Lipid droplet biogenesis: a novel process of self-digestion as a strategy of survival to stress

Memoria del trabajo experimental para optar al grado de doctor, correspondiente al Programa de Doctorado de Neurociencias del Instituto de Neurociencias de la Universidad Autónoma de Barcelona, llevado a cabo por Ainara González Cabodevilla bajo la dirección del Dr. Enrique Claro Izaguirre y del Dr. Albert Gubern Burset.

Ainara González Cabodevilla

Enrique Claro Izaguirre

Albert Gubern Burset

Bellaterra, Diciembre de 2014

INDEX

FIGURE INDEX

ABBREVIATIONS

3-MA, 3-methyladenine
ACSL, long-chain acyl-coenzyme A synthetase
Acyl-CoA, acyl-coenzyme A
Atg5, autophagy related protein 5
BEL, bromoenol lactone
CPT1, carnitine-palmitoyl transferase 1
CERK, ceramide kinase
EX, etomoxir
FAS, fatty acid synthase
FBS, Fetal bovine serum
KH buffer, Krebs-Helseleit buffer
LC3, microtubule-associated protein light chain 3
LDH, lactate dehydrogenase
PLA, phospholipase
Py-2, pyrrolidine 2
SiRNA, short interfering RNA
TAG, triacylglycerol

INTRODUCTION

CHAPTER 1. LIPID DROPLETS: DEFINITION AND ORIGIN

1. Lipid droplets

Lipids are essential for life, and the existence of cells specialized in fat storage has been conserved from flies and worms to humans (Pol et al., 2014; Murphy, 2012). However, almost all cells maintain the capability to retain and accumulate lipids.

Lipid droplets are the intracellular organelles specialized in assembling, storing and supplying lipids. They consist of a core of neutral lipids, mainly triacylglycerol and cholesterol esters, surrounded by a monolayer of phospholipids and a variety of associated proteins (Farese and Walther, 2009). All eukaryotic cell types are able to synthesize lipid droplets in response to elevated fatty acid levels. Although fatty acids supply a major source of energy for organisms, they can also be toxic. Cells escape cytotoxicity by esterifying fatty acids into neutral lipids and packaging them into lipid droplets ((Brasaemle and Wolins, 2012). Those neutral lipids can subsequently be metabolized when conditions are reversed, supplying cells with energy and membrane-building material (Martin and Parton, 2005).

Other than morphological studies, lipid droplets received little attention for decades, and were generally dismissed as inert lipid storage depots. In 1991, the discovery of perilipin1, a phosphoprotein that coats lipid droplets in adipocytes (Greenberg et al., 1991), brought new attention to the organelle. Since then, research on lipid droplets has experienced a dramatic increase, providing evidence for their central role on intracellular lipid homeostasis.

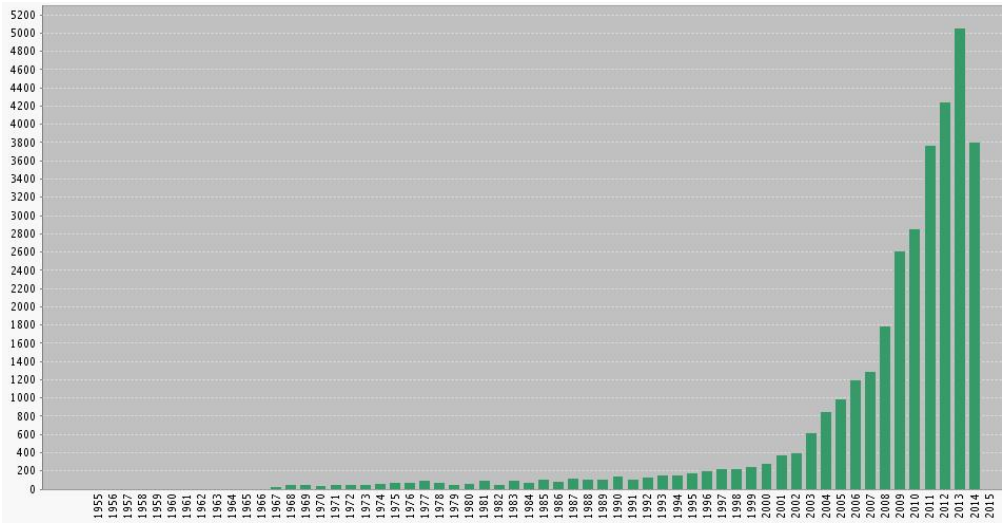

Figure 1: ***Citation report of the term"lipid droplets" in the last 50 years.*** *This figure shows the number of citations received by papers containing the words "lipid droplet" in their title. The exponential increase of citations is a good indicator of the growing interest of the scientific community for the organelle.*

Apart from storing neutral lipids for later use as metabolic fuel, lipid droplets have been seen to participate in processes of membrane building, lipid buffering, intracellular signaling, and protein storage. In human hepatocyte cell lines, the amphipatic protein Apolipoprotein B (ApoB) accumulates heavily on lipid droplets when it is in excess, before being degraded by both proteasomal and non-proteasomal pathways. In this case, lipid droplets might serve as platforms to process the unused ApoB molecules effectively and prevent them from forming toxic aggregates (Ohsaki et al., 2006). Lipid droplets have also been linked with development. In *Drosophila melanogaster*, lipid droplets coated with maternal core histones H2A and H2Av support the early cell cycles, and they can also transiently sequester H2Av produced in excess, ensuring proper histone balance in the nucleus (Li et al., 2014).

These data support that lipid droplets, far from being restricted to specialized lipid storage tissues, are a universal feature of eukaryotic cells, and intervene in a variety of important cell biology processes.

2. The Perilipin family of lipid droplet proteins

In 1991, the laboratory of Consantin Londos identified perilipin 1 as a lipid droplet protein which was phosphorylated in response to signals that stimulated lipolysis in adipocytes (Greenberg et al., 1991). The paradigm shifting discovery that proteins coated the surface of lipid droplets renewed the interest in the organelle, and led to the identification of four further members of the perilipin family of lipid droplet proteins.

Perilipins are an ancient family of proteins, which have been evolutionarily conserved from insects to mammals. They all share sequence similarity and the ability to bind lipid droplets (Figure 1), and differ from one another in size, tissue expression, affinity to lipid droplets and transcriptional regulation (Kimmel et al., 2010). Perilipins can be conceptually divided into those that are expressed in a tissue-restricted manner (perilipin 1, perilipin 4 and perilipin 5) versus ubiquitous manner (perilipin 2 and perilipin 3); as well as into those that are constitutively bound to lipid droplets (perilipin 1 and perilipin 2) versus those that demonstrate exchangeable lipid droplet binding (perilipin 3, perilipin 4 and perilipin 5) (Bickel et al., 2009).

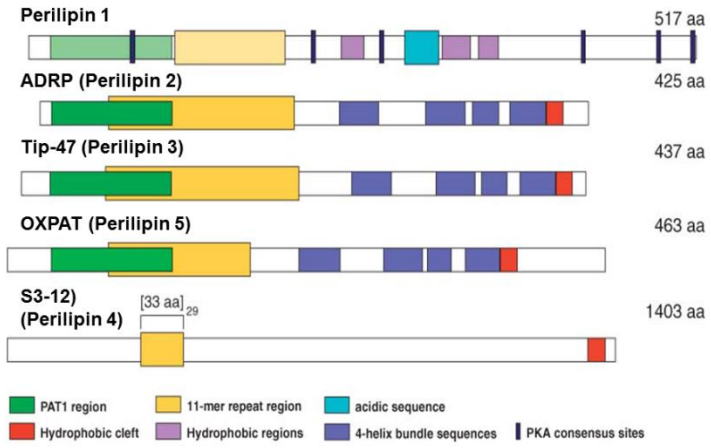

***Figure 2**. The Perilipin family of lipid droplet proteins.*

2.1 Perilipin 1

Perilipin 1 is the founding and best characterized member of the perilipin family. It is expressed in adipocytes and, to a lesser extent, steroidogenic cells, where it remains bound to the cytosolic lipid droplet and participates in the regulation of triacylglycerol storage and breakdown. Under basal conditions, perilipin 1 restricts access of cytosolic lipases to the neutral lipid core, thus promoting triacylglycerol storage (Lafontan, 2008). This is evidenced by the phenotype of perilipin *null* mice, which have a 65-70% reduction of adipose triacylglycerol storage as compared to wild type animals and are resistant to diet-induced obesity. Adipocytes isolated from perilipin *null* mice have a higher rate of basal lipolysis, consistent with a role for perilipin in protecting the core of the lipid droplet from the action of lipases (Tansey et al., 2001).

The role of perilipin 1 is not limited to ensuring the accumulation of triacylglycerol. It has been observed that perilipin 1 is phosphorylated upon activation of protein kinase A (PKA) by cyclic AMP (Greenberg et al., 1991), and that, in times of energy deficit, phosphorylation of perilipin 1 is necessary to ensure maximal lipolysis by lipases (Sztalryd et al., 2003).

2.2 Perilipin 2 (ADRP)

Perilipin 2, formerly known as adipocyte-differentiation related protein (ADRP), was first identified as a mRNA induced early during adipocyte differentiation (Jiang and Serrero, 1992). Its sequence similarity to perilipin 1 triggered the interest of the laboratory of

Constantin Londos, which reported that ADRP was in fact a ubiquitously expressed lipid droplet protein (Brasaemle et al., 1997).

Perilipin 2 binds constitutively the coat of lipid droplets, and is degraded by the proteasome in situations that preclude lipid droplet formation (Xu et al., 2005). Its presence at the lipid droplet surface promotes the accumulation of triacylglycerol (Imamura et al., 2002), likely by limiting access of cytosolic lipases to the neutral lipid core (Listenberger et al., 2007). As opposed to perilipin 1, perilipin 2 does not contain known sites for PKA phosphorylation or interaction with lipases (Bickel et al., 2009).

2.3 Perilipin 3 (Tip47)

Perilipin 3 was first identified as a possible cargo protein involved in the trafficking of the manose-6-phosphate receptor and studied as such (Miura et al., 2002), but its sequence similarities to Perilipin 2 prompted studies that confirmed its localization to lipid droplets (Than et al., 2003; Wolins et al., 2005).

Like perilipin 2, perilipin 3 is widely distributed among non-adipose tissues, but unlike perilipins 1 and 2, it is present in both lipid droplets and cytosolic compartments (Wolins et al., 2001; Barbero et al., 2001). In perilipin 2-null mice, lipid droplets appear coated by perilipin 3, which exerts a functional compensation ensuring lipid storage (Sztalryd et al., 2006).

2.4 Perilipin 4 (S3-12)

Perilipin 4 was first identified in a screen for adipocyte specific proteins, and found to be induced during adipocyte differentiation (Scherer et al., 1998). Its expression is highest in white adipocytes, with very low expression in heart and skeletal muscle and little or no expression in brown adipose tissue (Brasaemle, 2007). A sequence analysis revealed that approximately two thirds of its sequence was composed of tandem repeats of a 33-residue motif, which was similar to a region in the PAT1 domain of perilipins (Figure 2). However, the localization of perilipin 4 to the lipid droplet coat was not confirmed until 2003. A study performed by Wolins and colleagues showed that supplementing 3T3-L1 adipocytes with fatty acids caused perilipin 4 to move from the cytoplasm, where it was distributed diffusely, to the coat of nascent lipid droplets, where it co-localized with perilipin 3 (Wolins et al., 2003).

Further studies evidenced that inhibition of protein synthesis with cycloheximide did not block the fatty acid-induced appearance of lipid droplets, suggesting that the cytoplasmic pools of perilipins 3 and 4 constitute a ready reservoir of coat proteins to permit rapid packaging of newly synthesized triacylglycerol and to maximize energy storage during nutrient excess (Wolins et al., 2005).

2.5 Perilipin 5 (OXPAT)

Perilipin 5 was the last identified member of the perilipin family. It is preferentially expressed in tissues that catabolize large amounts of fatty acids, such as brown adipose tissue, skeletal muscle and heart. Similar to perilipins 2 and 3, perilipin 5 has been observed to promote triacylglycerol accumulation (Dalen et al., 2007). In liver, fasting-induced activation of the transcription factor PPARα triggers perilipin 5 expression and localization to lipid droplets (Wolins et al., 2006). Perilipin 5 overexpression in vitro in OP-9 and COS-7 cells increased cellular triglyceride storage in paralel with increases in fatty acid oxidation and induction of gene expression of mitochondrial enzymes involved in oxidative metabolism (Wolins et al. 2006). These results suggest involvement of perilipin 5 in triglyceride storage as well as oxidative degradation of fatty acids released from the droplet, and suggest involvement of perilipin 5 in lipid turnover.

3. Current model of lipid droplet biogenesis

Lipid droplets likely appear *de novo* by accumulation of neutral lipids in the endoplasmic reticulum (ER), although fusion of preexisting lipid droplets has been observed in yeast (Kassan et al., 2013). The currently accepted model of lipid droplet biogenesis from the ER is a three step process that includes neutral lipid synthesis, accumulation of neutral lipids within the bilayer of the ER, and droplet formation (Wilfling et al., 2014). Although the molecular mechanisms involved in each of the steps are still not fully understood, research carried out in recent years has shown that lipid droplet biogenesis is a highly orchestrated process that requires the coordinated activity of an important number of players.

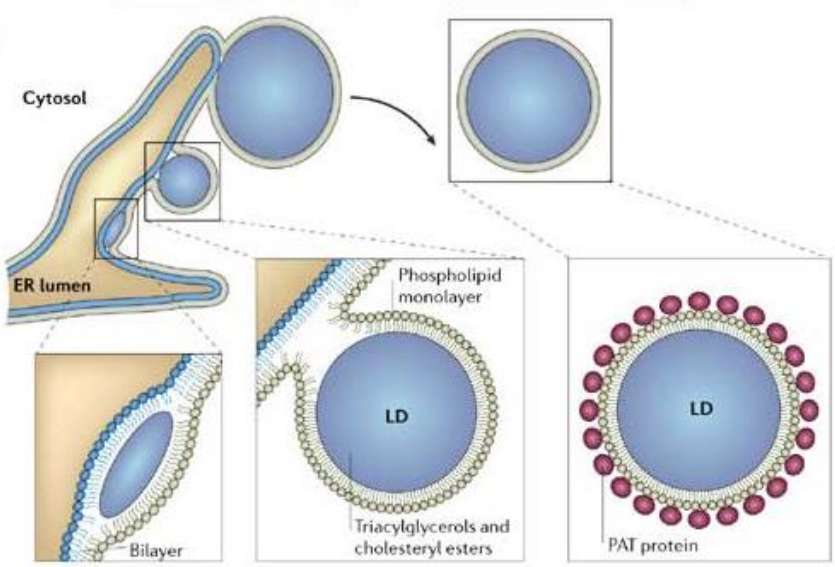

***Figure 3**: Current model of lipid droplet biogenesis from the ER*

According to the accepted model of lipid droplet biogenesis from the ER, neutral lipids synthesized in the ER accumulate within the ER bilayer, forming a lens. The mature lipid droplet is thought to bud from the ER to form an independent organelle, which consists on a neutral lipid core surrounded by a phospholipid monolayer and a variety of proteins, the best characterized being the members of the PAT (Perilipin, ADRP and Tip47) family of proteins (Martin and Parton, 2006)

3.1 Step 1: Neutral lipid synthesis

Neutral lipids are synthesized in the ER by members of the Membrane-Bound O Acyltransferase (MBOAT) and acyl-CoA:diacylglycerol acyltransferase (DGAT)-2 gene families. Members of the MBOAT family include acyl-CoA:cholesterol acyltransferase (ACAT)-1 and ACAT2; and DGAT1 (Buhman et al., 2001). Generally, those enzymes localize to the ER, where they can access their substrates.

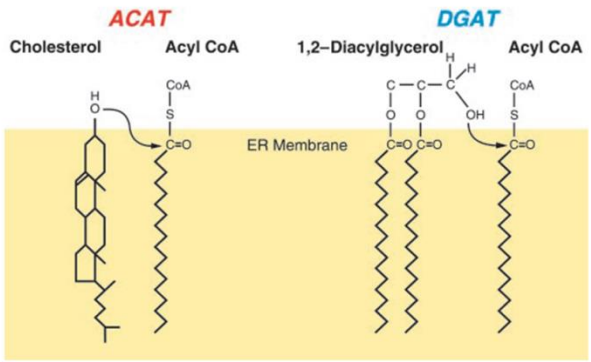

***Figure 4:* The enzymes of neutral lipid synthesis**

ACAT catalyzes the covalent joining of cholesterol with long chain fatty acyl-CoA moieties to form cholesterol esters. DGAT catalyzes a similar reaction in which diacylglycerol serves as the acyl acceptor molecule. Both enzymes function at the ER (Buhman et al., 2001).

An important step for triacylglycerol synthesis is the activation of fatty acids by the family of acyl-CoA synthetase enzymes (ACSL) (Ellis et al., 2010), which allows their use in metabolic pathways. Fatty acyl-CoAs are used by DGAT enzymes to generate triacylglycerol by joining them to diacylglycerol. Similarly, cholesterol esters are produced by condensation of fatty acyl-CoA to cholesterol (Wilfling et al., 2014).

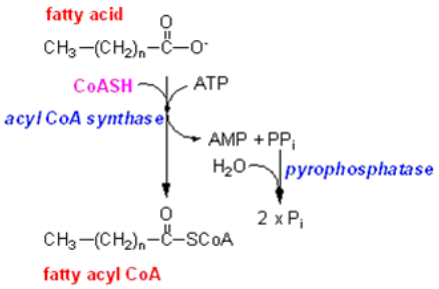

***Figure 5*. Fatty acid activation is a two-step reaction catalyzed by ACSL**

Fatty acid activation is catalyzed by acyl-CoA synthetase (ACS) via a two-step reaction: 1) the formation of an intermediate fatty acyl-AMP with the release of pyrophosphate, and 2) the formation of a fatty acyl-CoA with the release of AMP

Neutral lipid synthesis is essential for lipid droplet formation. The inhibition of the proposed lipid droplet-bound ACSL (ACSL1, ACSL3 and ACSL4,) with Triacsin C blocks triacylglycerol and cholesterol ester synthesis (Igal et al., 1997) and completely inhibits the formation of lipid droplets (Liefhebber et al., 2014). In yeast, the absence of all enzymes of neutral lipid synthesis does not affect viability, but results in the lack of any detectable lipid droplets (Sandager et al., 2002).

3.2 Step 2: Neutral lipid accumulation and lens formation

As the concentration of newly synthesized neutral lipids increases, the capacity of the ER bilayer to hold triacylglycerol is exceeded. At that point, lipid lenses are proposed to form in the ER bilayer (Brasaemle and Wolins, 2012), marking the beginning of lipid droplet biogenesis. The mechanisms that govern lens formation remain unclear, but recent studies indicate that they form in discrete regions dispersed throughout the ER (Jacquier et al., 2013; Kassan et al., 2013). It has also been observed that triacylglycerol enrichment in the ER

bilayer alone is insufficient to give raise to lipid droplets (Gubern et al., 2008). These findings suggest that lens formation, and the subsequent process of lipid droplet maturation, are governed by a mechanism other than mere neutral lipid accumulation.

Several proteins have been linked to the organization of lipid droplet formation sites. The ER protein seipin localizes at lipid droplet-ER junctions in yeast (Jacquier et al., 2013), and its deficiency dramatically alters lipid droplet size and number. Loss of function mutations in the BSCL2/SEIPIN gene cause Berardinelli-Seip congenital lipodystrophy 2 (BSCL2), a condition characterized by an almost complete loss of adipose tissue (Wee et al., 2014). Although the physiological role of seipin remains unknown, studies performed in yeast and fibroblasts from BSCL2 patients show that, in the absence of seipin, lipid droplets seem to bud chaotically from the ER, and exhibit dramatic morphological alterations (Liu et al., 2014), suggesting that seipin is necessary to organize the assembly of lipid droplets.

A recent study performed in COS-1 cells proposed that lipid droplets arise from restricted microdomains in the ER (Kassan et al., 2013). According to this model, newly synthesized neutral lipids accumulate within the bilayer of the ER until their concentration induces a curvature of the ER membrane. Proteins with amphipathic α helices, such as caveolin 1 or acyl-CoA synthetase 3 (ACSL3) are then attracted to these regions, where they form a stable interaction that nucleates unstable neutral lipid globules, marking the onset of lipid droplet assembly. At that early stage, ACSL3 enzymatic activity is not necessary to ensure nucleation, which can be promoted by the inactive mutant ACSL3Δgate, but is impaired when expression of ACSL3 is completely silenced. Given its ability to interact with other lipid droplet proteins, ACSL3 might contribute to organize specific regions of lipid droplet assembly within the ER (Pol et al., 2014)

3.3 Step 3: Lipid droplet formation

Once the nascent lipid droplets have accumulated sufficient neutral lipids, they are thought to bud from the ER, although whether they dissociate completely or remain attached to the ER is still unclear. The existence of intimate connections between lipid droplets and the ER has been observed in yeast (Jacquier et al., 2013) and animal cells (Kassan et al., 2013; Wilfling et al., 2013), but completely dissociated lipid droplets have also been seen in animal cells (Robenek et al., 2006)

In any case, the mechanism that guides lipid droplet budding from the ER is poorly understood. Some authors propose that, above a certain size, lipid droplets bud spontaneously from the ER due to thermal fluctuations, without the intervention of proteins (Wilfling et al., 2014). However, the ubiquity of lipid droplets across species and their physiological significance seem to argue for the presence of a highly conserved mechanism. In keeping with that idea, it has been observed that accumulation of neutral lipids within the ER bilayer alone is not sufficient to trigger lipid droplet formation (Gubern et al., 2008).

The transition between neutral lipid accumulation and the appearance of a globular droplet requires a reorganization of the ER phospholipid membrane (Pol et al., 2014). The regulated hydrolysis of phospholipids by phospholipases affects the biophysical properties of membranes, and may play a key role at this stage of lipid droplet biogenesis. In fact, results from a cell-free system showed that phosphatidic acid, a product of phospholipase activities, strongly induced lipid droplet formation (Marchesan et al., 2003). The effect of phosphatidic acid may be related to its ability to induce membrane bending and destabilization (Kooijman et al., 2003), which could facilitate the budding process.

3.3.1 Group IV Phospholipase A_2 in lipid droplet formation

A study performed by Gubern *et al* provided evidence that Group IVA Phospholipase A_2 (also known as cPLA$_2$α) was required at a step beyond the synthesis of neutral lipids (Gubern et al., 2008). cPLA$_2$α activity was found to be essential for lipid droplet biogenesis in all cell types tested, and those results have been reproduced in both cell lines and primary cultures (Gubern et al., 2008; Du et al., 2009; Cabodevilla et al., 2013). Those findings, together with the ubiquitous expression of cPLA$_2$α in mammalian tissues, argue for a general implication of the enzyme in lipid droplet biogenesis.

cPLA$_2$α is a member of the cytosolic PLA$_2$ family of phospholipases. PLA$_2$ phospholipases catalyze the hydrolysis of the middle (*sn-2*) ester bond of substrate phospholipids to release free fatty acids and lysophospholipids (Yu et al., 1998). Of all six isoforms of cytosolic PLA$_2$, cPLA$_2$α has been the most extensively studied, because its preference for arachidonic acid at the *sn-2* position makes it essential for eicosanoid production (Diez et al., 1992).

Exposure of serum-starved cells to fetal bovine serum (FBS), a treatment that induces lipid droplet biogenesis, triggered the release of arachidonic acid, which was precluded by inhibition of cPLA$_2$α with its specific inhibitor pyrrolidin-2 (py-2), or by silenced expression of

the enzyme. Under these conditions, inhibition of $cPLA_2\alpha$ dose-dependently blocked lipid droplet formation. These findings suggest that treatment with FBS stimulates $cPLA_2\alpha$, and that its activity is somehow necessary for FBS-induced biogenesis of lipid droplets (Gubern et al., 2008).

To test whether the role of $cPLA_2\alpha$ in lipid droplet formation was to provide arachidonic acid for neutral lipid synthesis, serum-starved cells were exposed to different concentrations of the fatty acid. Although arachidonic acid was able to induce lipid droplet biogenesis at high enough concentrations, its effect was sensitive to $cPLA_2\alpha$ inhibition. This showed that $cPLA_2\alpha$ activity was necessary in the formation of lipid droplets triggered by exogenous fatty acids, and that its loss of function could not be overcome by supplementation of its product. Further evidence that $cPLA_2\alpha$ was not involved in the step of neutral lipid synthesis was that its inhibition did not preclude incorporation of exogenous arachidonic acid into triacylglycerol or cholesterol esters. Taken together, these results suggest that $cPLA_2\alpha$ activity is necessary for lipid droplet biogenesis at a step beyond neutral lipid synthesis. This hypothesis was supported by the finding that, under conditions that stimulated lipid droplet formation, inhibition of $cPLA_2\alpha$ led to neutral lipid retention within membranes, and altered the structure of the ER, leading to the formation of aberrant membrane sacks (Figure 6).

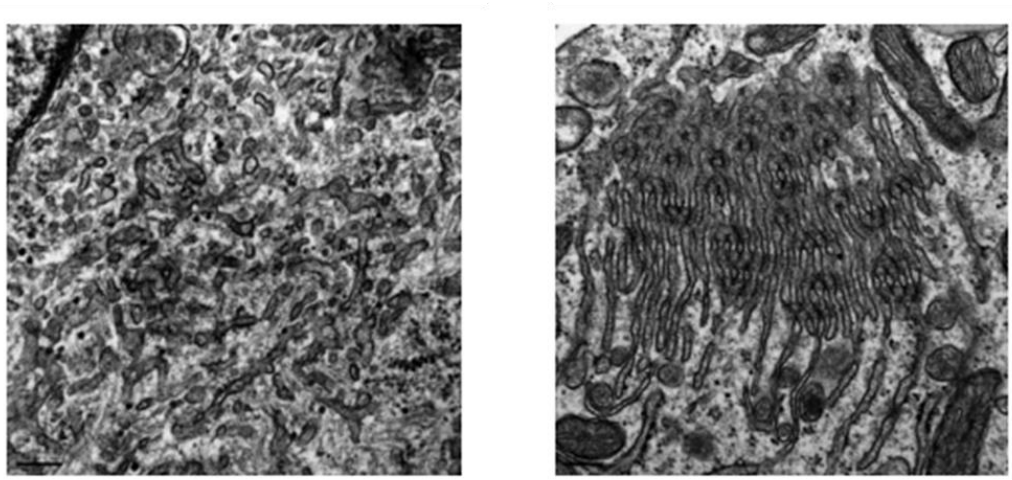

Figure 6. *Inhibition of $cPLA_{2\alpha}$ in conditions leading to lipid droplet formation resulted in the appearance of abnormal tubulovesicular structures associated with the smooth ER* (Gubern et al., 2008)

This is consistent with a model in which $cPLA_2\alpha$ activity would be necessary for the budding of the lipid droplet from the ER (Gubern et al., 2008). This effect could be favored by $cPLA_2\alpha$-

generated lysophospholipids, which are known to induce membrane curvature due to their inverted cone shape (Brown et al., 2003).

3.3.2 Activation of cPLA$_2$α for lipid droplet biogenesis

In order to promote lipid droplet biogenesis, cPLA$_2$α has to be activated by phosphorylation at Ser-505 (Gubern et al., 2008). This activation is achieved through a pathway that involves the mitogen-activated protein kinase JNK and ceramide kinase (CERK), in a calcium-independent manner (Gubern et al., 2009a). Exposure of serum-starved Chinese hamster ovary cells to FBS induced phosphorylation of JNK, which in turn phosphorylated cPLA$_2$α at Ser-505. Inhibition of JNK or expression of a dominant-negative form of its upstream activator MEKK1 precluded cPLA$_2$α phosphorylation triggered by FBS, and blocked lipid droplet biogenesis.

It was also observed that CERK was necessary to trigger activation of JNK. Silenced expression of the enzyme inhibited the phosphorylation of JNK and cPLA$_2$α induced by FBS, therefore precluding lipid droplet formation. Consistently, treatment with ceramide 1-phosphate (Cer-1-P), the product of CERK activity, induced both JNK and cPLA$_2$α phosphorylation, and lipid droplet formation. These findings showed for the first time the crucial role of the JNK cascade in lipid droplet biogenesis, through the activation of cPLA$_2$α (Gubern et al., 2009a). Although this work was performed in a Chinese hamster ovary cell model, the involvement of CERK in lipid droplet biogenesis has also been assessed in LN18 human glioma cells (Cabodevilla et al., 2013). Given that cPLA$_2$α has been implicated in lipid droplet formation in a variety of cell types, the same generalization might stand for its activation mechanism.

4. Lipid droplet biogenesis triggered by stress

Exogenous lipid availability is not the only physiological situation that stimulates lipid droplet biogenesis. In fact, lipid droplet formation is a hallmark of cellular stress. Many kinds of stress, including inflammation, apoptosis induced by different insults, hypoxia or nutrient deprivation trigger the appearance of lipid droplets (Weng et al., 2014; Lee et al., 2013). It is also considered that NMR-visible lipids (the neutral lipid core of lipid droplets) appear in cancer cells and human tumors as a stress response to the tumor microenvironment (Delikatny et al., 2011), and may also arise as a response to treatment (Lee et al., 2010).

As discussed above, lipid droplet biogenesis from the ER is initiated by the esterification of exogenous fatty acids and cholesterol to form triacylglycerol and cholesteryl esters. In that case, lipid droplets have a storage purpose for energy generation and membrane building, and they also buffer cells from the toxic effects of excess lipids. However, the origin and physiological role of stress-triggered lipid droplets have not been extensively studied, and many questions remain to be elucidated.

4.1 Origin of triacylglycerol in stress-triggered lipid droplets

Apoptosis often alters phospholipid metabolism, resulting in the release of fatty acid and lysophospholipids. Evidence suggests that group VIA PLA_2 ($iPLA_2$–VIA) is involved in the generation of lysophosphatidylcholine during programmed cell death, which may play a prominent role in mediating the chemoattractant and recognition/engulfment signals that accompany the process of apoptotic cell death, facilitating efficient clearance of dying cells by phagocytes (Balsinde et al., 2006).

Unlike $cPLA_2\alpha$, which has a marked preference for arachidonic acid, $iPLA_2$–VIA has no substrate specificity for the fatty acid at the *sn-2* position. Therefore, it is able of hydrolyze a wide variety of phospholipid substrates and serves a housekeeping role mediating membrane phospholipid remodeling, in what is called the Land's cycle (Winstead et al., 2000).

Taking these ideas into account, it has been hypothesized that, during cellular stress, part of the fatty acids released by $iPLA_2$–VIA may be incorporated into triacylglycerol and stored in lipid droplets (Gubern et al., 2009b).

Cells cultured in the absence of serum and subjected to different types of stress synthesized triacylglycerol and lipid droplets in the absence of an external lipid source (Figure 6). It was observed that inhibition of *de novo* fatty acid synthesis with fatty acid synthase (FAS) inhibitors cerulenin and C75 induced lipid droplet biogenesis and triacylglycerol synthesis which necessarily had to take place from endogenous sources.

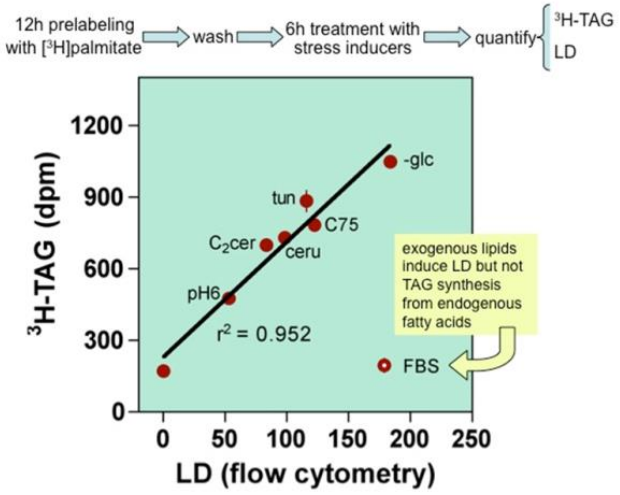

Figure 6. ***Stress-triggered triacylglycerol (TAG) and lipid droplet (LD) synthesis in the absence of an external source of fatty acids.***

This figure shows the correlation between TAG synthesis and LD occurrence as induced by six different stressors: acidic pH, C2-ceramide, FAS inhibitors cerulenin and C75, tunicamycin and glucose deprivation. All stressors triggered TAG synthesis from pre-existing fatty acids, and induced lipid droplet formation. Lipid droplet induction with FBS did not stimulate the synthesis of TAG from endogenous fatty acids (Gubern et al., 2009b)

Under these conditions, pharmacological inhibition or silenced expression of $iPLA_2$-VIA completely blocked TAG synthesis and lipid droplet occurrence. Further, cells prelabeled with the fluorescent fatty acid analog C_1-BODIPY-C_{12} generated intensely fluorescent lipid droplets when challenged with FAS inhibitor C75. However, inhibition of $iPLA_2$-VIA resulted in the fluorescent label being retained in perinuclear membrane structures. $iPLA_2$-VIA downregulation had no effect on lipid droplet occurrence in cells treated with FBS (Gubern et al., 2009b)

4.2 Role of $cPLA_2\alpha$ in stress-triggered lipid droplet formation

When cells were subjected to stress, $cPLA_2\alpha$ activity was still required for lipid droplet formation. Treatment with cerulenin and C75 promoted the phosphorylation of $cPLA_2\alpha$ at Ser505, which is necessary for the enzyme activation during lipid droplet biogenesis. This was partially abrogated by pharmacological inhibition of $iPLA_2$-VIA, and increased by its overexpression, suggesting that $iPLA_2$-VIA might have a role in the events leading to $cPLA_2\alpha$ activation.

In addition, cells treated with C75 in the presence of $cPLA_2\alpha$ inhibitor py-2 synthesized triacylglycerol, but were unable to form lipid droplets, resulting in an accumulation of triacylglycerol in membrane structures (Gubern et al., 2009b).

4.3 Physiological role of stress-triggered lipid droplet formation

Although lipid droplet formation is a hallmark of cellular stress which has been observed both *in vivo* and *in vitro*, its physiological role has not been elucidated. Triacylglycerol synthesis, which is required for lipid droplet biogenesis, is an energy-consuming process that appears futile in cells committed to die. However, was observed that overexpression of $iPLA_2$-VIA increased triacylglycerol synthesis and delayed cell death under glucose deprivation. This protection was precluded by preventing lipid droplet biogenesis after $cPLA_2\alpha$ inhibition (Gubern et al., 2009b). Consistently, the ability to synthesize lipid droplets has been linked to neuron survival to starvation (Du et al., 2009), and the attenuation of ischemia-induced injury in the heart (Lei et al., 2013). These observations lead to hypothesize that lipid droplet biogenesis under stress might be a survival strategy.

Given the fact that triacylglycerol contained in stress-triggered lipid droplets is synthesized using fatty acids released from membrane phospholipids, it is tempting to speculate that, in this situation, lipid droplet biogenesis may represent a lipidic counterpart of autophagy: fatty acids from structural phospholipids might be reused for triacylglycerol synthesis in a process mediated by $iPLA_2$-VIA, and packed in lipid droplets for energetic purposes in a process requiring $cPLA_2\alpha$.

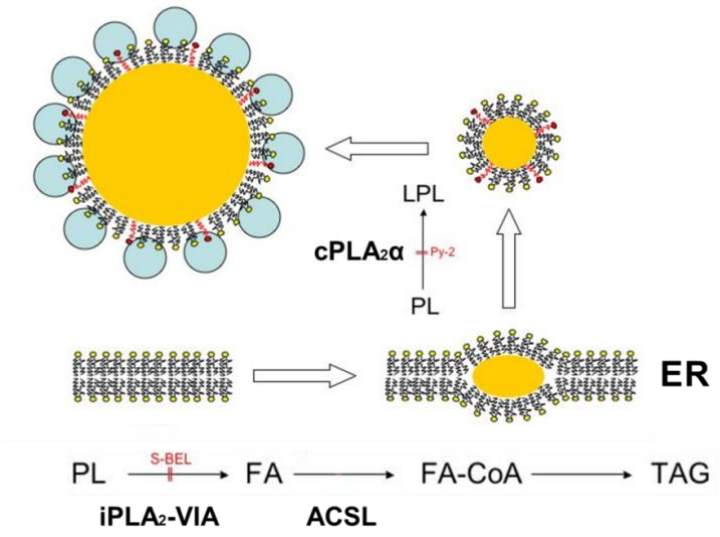

Figure 7. ***Proposed model of lipid droplet formation from the ER.***

Lipid droplet biogenesis from the ER is triggered by exogenous lipid availability or a variety of stressors. In any case, neutral lipid synthesis takes place in the ER, and $cPLA_2\alpha$ is necessary to ensure lipid droplet formation, likely by the synthesis of lysophospholipids, which are known to induce membrane curvature due to their inverted cone shape. When lipid droplet biogenesis is triggered by stress, fatty acids released from membrane phospholipids by $iPLA_2$-VI are esterified into triacylglycerols, which will conform the neutral lipid core of lipid droplets.

CHAPTER 2: LIPID DROPLET MOBILIZATION AND UTILIZATION

The balance of lipids stored within lipid droplets is controlled by the net cycle of neutral lipid synthesis and degradation. Neutral lipids in the core of lipid droplets are hydrolyzed by intracellular lipases, yielding fatty acids for energy generation and building of membrane phospholipids. Although all cells are equipped to perform lipolysis, little is known about the processes involved in the mobilization of lipid droplets in non-adipose tissues. However, basal levels of lipolysis are detectable in most cells, where cycles of esterification and lipolysis are likely to be continuously active (Walther and Farese, 2009). Conversely, the lipid droplets occupying most of the cytoplasm of adipocytes are a major energy reserve for the whole organism, and hydrolysis of the neutral lipids contained in their core involves a complex regulation (Lafontan, 2008).

1. **Mobilization of lipid droplets in adipocytes**

In the adipose tissue, the formation and catabolism of lipid droplets is strictly dependent on the energetic status of the organism. When there is lipid availability, excess fatty acids are used to synthesize neutral lipids, which are stored into lipid droplets until conditions are reversed. Then, when fatty acids are required by cells or tissues, cytosolic lipases hydrolyze triacylglycerol contained in lipid droplets (Chaves et al., 2011). In adipocytes, complete lipolysis is a three step process catalyzed sequentially by adipose triglyceride lipase (ATGL), hormone-sensitive lipase (HSL) and monoacylglycerol lipase (MGL). The liberated fatty acids and glycerol are subsequently released from the cell, to be used as metabolic fuel in peripheral tissues, mainly liver, heart and skeletal muscle (Viscarra and Ortiz, 2013).

1.1 Hormone-sensitive lipase (HSL)

Hormone-sensitive lipase (HSL) is the best characterized cytosolic lipase in adipocytes. It was initially identified in the white adipose tissue of mammals as an enzyme which was induced by fasting and stimulated by catabolic hormones (Lass et al., 2011). Early studies performed *in vitro* characterized the ability of HSL to catalyze all three steps of complete triacylglycerol hydrolysis to free fatty acids and glycerol (Belfrage et al., 1977).

It has long been known that the rate of release of free fatty acids from adipose tissue is controlled by regulation of the activity of HSL by protein kinase A (PKA) (Huttunen et al.,

1970), and abundant data support a model in which β-adrenergic agents lead to an increase in the intracellular concentration of the cyclic AMP that activates PKA, which in turn phosphorylates and stimulates HSL (Birnbaum, 2003).

A pitfall in this model was the early observation that *in vitro* stimulation of HSL with PKA increased the activity of the lipase less than twofold, a raise which did not correlate with the observed 30 to 100-fold increase in lipolysis observed *in vivo* upon PKA stimulation in mammalian adipocytes. It is now understood that activation of HSL is a two-step process that requires phosphorylation by PKA and binding to the lipid droplet through association with the lipid droplet protein perilipin 1 (Hirsch and Rosen, 1984; Egan et al., 1992; Sztalryd et al., 2003). Therefore, substrate access, rather than an increase in the specific activity of HSL, is likely to be the basis for the large PKA-stimulated lipolysis in adipocytes (Miyoshi et al., 2006)

The early observation that perilipin 1 was both the most abundant protein in the coat of lipid droplets and the major substrate of PKA in adipocytes (Greenberg et al., 1991) suggested that its phosphorylation might play an important role in the regulation of lipolysis. This was confirmed by mutagenesis experiments, which showed that simultaneous mutation of three serines in the N-terminal PKA site of perilipin 1 prevented phosphorylation and reduced maximal lipolysis catalyzed by HSL (Zhang et al., 2003). This effect was due to the inability of HSL to translocate to the membrane of lipid droplets upon phosphorylation by PKA, a process which was abrogated by expression of the mutant perilipin 1 and also in adipocytes of perilipin 1 *null* mice (Sztalryd et al., 2003).

Taken together, these findings allow proposing a model by which β-adrenergic agents activate PKA by G-protein mediated increase of cAMP levels. Once active, PKA phosphorylates HSL and perilipin 1, activating the lipase and allowing its translocation to the lipid droplet. Phosphorylated perilipin 1 might directly recruit HSL to the lipid droplet surface by interacting with the enzyme. Alternatively, phosphorylated perilipin 1 may modify the lipid droplet surface to indirectly facilitate interaction of HSL with the core triacylglycerols (Wang et al., 2009).

1.2 Adipose triglyceride lipase (ATGL)

In the early 2000s, studies performed on HSL *null* mice evidenced that, upon stimulation with β-adrenergic agents, those animals still retained 40% triacylglycerol lipase activity in their

white adipose tissue as compared to wild type controls (Osuga et al., 2000). This finding challenged the view, held for almost three decades, that HSL was the only, and therefore rate-limiting, enzyme for triacylglycerol hydrolysis in adipocytes. Interestingly, HSL null mice showed a significant accumulation of diacylglycerol in adipose tissue, suggesting that HSL is essential for diacylglycerol hydrolysis *in vivo* (Haemmerle et al., 2002), but not for the initiation of the lipolytic cascade. These results were in keeping with the 10-fold higher specific activity of the enzyme for diacylglycerol as compared to triacylglycerol or monoacylglycerol observed *in vitro* (Belfrage et al., 1977). Taken together, these findings led to hypothesize that, despite the ability of HSL to catalyze all three steps of complete triacylglycerol hydrolysis, it was not the only enzyme mediating the process in adipocytes.

The prediction that there must be other lipases at play was confirmed in 2004, when three different groups reported the identification of adipose triglyceride lipase (ATGL) as a new cytosolic enzyme participating in triacylglycerol hydrolysis (Zimmermann et al., 2004; Villena et al., 2004; Jenkins et al., 2004).

ATGL is highly expressed in the adipose tissue of mice and humans, and has detectable levels of expression in virtually all tissues (Lake et al., 2005). It exhibits a marked substrate preference for triacylglycerol, and minor or no activity when other lipids, such as diacylglycerol or monoacylglycerol, are provided as substrates (Zimmermann et al., 2004). Deficiency in ATGL activity leads to systemic accumulation of triacylglycerol, suggesting that the role of the enzyme in triacylglycerol breakdown is not limited to the adipose tissue (Haemmerle et al., 2006).

1.2.1 Regulation of ATGL by CGI-58

Efficient ATGL activity requires its interaction with CGI-58, a protein whose deficiency causes Chanarin-Dorfman Syndrome (CDS), a rare genetic disease where triacylglycerol accumulates excessively in multiple tissues (Yamaguchi and Osumi, 2009). The mechanism by which CGI-58 stimulates ATGL is not fully understood. The need of direct protein-protein interaction was demonstrated *in vitro*, but proved to be insufficient to elicit ATGL activity by itself (Lass et al., 2006). ATGL activation in living cells additionally requires the binding of CGI-58 to the lipid droplet (Lass et al., 2011), and truncated variants of CGI-58, which fail to localize to the lipid droplet, but bind to ATGL, are unable to stimulate ATGL activity (Gruber et al., 2010).

1.2.2 β-adrenergic stimulation of ATGL

ATGL can be activated by β-adrenergic stimulation, as suggested by the triacylglycerol lipase activity present in HSL *null* mice adipose tissue (Osuga et al., 2000). Further, ATGL-deficient mice are unable to achieve complete hormone-activated lipolysis, which is reduced by approximately 70% in the absence of ATGL (Haemmerle et al., 2006). The molecular mechanisms that regulate ATGL activity in response to β-adrenergic stimulation are not fully understood, but there is evidence that supports an indirect mechanism involving perilipin 1 and CGI-58 (Miyoshi et al., 2007).

In non-stimulated adipocytes, CGI-58 is located at the surface of lipid droplets, where it binds to perilipin 1 by a conserved region within the carboxy terminus of the lipid droplet protein. This interaction stabilizes CGI-58 by retarding its degradation by the proteasome (Patel et al., 2014). Upon β-adrenergic stimulation, perilipin 1 phosphorylation by PKA causes the dissociation of CGI-58, making it available for the activation of ATGL (Subramanian et al., 2004). These observations indicate that perilipin 1 indirectly controls the activation of ATGL in the adipose tissue by interacting with its co-activator CGI-58 in a cAMP-dependent manner (Lass et al., 2011).

1.3 Monoacylglycerol lipase (MGL)

Monoacylglycerol lipase (MGL) is responsible for catalyzing the final step in the separation of glycerol and fatty acids by hydrolyzing monoacylglycerol (Fredrikson et al., 1986). It was first identified in rat adipose tissue (Sites, 1976), and it is ubiquitously expressed at relatively high levels. This wide-spread distribution, together with the high specific activity of the enzyme toward medium- and long-chain monoacylglycerol, has led to hypothesize that the final step in triacylglycerol hydrolysis is not highly regulated (Zechner et al., 2009).

MGL-deficient mice exhibit systemic accumulation of monoacylglycerol and reduced adipose tissue lipolysis. However, MGL-deficient white adipose tissue is still able to degrade monoacylglycerol in response to lipolytic stimulation. In the absence of MGL, HSL accounts for the remaining monoacylglycerol-hydrolase activity (Taschler et al., 2011)

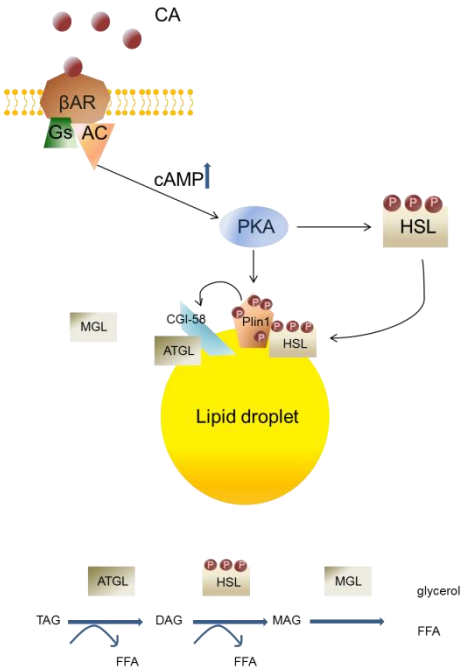

Figure 8. ***Model of the lipolytic cascade in adipocytes.***

When catecholamines (CA) bind to β-adrenergic receptors (βAR), G protein (Gs)-mediated signaling activates adenylyl cyclase (AC). Increased cAMP levels activate cAMP-dependent protein kinase A (PKA), which in turn phosphorylates HSL and perilipin 1 (Pln1). Phosphorylation of HSL activates the enzyme and triggers its translocation to the lipid droplet, where it binds phosphorylated perilipin 1 and gains access to its substrate. Phosphorylation of perilipin 1 induces the dissociation of CGI-58, which is bound to perilipin 1 in basal (unphosphorylated) conditions. Free CGI-58 is able to bind and activate ATGL. ATGL catalyzes the hydrolysis of triacylglycerol into diacylglycerol, which is hydrolyzed into monoacylglycerol by HSL. The final step of complete lipolysis is performed by cytosolic monoacylglycerol lipase (MGL), giving a net result of glycerol and three free fatty acids (FFA).

2. Mobilization of lipid droplets in non-adipose tissue

All cell types store triacylglycerol in lipid droplets, and are equipped to release fatty acids for energy use in times of nutrient deprivation (Zechner et al., 2009). However, the mechanisms governing lipolysis in non-adipose tissues are poorly understood. Since perilipin 1 expression is restricted to β-adrenergic stimulatable cells, such as adipocytes and steroidogenic cells, regulation of lipolysis in other tissues must be a perilipin 1-independent process.

2.1 Autophagy in the regulation of lipolysis

The process of lipolysis described in this section is a response aimed at maintaining systemic and cellular energy homeostasis. Thus, starvation triggers the release of free fatty acids stored as triacylglycerol in adipocyte lipid droplets for systemic energy generation. Lipolysis also takes place in non-adipose tissues, where fatty acids and cholesterol esters are released from the neutral core of lipid droplets for local use as metabolic fuel or membrane building. A second cellular response to starvation is the induction of macroautophagy (henceforth called autophagy) (Mizushima et al., 2008).

Autophagy is a catabolic process in which organelles and other cellular components are enveloped in double membrane vesicles (autophagosomes), which eventually fuse with lysosomes. In the resulting autolysosomes, acidic enzymes degrade the cargo of the autophagosome for reuse of its components, which are released back into the cytosol (Czaja et al., 2013). Autophagy occurs constitutively in all eukaryotic cells, and operates as a homeostatic mechanism. In addition, autophagy can be upregulated in response to various physiological and pathological stimuli, either to promote cell survival (as in the case of starvation or oxidative stress), or to act as a mode of cell death (type II programmed cell death, which is observed in development) (Abounit et al., 2012).

The functional and regulatory similarities shared by lipolysis and autophagy have attracted much attention in the last years. Further, the existence of an acidic lipase within lysosomes (Debeer et al., 1979), coupled with the ability of the autophagic machinery to degrade cellular organelles, led to hypothesize that autophagy might be involved in the mobilization of lipid droplets. In 2009, Singh and colleagues reported for the first time the identification of such a mechanism in cultured hepatocytes and mouse liver *in vivo* (Singh et al., 2009).

The authors observed that inhibition of autophagy increased triacylglycerol and lipid droplets *in vivo* and *in vitro*, and that loss of autophagy decreased triacylglycerol breakdown, as measured by the reduction of β-oxidation rates. In addition, both triacylglycerol and lipid droplet proteins co-localized with autophagic compartments, and several components of the autophagic machinery (such as LC3, Atg5 or Atg7) were seen to localize to newly synthesized membrane structures at the surface of lipid droplets. In many cases, those membranes curved to finally seal, giving raise to double-membrane vesicles which contained solely components of lipid droplets in their lumen (Singh et al., 2009). Although lipid droplet proteins and triacylglycerol were also found in autophagosomes under basal conditions, along with cytosolic components, prolonged starvation led to the preferential sequestration of lipid droplets, suggesting some level of selectivity in the process (Singh et al., 2009).

These findings led the authors to coin the term “lipophagy”, to describe a regulated process whereby portions of lipid droplets, or even whole lipid droplets, become trapped inside autophagosomes and transported to lysosomes, where they are degraded to fatty acids (Singh and Cuervo, 2012).

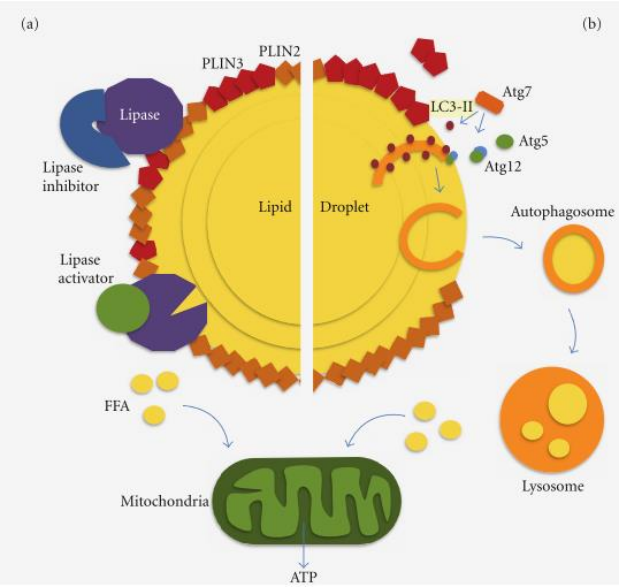

Figure 9. ***Lipolysis of lipid droplets by cytosolic lipases (a) or macrolipophagy (b)***

This figure is a schematic representation proposed by Singh and colleagues of the processes of lipolysis taking place in hepatocyte lipid droplets. The left part of the image represents the interactions between cytosolic lipases and perilipins at the lipid droplet coat, which have been described in the previous section of this introduction. The right part of the image depicts the formation of autophagic vacuoles at the surface of lipid droplets. In both cases, the ultimate products of lipolysis, free fatty acids (FFA) serve as fuel for the generation of ATP in mitochondria (Singh and Cuervo, 2012).

The publication of this seminal work significantly altered the view of lipid metabolism, providing an alternative mechanism by which cells mobilize lipid droplets in response to cellular needs or external stimuli (Liu and Czaja, 2013). Since then, the contribution of lipophagy to starvation-triggered lipid droplet mobilization in hepatocytes has been confirmed by several groups (Xiong et al., 2012; Skop et al., 2012; Jaber et al., 2012; Yang et al., 2010), and it has also been observed in other cell types, including neurons (Martinez-Vicente et al., 2010; Kaushik et al., 2011) and stellate cells (Hernández-Gea et al., 2012).

2.2 Regulation of cytosolic lipases by perilipins in non-adipose tissues

Despite the absence of perilipin 1 expression in non-adipose tissues, ATGL and its co-activator CGI-58 still play an essential role in triacylglycerol hydrolysis. This is evidenced by the systemic accumulation of triacylglycerol observed in ATGL- and CGI-58-defficient animals (Guo et al., 2013), as well as in patients affected with Chanarin-Dorfman Syndrome (Yamaguchi, 2010). Importantly, ATGL-null mice exhibit massive cardiac

triacylglycerol accumulation and impaired mitochondrial function, which results in the premature death of the animals (Haemmerle et al., 2006).

The importance of correct ATGL activity in non-adipose tissue evidences the need of an alternative, perilipin 1-independent regulation of the lipase. Evidence gathered by different groups supports that the protein composition of perilipins at the lipid droplet coat regulates the lipolytic activity of ATGL in various cell types.

2.2.1 Perilipins 2 and 3 limit the access of ATGL to the lipid droplet coat

Perilipins 2 and 3 are ubiquitously expressed in non-adipose tissue, where they promote triacylglycerol storage in the neutral core of lipid droplets (Paul et al., 2010). Perilipin 2 is the main perilipin present in non-adipose tissue, where it constituently binds the coat of lipid droplets. Conversely, perilipin 3 appears both in the lipid droplet phospholipid monolayer and the cytosol. It has been observed that increased expression of perilipin 2 induces triacylglycerol accumulation (Imamura et al., 2002; Xu et al., 2005). In perilipin 2-null mice, lipid droplets appear coated by perilipin 3, which exerts a functional compensation (Sztalryd et al., 2006). The absence of both perilipins leads to an increase in basal lipolysis, which is associated with a higher localization of ATGL to lipid droplets (Bell et al., 2008). Consistently, overexpression of both perilipins reduces ATGL presence in lipid droplets (Wang et al., 2011; Listenberger et al., 2007), suggesting that perilipins 2 and 3 regulate lipolysis by protecting the neutral lipid core from cytosolic lipases. The mechanism by which perilipins 2 and 3 limit the access of ATGL to lipid droplets is unclear, but it has been proposed that their binding might crowd together the phospholipid monolayer of lipid droplets, denying access to other proteins that rely on hydrophobic interactions with the neutral lipid core (Listenberger et al., 2007).

2.2.2 Perilipin 5 recruits ATGL and CGI-58 to the lipid droplet coat

Perilipin 5 was the last identified member of the perilipin family. It is preferentially expressed in highly oxidative tissues, such as brown adipose tissue, skeletal muscle and heart. Similar to perilipins 2 and 3, perilipin 5 has been observed to promote triacylglycerol accumulation (Dalen et al., 2007). In liver, fasting-induced activation of the transcription factor PPARα triggers perilipin 5 expression and localization to lipid droplets (Wolins et al., 2006).

It has been proposed that perilipin 5 exerts a negative regulatory role in lipid droplet hydrolysis, by binding and inhibiting ATGL at the lipid droplet surface under basal conditions. The ability of perilipin 5 to directly bind ATGL, which has been observed by independent groups (Wang et al., 2011; Granneman et al., 2011) is unique amongst the perilipin family of lipid droplet proteins. A study performed by Wang and colleagues analyzed the consequences of ectopic expression of perilipin 5 in AML12 cells (which contain endogenous ATGL, but not perilipin 5). The presence of perilipin 5 triggered the localization of ATGL to the lipid droplet coat and dramatically decreased basal lipolysis. Interestingly, stimulation of PKA induced perilipin 5 phosphorylation and a modest (two-fold) increase in lipolysis (Wang et al., 2011).

Perilipin 5 further regulates ATGL activity by binding its co-activator CGI-58 and recruiting it to the lipid droplet coat. Thus, through its ability to bind both proteins, perilipin 5 likely has a role in coordinating the interaction between ATGL and CGI-58 (Granneman et al., 2011).

The strong inhibition of basal lipolysis exerted by perilipin 5, as well as the modest increase triggered by its phosphorylation, has led to hypothesize that perilipin 5 might play a role in protecting mitochondria from a rapid influx of fatty acids during lipolysis in highly oxidative tissues (Wang et al., 2011). In keeping with this idea, perilipin 5-null mice exhibit enhanced mitochondrial oxidation of fatty acids in the heart, which leads to increased production of reactive oxygen species and eventual decline of the heart function (Kuramoto et al., 2012). Since ATGL-mediated triacylglycerol hydrolysis is known to induce PPARα signaling (Kratky et al., 2014), which in turn promotes perilipin 5 expression (Wolins et al., 2006; Yamaguchi et al., 2006), this mechanism could be a form of negative feedback aimed at controlling the rate of fatty acid release.

3. **Activation of fatty acids generated by lipolysis**

Lipolysis, whether performed by cytosolic lipases or through lipophagy, results in the release of free fatty acids, which are essential substrates for energy production and lipid synthesis. Thus, fatty acids hydrolyzed from lipid droplet triacylglycerols are subsequently used to fuel β-oxidation in mitochondria or to synthesize membrane lipids and lipid intermediates involved in cellular signaling (Beller et al., 2010). Occasionally, newly released fatty acids are re-esterified into triacylglycerol (Edens et al., 1990). In any case, all pathways of fatty acid metabolism require the acyl-coenzyme A synthetase (ACS)–mediated conversion of fatty acids to acyl-CoAs.

Recent findings have revealed the existence of 26 distinct ACS genes in the human genome, which can be divided into five sub-families based on the chain length of their preferred fatty acid substrates (Watkins et al., 2007; Lopes-Marques et al., 2013). The variety of ACS enzymes has led to hypothesize that they each play a unique role, directing their acyl-CoA product to specific metabolic fates (Watkins et al., 2007; Li et al., 2009).

3.1 Long chain Acyl Coenzyme A Synthetases (ACSL)

ACSL is the sub-family of ACS enzymes which activate fatty acids with chain lengths of 12 to 20 carbon atoms (Ellis et al., 2010). The five ACSL genes are annotated as members 1, 3, 4, 5, and 6 (ACSL1 to ACSL6), and all are represented by many spliced transcript variants. The cDNAs of ACSL2 were found to correspond to the same gene as ACSL1; consequently, ACSL2 was deleted from the databases (Soupene and Kuypers, 2008).

ACSL isoenzymes are intrinsic membrane proteins whose active sites face the cytosol. Their acyl-CoA products are either partitioned into the facing membrane monolayer, where they can encounter downstream metabolic enzymes (Coleman and Bell, 1978), or transported to different organelles by the cytosolic acyl-CoA binding protein (Stremmel et al., 2001).

Of the 5 isoforms of ACSL, three of them (ACSL1, 3 and 4) have been found in association with lipid droplets (reviewed by Mashek et al., 2010), and their competitive inhibitor Triacsin C has been reported to block neutral lipid synthesis and lipid droplet formation as a response to an external lipid influx (Igal et al., 1997; Namatame et al., 1999 Ujimoto et al., 2006; Fujimoto et al., 2007; Liefhebber et al., 2014). In fact, Triacsin C is considered to be a potent inhibitor of lipid droplet biogenesis (Zou et al., 2014).

4. **Mitochondrial β-oxidation of fatty acids**

Relative to their mass, fatty acids are the most efficient molecules in terms of ATP generation, through the pathways of mitochondrial β-oxidation and oxidative phosphorylation (Da Poian et al., 2010).

Upon their release from lipid droplet triacylglycerol, long-chain fatty acids are activated by ACSL as described above, forming acyl-CoA. However, the inner membrane of mitochondria is not permeable to long-chain acyl-CoA. Carnitine-palmitoyl transferase (CPT1), an enzyme

located in the outer membrane of mitochondria, catalyzes the conversion of long-chain acyl-CoA to acylcarnitine, which is subsequently shuttled into the mitochondria and converted back to acyl-CoA for its catabolism via β-oxidation (Lapaschuck et al., 2010) (Figure 10).

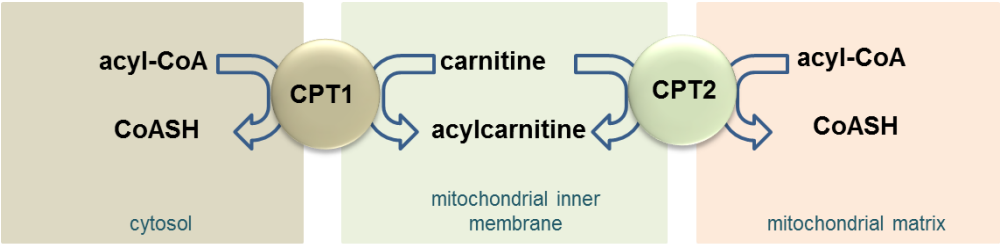

***Figure 10*.The access of long-chain acyl-CoA to the mitochondria is regulated by CPT1.**

CPT1 catalyzes the conversion of acyl-CoA to acylcarnitine, and shuttles the entrance of long-chain fatty acids into the mitochondria. Once there, acylcarnitine is converted back to acyl-CoA for its catabolism via β-oxidation.

The β-oxidation of activated fatty acids is catalyzed by the sequential action of four enzyme families (acyl-CoA dehydrogenase, enoyl-CoA hydratase, β-hydroxyacyl-CoA dehydrogenase and acyl-CoA acetyltransferase). The end product of each cycle of β-oxidation is acetyl-CoA, shortening the long-chain fatty acid by two carbons (Figure 11). Acetyl-CoA then enters the tricarboxylic acid cycle, rendering NADH and $FADH_2$, and leading to ATP synthesis via oxidative phosphorylation in the mitochondrial respiratory chain (Aon et al., 2014)

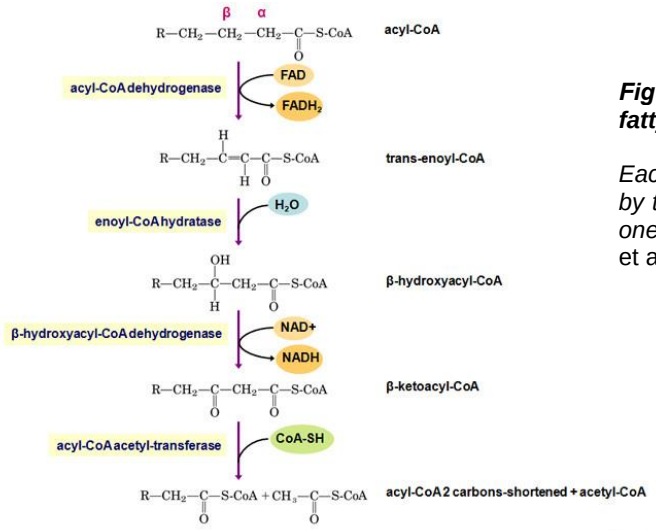

Figure 11: Cycle of mitochondrial β-oxidation of fatty acids.

Each repetition of the cycle shortens the acyl-CoA by two carbons. The cycle is repeated until the last one yields two molecules of acetyl-CoA (Da Poian et al., 2010)

CHAPTER 3: LIPID DROPLETS IN DISEASE

Some of the most prevalent diseases in the western society are associated with an alteration in the size, number or regulation of lipid droplets, making them an appealing new therapeutic target.

1. Type 2 diabetes

In humans, the ability of the adipose tissue to sequester free fatty acids into triacylglycerol and store them into lipid droplets highly correlates with whole-body insulin sensitivity (Puri et al., 2008). The presence of circulating free fatty acids and other bioactive lipids, which is observed in obesity and lipoatrophy, interferes with insulin signaling pathways and dose-dependently decreases glucose uptake in muscle (Boden et al., 1994). Consistently, genetically modified “fatless” mice, which are devoid of adipocytes, can be protected from insulin resistance by transplantation of adipose tissue (Lewis et al., 2002).

Further evidence of the implication of lipid droplets in type 2 diabetes was presented by Boström *et al* (Boström et al., 2007)**.** They showed that, in the presence of free circulating fatty acids, muscle and liver cells increased the number and size of intracellular lipid droplets. SNAP-23, a protein required for lipid droplet fusion, did not increase its expression, but relocated to cytosolic and lipid droplet-associated pools, decreasing the plasma membrane pool to 50%. This had functional consequences for glucose uptake, since SNAP-23 is necessary at the plasma membrane for the fusion of glucose transporter (Glut4)-containing secretory vessels which is triggered by insulin (Söllner, 2007).

2. Hepatitis C

The life cycle of the Hepatitis C Virus (HCV) is tightly associated with the lipid metabolism of liver cells, and lipid droplets play a central role in HCV propagation (Harris et al., 2011; Bose and Ray, 2014; Alonzi et al., 2004). The viral protein core contains a lipid droplet-binding domain, and its localization to lipid droplets is crucial for successful viral assembly (Herker and Ott, 2011). In cultured hepatoma cells, core was seen to localize to lipid droplets and progressively coat them, displacing perilipin 2 until it was below detectable levels. This

substitution of perilipin 2 with core resulted in the transport of lipid droplets towards the microtubule organizing center (Boulant et al., 2008), which is in close proximity to the HCV replication sites (Alvisi et al., 2011). The viral protein NS5A, which bridges viral RNA replication and virion assembly, colocalizes with core on lipid droplets, and mutations that disrupt this colocalization lead to impaired virion assembly (Herker and Ott, 2011).

3, Parkinson's disease

α-Synuclein is one of the main components of Lewy bodies and Lewy neurites, the fibrillary lesions that are the pathologic hallmark of Parkinson's disease. Studies performed in cell lines and primary neuronal cultures showed that wild type α-synuclein associated with lipid droplets and was able to regulate triacylglycerol turnover. However, point mutants of α-synuclein were only partially targeted to lipid droplets and showed less efficiency in protecting core triacylglycerol from lipolysis (Cole et al., 2002). Wild type α-synuclein formed oligomers upon associating with lipid droplets, leading to the suggestion that the conformational changes induced by lipid droplet binding promoted oligomerization of α-synuclein, providing nuclei to seed the formation of synuclein aggregates (Cole et al., 2002). Consistently, a correlation between increased lipid droplet content and synuclein oligomerization has recently been reported in 3D5 cells overexpressing α-synuclein (Jiang et al., 2014).

4. Cancer

Lipid droplets are the source of nuclear magnetic resonance (NMR)-visible lipids (Gujar et al., 2005), and their appearance in tumors is commonly used to monitor malignancy, metastasis and response to treatment (Hakumäki and Kauppinen, 2000).

It has been observed that lipid droplets accumulate in cultured cells as a response to external stimuli such as those present in the tumor microenvironment, such as acidic pH or nutrient deprivation (Delikatny et al., 1996); as well as in tumors in vivo, as a response to drugs or radiation therapy (Milkevitch et al., 2005; Lee et al., 2010), or in situations of hypoxia or acidic pH (Freitas et al., 1990, 1996; Zoula et al., 2003; Milkevitch et al., 2005; Jiang et al., 2012) Recently, high levels of NMR-visible lipid droplets have been identified as a distinctive marker of cancer stem cells in colorectal cancer, and xenotransplantation

experiments demonstrate that colorectal cancer stem cells overexpressing lipid droplets retain most tumorigenic potential (Tirinato et al., 2014).

These observations have led to hypothesize that lipid droplet synthesis might be triggered in tumors as a response to stressors, and might embody an attempt of cancer cells to adapt themselves to the tumor microenvironment (Delikatny et al., 2011). Given the fact that metabolic adaptations are central to the biology of cancer cells (Kim and Dang, 2006; Vander Heiden et al., 2009), the biogenesis of lipid droplets triggered by the stressors of the tumor microenvironment might offer a selective advantage, by providing fatty acids for ATP generation through mitochondrial oxidation.

OBJECTIVES

The global objective of this thesis is to understand the biology of lipid droplets induced by stress. This general objective can be divided into four more specific ones:

- To address the hypothesis that lipid droplet biogenesis induced by stress is a cell survival strategy

- To study the mechanisms whereby stress-triggered lipid droplets exert their protection

- To dissect as much as possible the mechanisms governing stress-triggered lipid droplet formation and mobilization

- To identify possible differences in the biology of lipid droplets when they are triggered by lipid availability, or stress due to complete nutrient deprivation

EXPERIMENTAL PROCEDURES

1. Materials

[9,10^{3}H(N)]-palmitic acid (60 Ci/mmol) was purchased from American Radiolabeled Chemicals, Inc. Dowex 1x2-400 anion exchange resine was from Sigma. Lipofectamine™ RNAiMAX Transfection Reagent was from Invitrogen. $cPLA_2$ α inhibitor pyrrolidine-2 (py-2, catalog number 525143) was from Calbiochem; CPT-1 inhibitor etomoxir (EX) and autophagy inhibitor 3-methyladenine (3-MA) were from Sigma. Rabbit anti- $cPLA_2α$ and anti-phospho-Ser^{505} $cPLA_2α$ antibodies were from Cell Signaling; rabbit anti-perilipin 2, rabbit anti perilipin 3 and rabbit anti-LC3B were from abcam; rabbit anti-CPT-1 was from abcam, and mouse anti-β-actin was from Sigma. Sodium oleate, primuline and Nile red were from Sigma; 4,4-difluoro-5-methyl-4-bora-3*a*,4*a*-diaza-*s*-indacene-3-dodecanoic acid (C_1-BODIPY® 500/510-C_{12}) and LysoTracker® Red DND-99 were from Molecular Probes, and Oil Red O and propidium iodide (PI) were from Sigma.

2. Cells

Human glioblastoma LN18 cells, primary astrocytes from rat cerebral cortex, HeLa cells and MEF cells (wild type and Atg5 KO) were cultured in Dulbecco's modified Eagle's medium (Sigma), containing 10% fetal bovine serum (FBS, Sigma), 100 units/ml penicillin (Invitrogen), and 100 µg/ml streptomycin (Invitrogen). CHO-K1 cells were cultured in Ham's F12 medium (Sigma), containing 7.5% FBS, 100 units/ml penicillin and 100 µg/ml streptomycin. Cell passages were made once a week by trypsinization (Sigma).

3. Fluorescence microscopy

Cells cultured on glass bottom culture dishes were washed with phosphate-buffered saline (PBS, Sigma), fixed with 3% paraformaldehyde (Sigma) for 10 min, and washed twice with PBS. For Nile red staining of LD, cells were overlaid with 0.5 ml of PBS, to which 1 µl of a stock solution of Nile red in acetone (0.2 mg/ml) was added. For C_1-BODIPY® 500/510-C_{12} staining of LD, cells were overlaid with 0.5 ml PBS, to which 5 µl of a stock solution of 1 mg C_1-BODIPY® 500/510-C_{12} in 1 ml 98% ethanol (3.8 mM) were added. For Oil Red O staining of LD, a working solution of Oil Red O was made with 6 parts of Oil Red O stock solution (5 mg Oil Red O per mL of 60% triethylphosphate) and 4 parts of deionized water. The working

solution was then filtered through a 0.2 µm filter to remove cyrstallized Oil Red O. Cells were overlaid with 0.5 µl of Oil Red O working solution and kept for 1 hour in the dark. Coverslips were mounted with 10% glycerol in PBS and sealed with nail polish. For lysosome labeling, unfixed cells were overlaid with pre-warmed culture medium or buffer, containing 0.0375 µl/ml of LysoTracker® Red DND-99 stock solution (1 mM in anhydrous DMSO). The final concentration of LysoTracker® Red DND-99 was of 75 nM. Cells were incubated for 30 minutes at 37ºC and 4% CO_2 and then washed with PBS and fixed with 3% paraformaldehyde. Samples were kept in the dark until photographed in a Leica Qwin 500 microscope with a Leica DFC500 camera, using the Leica DCviewer 3.2.0.0 software. Analysis of photomicrographs was performed with ImageJ 1.38x public software (Wayne Rasband, National Institutes of Health; rsb.info.nih.gov)

4. Electron microscopy

Cells were rinsed twice with 0.1 M phosphate-buffered saline (PBS), pH 7.4, and fixed with PBS containing 2.5% (v/v) glutaraldehyde and 2% (v/v) paraformaldehyde for 2 h at 4 °C. After four 10-min washes in PBS, cells were postfixed with 1% osmium tetroxide in PBS for 2 h at 4 °C, washed in PBS, dehydrated through an ascending series of acetone concentrations up to 100%, and included in EPON resin. Micrographs were taken with a JEOL JEM-2011 electron microscope equipped with a CCD GATAN 794 MSC 600HP camera.

5. Flow cytometry

Indirect quantification of Nile red-stained LD by flow cytometry was performed as described by Gubern et al (cita). Briefly, harvested cells were transferred to a 15 ml falcon, as well as their overlaying medium or buffer, to prevent the loss of floating dead cells. After two PBS washes, they were resuspended in 0.5 ml PBS containing 0.2 µg/ml of the Nile red stock solution. Samples were kept at least 45 min in the dark to attain equilibrium with the dye. Analysis was carried out with a Cytomics FC 500 (Beckman Coulter) equipped with an argon laser (488 nm), in the FL1 channel (505–545 nm), with the photomultiplier set at 600 V and a

gain value of 1. After gating out cellular debris, 10000-30000 events were taken. For each assay, we obtained a Forward/Side Scatter plot (FS/SS plot), a bidimensional representation of each event in terms of size (FS) and structural complexity (SS). Each sample appeared divided into two populations, which differed in FS value (size). Staining with propidium iodide evidenced that the population with a lower FS value (smaller cells) was composed of dead cells. This shift of dead cells to lower FS values allowed us to separately study LD content in viable and dead cells, even though Nile red's emission spectrum does not allow co-staining with PI. Alternatively, cells were stained with PI and C_1-BODIPY® 500/510-C_{12}. After treatment, cells were processed as described above, and resuspended in 0.5 PBS containing 2.5 µl of the C_1-BODIPY® 500/510-C_{12} stock solution and 2.5 µl of the PI stock solution. Samples were kept in the dark at 4ºC for 20 minutes before carrying out the analysis, in the FL1 (405 nm) and the FL3 channels (610 nm).

6. β-oxidation analysis

Serum-starved cells, seeded in 24-well plates, were labeled overnight with 1 µCi/ml [^{3}H]palmitic acid in culture medium supplemented with 0.5% delipidated bovine serum albumine (BSA, Sigma). After labeling, cells were washed once with BSA-containing culture medium and twice with PBS, and left for 30 minutes in serum-free culture medium, to make sure cells were devoid of LD before treatment. □-oxidation was monitored through the generation of [^{3}H]-water. After treatment, the medium or buffer overlaying each sample was transferred to a polypropilene tube containing 1 ml of Dowex 1x2-400 anionic exchange resine (1:2 in distilled water). Tubes were vigorously shaken and centrifuged for 10 minutes at 1000 rpm. Any radioactive metabolic intermediate other than [^{3}H]-water was trapped by the resine, and 500 µl of the overlaying [^{3}H]-water were transferred to vials and counted for radiactivity.

7. Quantification of [^{3}H]-lipids

Cells seeded in 24-well plates were labeled overnight with 1 µCi/ml [^{3}H]palmitic acid, washed and treated as explained above. After treatment, lipids were extracted as described. To separate the major lipid species, 0.2-ml aliquots of the chloroform phases were evaporated under vacuum, resuspended in 15 µl of chloroform/methanol (3:1, v/v), and spotted onto Silica Gel G thin layer chromatography plates (Merck), which were developed in

hexane/diethyl ether/acetic acid (70: 30:1, v/v), and stained with primuline spray (5 mg of primuline in 100 ml of acetone/water (80:20, v/v)). Identification of phospholipids, TAG, and cholesteryl esters was made by co-migration with authentic standards. Quantification of radioactive lipids was done by scraping into vials the silica gel from regions corresponding to migration of the standards.

8. Immunoblots

Cells were lysed with 62.5 mm Tris-HCl buffer, pH 6.8, containing 2% SDS, 10% glycerol, 50 mm dithiothreitol, and 0.01% bromphenol blue, and around 20 µg of protein were separated by standard 8%, 10% or 15% SDS-PAGE and transferred to nitrocellulose membranes. Primary (1:1,000) and secondary antibodies (1:5,000) were diluted in 25 mm Tris-HCl buffer, pH 7.4, containing 140 mm NaCl, 0.5% defatted dry milk or bovine serum albumine (depending on each antibody's manufacturer's advice) and 0.1% Tween 20. Membranes were developed using ECL detection reagents from Amersham Biosciences

9. *siRNA transfection*

A pre-designed siRNA (sense and antisense PLA2G4A2-(2424), Gene Link) directed against human cPLA2α was used. Cells were transfected at 60% confluence by adding to each 35-mm culture well 1 ml of Opti-MEM (Invitrogen) containing 1.5 µl of the stock siRNA solution (20 µm) and 5 µl of Lipofectamine™ RNAiMAX Transfection Reagent (1 mg/ml). After 5 h, 1 ml of Ham's F-12 medium containing 7.5% FBS was added, and the cells were incubated for 48 h and then changed to serum-free medium during 24 h prior to treatment.

10. Statistical analysis

Data analysis was carried out with Prism software (GraphPad). Values are expressed as mean ± S.E.M. Significant differences between mean values were determined by applying the unpaired Student's one-tailed t-test. Differences between groups were considered significant if $P<0.05$.

RESULTS

1. Flow cytometry as a tool to monitor lipid droplet occurrence and cell death

The aim of this work was to study the physiological role of lipid droplet biogenesis induced by stress, and to determine possible functional or regulatory differences in the biology of lipid droplets when they are induced by stress or an external lipid source.

In order to address these objectives, we needed a reliable way to assess cell viability and lipid droplet occurrence in response to different treatments, and we found that flow cytometry was an ideal tool, since it allowed us to measure both parameters in the same sample.

Flow cytometry is a technology that simultaneously measures and then analyzes multiple physical characteristics of single particles, usually cells, as they flow in a fluid stream through a beam of light. The properties measured include a particle's relative size, relative granularity or internal complexity, and relative fluorescence intensity. These characteristics are determined using an optical-to-electronic coupling system that records how the cell or particle scatters incident laser light and emits fluorescence (BD Biosciences, 2000).

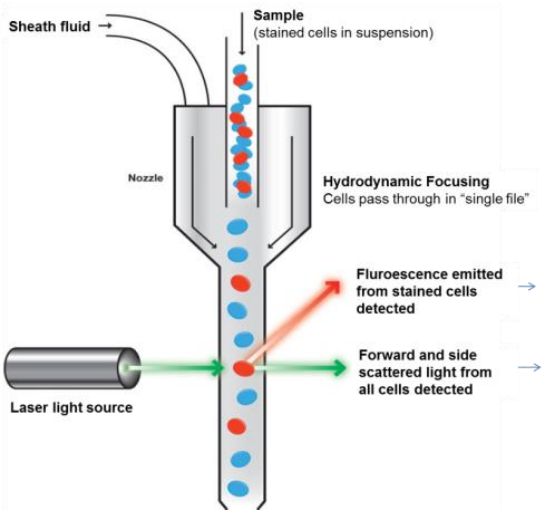

***Figure 12*: Structure of a flow cytometer**

When a stained cell sample in suspension buffer is run through the cytometer, it is hydrodynamically focused, using sheath fluid, through a very small nozzle. The stream of fluid takes the cells past the laser light one cell at a time. There are a number of detectors to detect the light scattered from the cells/particles as they go through the beam. There is one in front of the light beam (Forward Scatter or FS) and several to the side (Side Scatter or SS). Fluorescent detectors are used for the detection of fluorescence emitted from positively stained cells/particles (Flow cytometry guide, abcam).

Flow cytometry of cells stained with Nile red has proved to be a very effective way to indirectly quantify lipid droplets. Nile red is a lipophilic dye widely used in the study of lipid droplets, with an emission spectrum that shifts to shorter wavelengths in hydrophobic environments. When Nile red-stained cells are examined at wavelengths of 580 nm or less, the fluorescence of the prove in the extremely hydrophobic environment of the droplets is maximized, whereas that of cellular membranes is minimized (Greenspan et al., 1985).

Indirect quantification of lipid droplets by flow cytometry has shown a very strong correlation with image analysis of photomicrographs (Gubern et al., 2008), and it provides the advantage of allowing a very fast and reproducible assessment of overall lipid droplet occurrence in a high number of cells.

Figure 13 depicts the correlation between lipid droplet occurrence and the distribution of Nile red fluorescence in the FL1 channel. CHO-K1 cells were cultured in complete F12-Ham's culture medium and switched to fetal bovine serum- (FBS)-free medium overnight. Serum starvation was used to set a control condition in which lipid droplet occurrence was minimal (Kassan et al., 2013; Gubern et al., 2008). Then, lipid droplet biogenesis was induced by treatment with FBS, or FBS supplemented with 100 µM sodium oleate. After the treatment, cells were stained with Nile red and analyzed by fluorescence microscopy or flow cytometry. As expected, serum starvation completely depleted lipid droplets (Figure 13A, left panel), which appeared in response to treatment with FBS (Figure 13A, central panel) or FBS + 100 µM sodium oleate (Figure 13A, right panel). Visual inspection of photomicrographs evidenced that the addition of sodium oleate greatly enhanced lipid droplet occurrence as compared to FBS alone. This increase could be indirectly quantified by flow cytometry analysis of Nile red-stained cells. Panel B shows the fluorescence distribution in FL1 of 15000 events for each treatment. The presence of Nile-red stained lipid droplets leads to an increase of the fluorescence median, which can be used to indirectly quantify lipid droplets (Figure 13, panel C). In this work, all the results regarding lipid droplet quantification are expressed as the increase of the fluorescence median in FL1 over control, which is the fluorescence median of serum-starved cells stained with Nile-red.

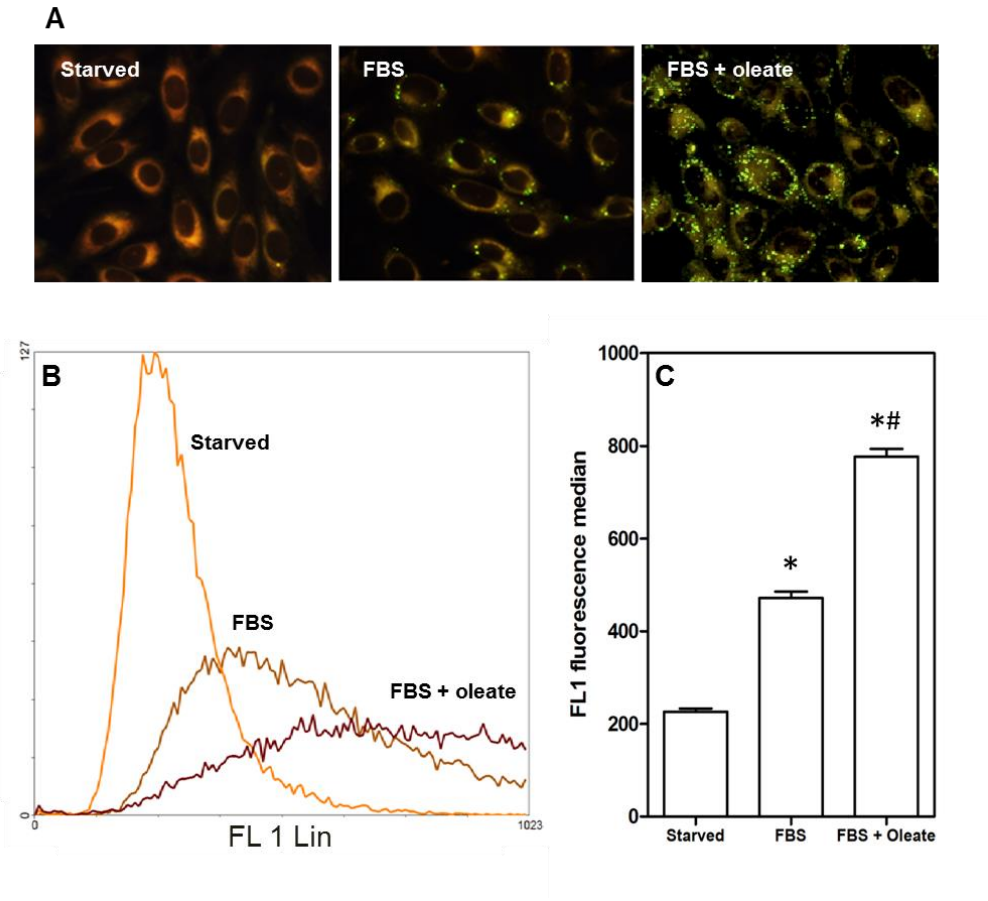

Figure 13. Flow cytometry of Nile red-stained cells allows the indirect quantification of lipid droplets.

*Panel A shows photomicrographs of Nile red-stained CHO K1 cells treated with serum-free culture medium (left panel), or culture medium with FBS alone (middle panel), or in combination with 100 µM sodium oleate (right panel). Whereas serum-starved cells are devoid of lipid droplets, cells kept in FBS with or without oleate contain them, and simple visual inspection confirms that the presence of oleate increases lipid droplet occurrence. This increase can be indirectly quantified by flow cytometry. Panel B shows the distribution of 15000 events for each condition in the FL1 channel. Fluorescence intensities, quantified as the median value of each event distribution, are represented in panel C, which shows the median ± SEM of three independent experiments. *p<0.0001 compared to control in the absence of FBS; $^{\#}$p<0.0001 compared to FBS alone.*

Although Nile red is an ideal probe for the detection of lipid droplets, it has a major drawback for costaining studies. As mentioned before, Nile red exhibits high affinity for lipids, as well as sensitivity to the degree of hydrophobicity of lipids. The latter feature results in a shift of the emission spectrum from red to yellow, in the presence of polar and non-polar lipids, respectively (Diaz et al., 2008). Figure 14 is a representative example of Nile red-stained CHO K1 cells examined by fluorescence microscopy at increasing wavelengths. Lipid droplets, which are composed mainly of triacylglycerol, are stained in yellow (panel A) and

green (panel B), whereas cytoplasmic membranes, composed mostly of phospholipids, are stained in red (panel C). This characteristic of the dye hinders the possibility of costaining with other green or red fluorescence probes, making it difficult to monitor lipid droplet occurrence and cell survival in the same sample.

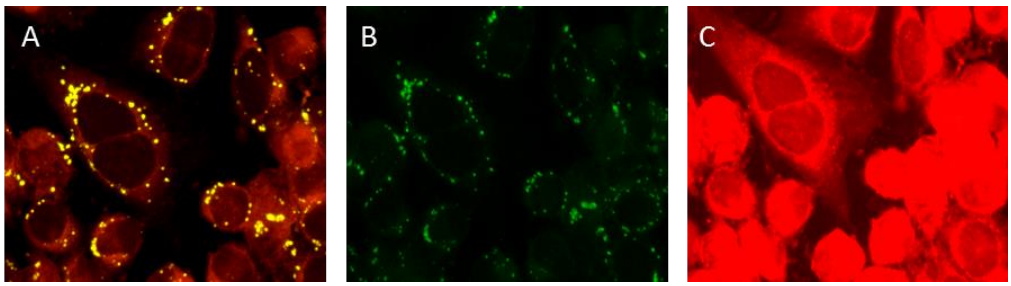

***Figure 14:* Nile red has a wide emission spectrum, which shifts to shorter wavelengths in highly hydrophobic environments.**

CHO K1 cells were maintained in complete F12 Ham's culture medium supplemented with FBS, stained with Nile red and analyzed by fluorescence microscopy using different emission filters with increasing wavelengths. When excited, the fluorescence of Nile red interacting with the highly hydrophobic lipid droplets was maximized, allowing the specific marking of lipid droplets. However, Nile red in less hydrophobic environments, like membrane leaflets, could also be observed at longer wavelengths, eventually losing its selectivity for lipid droplets. Nile red could be viewed for yellow-gold fluorescence (A), green fluorescence (B) or red fluorescence (C).

Propidium iodide (PI) staining is the most common way to quantify cell death by flow cytometry. PI is a red fluorescent molecule that binds nucleic acids. It is membrane-impermeant, so, in the absence of a permeabilizing treatiment, it can only penetrate cells with compromised membrane integrity. Loss of membrane integrity is a very direct evidence of cell death, which makes PI staining a widely used method to evaluate viability (Ross et al., 1989; Lecoeur, 2002).

Figure 15 shows the results of a representative experiment in which CHO K1 cells were maintained in serum-free DMEM for 24 hours, harvested and stained with PI. Panel A is a Forward/Side Scatter plot, which represents the distribution of 15000 cells in terms of size (Forward Scatter, FS) and structural complexity (Side Scatter, SS). Panel B shows the distribution of PI fluorescence in the same sample. Since PI is only able to penetrate dead cells, viability can be measured as the percentage of cells able to exclude PI (depicted as the black peak in Figure 15, panel B). The red fluorescence emitted by PI-permeant dead cells

allows us to recognize the different phases of the cell cycle, as represented by the red peak in panel B.

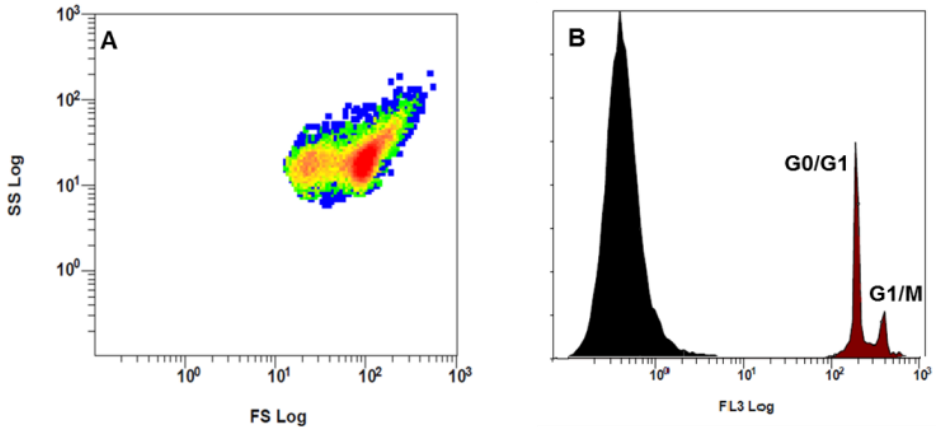

,

***Figure 15:* Flow cytometry analysis of PI-stained cells.**

Serum-deprived CHO K1 cells were harvested and stained with PI, and flow cytometry was used to analyze cell size (FS) and structural complexity (SS) (A), and PI fluorescence emission (B). Viability was measured as the percentage of cells able to exclude PI (black peak, panel B). Dead cells emitted PI fluorescence (red peak, panel B).

Interestingly, the Forward/Side Scatter plot revealed that cells were distributed into two distinct populations, characterized by a different size (FS value) (Figure 16, panel A). Since loss of cell volume is a universal characteristic of programmed cell death (Trump et al., 1997; Bortner and Cidlowski, 2002; Friis et al., 2005), we hypothesized that the population characterized by a lower FS value was composed of dead cells. In order to test our hypothesis, we gated each population separately and analyzed their respective PI fluorescence emissions (Figure 16). As we expected, the population composed of bigger cells was viable, and therefore able to exclude PI. The population composed of smaller cells was responsible for the PI emission of the sample.

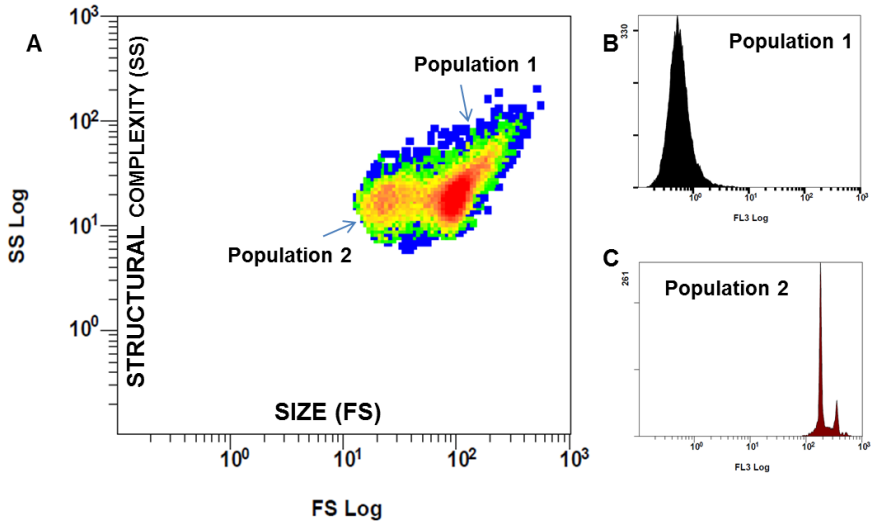

<u>Figure 16.</u> PI fluorescence emission is restricted to the population composed of smaller cells (lower FS value)

The FS/SS plot revealed that cells are distributed into two populations with different FS values (A). Gating each population separately allowed us to determine that the population composed by bigger cells was able to exclude PI (B), whereas the population composed by smaller cells emitted PI fluorescence (C).

We found a consistent correlation between cell shrinkage and PI permeability in all cell types tested. Figure 17 is a representative example of experiments performed on human glioblastoma LN18 cells. After 24 hours of serum starvation, cells were harvested and stained with PI. Flow cytometry analysis revealed that LN18 cells were also distributed into two distinct populations (panel A). A representation of the events in terms of size and PI fluorescence evidenced that only the population with a smaller size was permeable to PI (panel B).

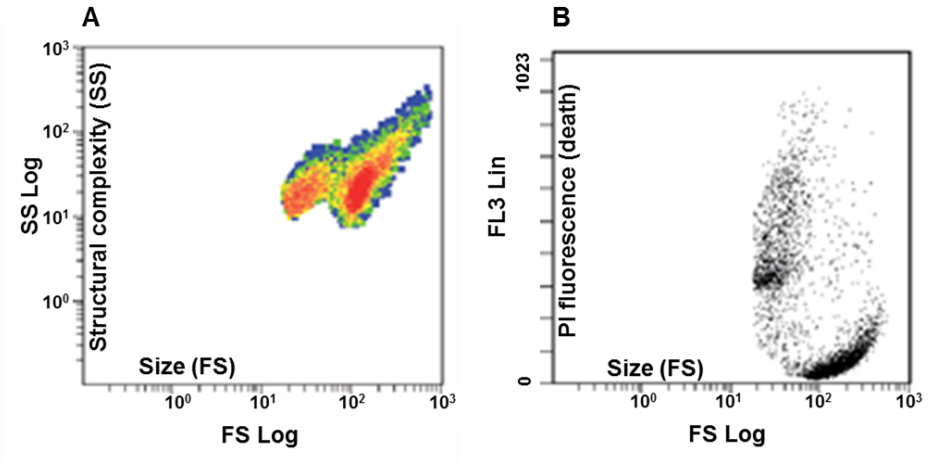

***Figure 17* Flow cytometry can be used to monitor viability by measuring cell shrinkage**

Representative distribution of serum-starved LN18 cells after 24 hours in culture. As seen in panel A, cells appear divided into two distinct populations that differ in FS value. A representation of the same events plotted in terms of size and PI-induced fluorescence shows that only the population composed by smaller cells (lower FS value) is stained by PI. However, the population with a higher FS value is able to exclude the dye (B).

This allowed us to measure viability by flow cytometry as the percentage of cells in the higher FS population, without the need of staining with PI. The possibility of identifying viable and dead cells based on size alone allowed us to quantify both lipid droplet content and viability of Nile-red stained cells in the same sample.

2. Complete nutrient deprivation triggers lipid droplet biogenesis, in a process dependent on cPLA$_2$α activity

To investigate the physiological role of lipid droplet biogenesis induced by stress, we selected complete nutrient deprivation as a model. This decision was motivated by the fact that, of all the types of stress previously tested by our group, complete nutrient deprivation was the strongest in terms of induction of TAG synthesis and lipid droplet formation (Gubern et al., 2009b). Complete nutrient deprivation was accomplished by treating serum-starved cells with Krebs-Henseleit buffer without glucose (KH buffer without glucose).

As a first approach o test the validity of our model, we deprived CHO K1 cells of serum overnight, to ensure lipid droplet depletion, and switched them to KH buffer without glucose. After an 8 hour treatment, cells were stained with Nile red and analyzed by fluorescence

microscopy or flow cytometry to monitor lipid droplet occurrence. Complete nutrient deprivation induced lipid droplet formation (Figure 18, panel A), which was precluded by inhibition of cPLA$_2$α with its specific inhibitor pyrrolidin-2 (py-2) (Figure 18, panel B). This was in keeping with previous results from our group, which had shown that cPLA$_2$α activity is necessary for lipid droplet biogenesis (Gubern et al., 2008, 2009b). Flow cytometry analysis revealed that py-2 dose-dependently blocked the formation of lipid droplets triggered by complete nutrient deprivation (Figure 18, panel B).

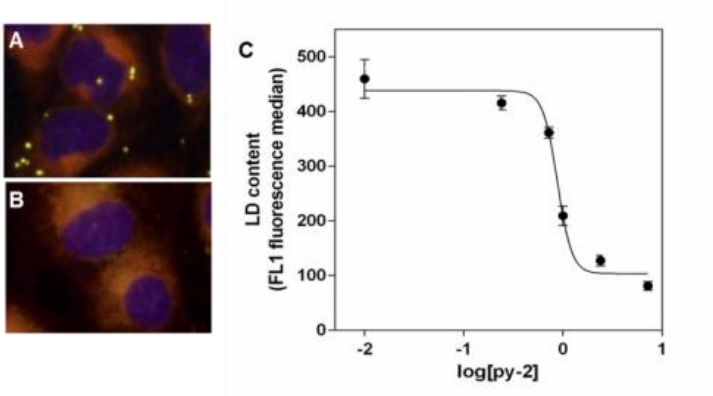

<u>Figure 18.</u> CHO K1 cells treated with KH buffer without glucose synthesize lipid droplets in a manner sensitive to cPLA$_2$α inhibition.
Serum-starved CHO K1 cells were treated with KH buffer without glucose in the absence (A) or presence (B, C) of cPLA$_2$α inhibitor py-2. Complete nutrient deprivation induced the appearance of lipid droplets, which was dose-dependently precluded by py-2.

Alternatively, CHO K1 cells were transfected with siRNA designed against cPLA$_2$α or control siRNA, and deprived of serum overnight. Cells were then switched to KH buffer without glucose, in the presence or absence of py-2, and the occurrence of lipid droplets was monitored by flow cytometry over a 20-hour period (Figure 19). Lipid droplet occurrence reached a maximum at 8-12 hours of treatment and decreased thereafter, and was sensitive to pharmacological inhibition or silenced expression of cPLA$_2$α (Figure 19, panels A and B).

Previous results from our group had shown that phosphorylation of cPLA$_2$α by JNK at Ser505 is required for the activation of the enzyme in situations leading to lipid droplet formation (Gubern et al., 2009a). Consistently, cells kept in KH buffer without glucose exhibited increased phosphorylation of cPLA$_2$α at Ser505, as well as increased expression of perilipin 2 (Figure 19, panel C).

Taken together, these results showed that our selected model of stress led to the formation of lipid droplets in CHO K1 cells, in a manner consistent with previous observations.

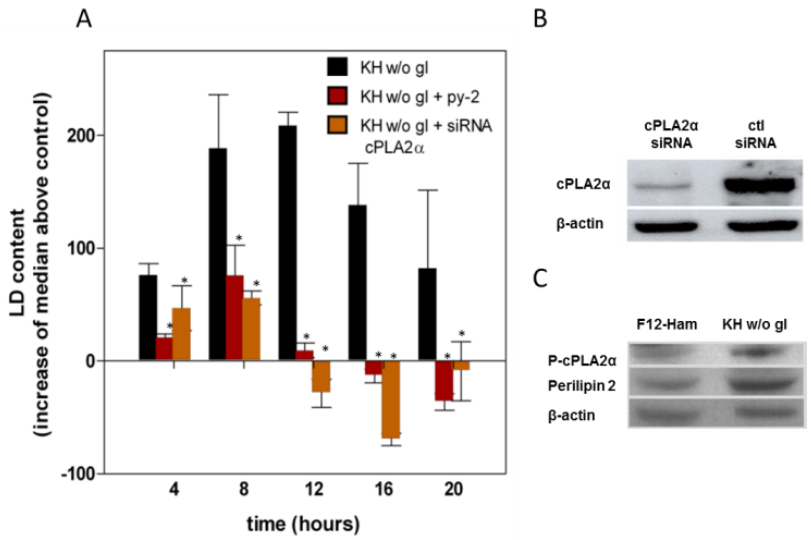

Figure 19. ***Stress triggered by complete nutrient deprivation induces lipid droplet biogenesis in CHO-K1 cells in a cPLA2α-dependent manner****.*

*CHO-K1 cells were transfected with siRNA designed against cPLA2α (gray bars) or with a control siRNA (solid and open bars) and then kept in culture medium without serum for 24 h to deplete LD. Afterward, cells were switched to KH buffer without glucose in the absence (solid and gray bars) or presence of 1 M py-2 (open bars), harvested at the times indicated, and stained with Nile red. The occurrence of LD was assessed by flow cytometry. Intensities in FL1 were quantified as the median values of the event distributions of each condition. Here, LD content is expressed as the increase of the median values above control (cells kept in FBS-free culture medium), and the results are means ± SEM of 3–5 independent experiments carried out with duplicate determinations. C, cells maintained in KH buffer without glucose had increased expression of perilipin 2 and phosphorylation of cPLA$_2$α at Ser^{505}. *, significantly different from KH without glucose.*

Our next step was to establish whether complete nutrient deprivation induced cPLA$_2$α-dependent lipid droplet formation in other cell types. To that purpose, we selected the human HeLa and glioblastoma LN18 cell lines, as well as primary rat astrocytes. Cells were deprived of serum overnight and switched to KH buffer without glucose, in the absence or presence of py-2 (Figure 18). After 16 hours of treatment, the occurrence of lipid droplets was assessed by fluorescence microscopy or flow cytometry. In all cases, KH buffer w/o glucose induced the formation of lipid droplets, which was evident upon visualization of lipophylic-dye stained cells (Figure 14, panels A, C and E) or by the increase in the fluorescence median of Nile red-stained cells (Figure 20, panels G, I and H). In all cell types, lipid droplet formation was abrogated by inhibition of cPLA$_2$α with py-2 (Figure 20, panels B, D, F and G-H).

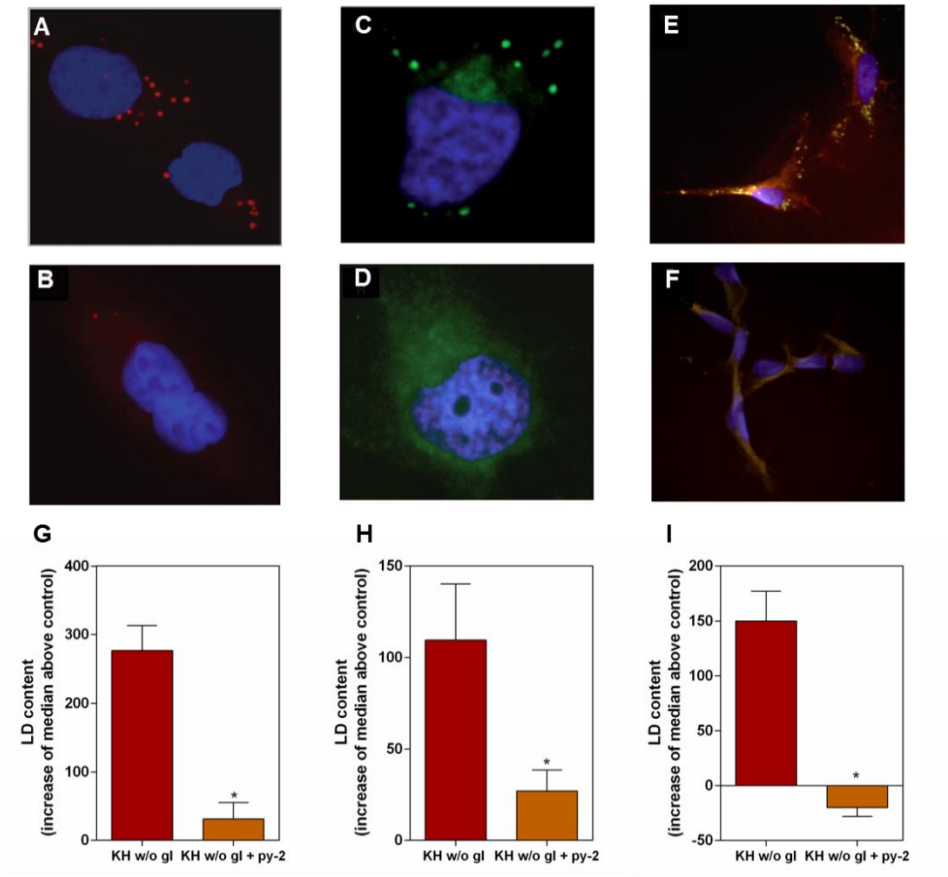

***Figure 20.* Complete nutrient deprivation induces cPLA$_2$α-dependent lipid droplet biogenesis in a variety of cell types.**

*Human glioblastoma LN18 (A,B) and HeLa cells (C,D); and primary rat astrocytes (E,F) were kept in KH buffer without glucose for 16 hours in the absence (top panels) or presence (bottom panels) of 1 μM py-2. Lipid droplets were stained with Oil Red O (A and B), BODIPY 493/503 (C and D) or Nile red (E and F). In all cases, treatment with KH without glucose triggered lipid droplet biogenesis, which was blocked by py-2. Panels G to I show the indirect quantification of lipid droplet occurrence by flow cytometry after a 16 hour treatment with KH buffer without glucose in the absence or presence of py-2. In each experiment, lipid droplet content was quantified as the median of the fluorescence distribution of 15000 events in FL1. Each result is the mean ± SEM of 3 (G and I) or two (H) independent experiments carried out with duplicates. *p<0.0001 compared to KH buffer without glucose.*

As mentioned above, cPLA$_2$α must be activated by phosphorylation at Ser505 to participate in the biogenesis of lipid droplets. This activation is mediated by the SAPK/JNK pathway, in a process that requires upstream generation of ceramide 1-phosphate (C1P) by ceramide kinase (CERK) (Gubern et al., 2009a). To assess whether this mechanism was still relevant when the biogenesis of lipid droplets was triggered by stress, we transfected LN18 cells with siRNA designed against CERK, or a control siRNA, and maintained them in serum-free culture medium before treatment with KH buffer without glucose. After a 16 or 24 hour treatment, cells were harvested and stained with Nile red to quantify lipid droplets by flow

cytometry. Silenced expression of CERK significantly reduced lipid droplet occurrence (Figure 21).

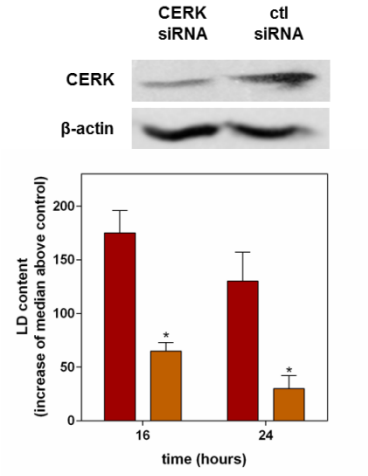

***Figure 21.* Silenced expression of CERK blocks lipid droplet biogenesis induced by complete nutrient deprivation.**

*LN18 cells were transfected with siRNA designed against CERK (open bars) or control (filled bars) and treated with KH buffer without glucose for 16 and 24 hours. Lipid droplet occurrence was assessed by flow cytometry of Nile red- stained cells. Complete nutrient deprivation induced lipid droplet biogenesis, which was precluded by silenced expression of CERK. *, significantly different to control siRNA*

.

The results presented so far show that complete nutrient deprivation induces the biogenesis of lipid droplets in all cell types tested, in a process that requires cPLA$_2$α activity. The consistency of this response argues for a conserved physiological role of lipid droplets in situations of stress. As discussed previously, TAG at the core of stress-induced lipid droplets are synthesized with fatty acids released from membrane phospholipids (Gubern et al., 2009b). TAG synthesis is an energy-consuming process that appears futile in a situation in which cells are committed to die. However, lipid droplets seem to have a protective effect on starving neurons or ischemic cardiac tissue (Du et al., 2009; Lei et al., 2013).

Taken together, these observations lead to hypothesize that lipid droplet biogenesis induced by stress is a cell survival strategy.

3. Inhibition of lipid droplet biogenesis accelerates death of nutrient-deprived cells

In order to test the hypothesis that survival is linked to the ability of cells to generate lipid droplets, we studied the effect of pharmacological inhibition of cPLA$_2$α on the viability of nutrient-deprived cells. Serum-starved LN18 cells were treated with FBS-free culture medium or KH buffer without glucose, in the presence or absence of py-2. After 16 hours of treatment, cells were harvested and stained with PI in the absence of a permeabilizing treatment, to ensure that the probe only penetrated dead cells. Figure 22 shows the results of a representative experiment. Panels A, B and C are FS/SS plots, depicting the distribution

of 10000 cells in terms of size (FS) and structural complexity (SS). Cells treated with serum-free culture medium (panel A) or KH buffer without glucose (panel B) were mostly found on the population with a higher FS value. However, treatment with py-2 caused nutrient-deprived cells to accumulate in the low-FS population (panel C). Panels D, E and F show the distribution of the same samples in terms of size (FS) and PI fluorescence emission (FL3 Lin). In all cases, only the population composed of smaller cells was stained with PI.

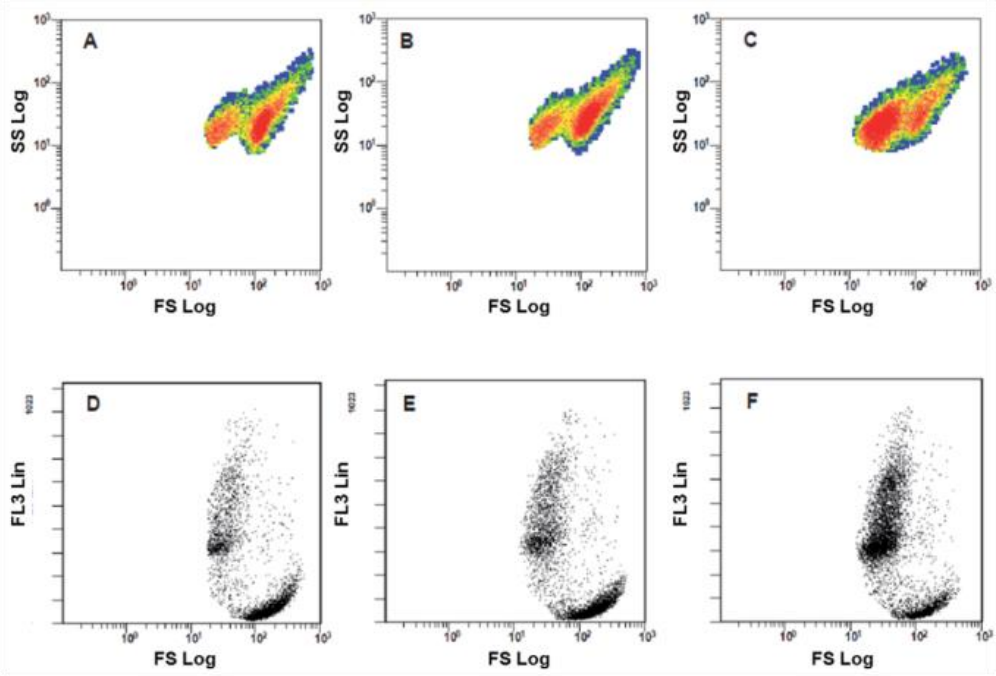

<u>Figure 22</u>. Inhibition of lipid droplet biogenesis with py-2 is toxic for nutrient-deprived cells

LN18 cells were kept for 16 h in DMEM (A and D) or KH without glucose in the absence (B and E) or presence of 1 M py-2, harvested, stained with PI and analyzed by flow cytometry. A–C show the distribution of 10,000 events for each condition in terms of shape (SS) and size (FS). In all cases, events were distribued in two distinct populations, characterized by a different FS value. Cells kept in DMEM (A) and KH without glucose (B) appeared mostly in the population with a higher FS value, whereas those treated with KH without glucose 1 µM py-2 (C) were in the low FS population. D–F show the distribution of the same samples in terms of viability, measured according to the ability of cells to exclude PI, which is expressed as FL3, and size (FS). In all cases, the high FS population excluded PI, as evidenced by the lower FL3 fluorescence. py-2 promoted an increase of the PI-stained population.

Using cell shrinkage as a criterion of cell death, we studied the effect of lipid droplet inhibition over a 24 hour period. Flow cytometry analysis revealed that LN18 cells were able to maintain viability during 24 hours of complete nutrient deprivation. However, the same treatment in the presence of 1 µM py-2 induced cell death after a lag of 8 hours, leaving only approximately 10% viable cells after 24 hours. This contrasted with the complete lack of

toxicity of the cPLA$_2$α inhibitor in control cells maintained in culture medium (Figure 23, panel A).

As an alternative to flow cytometry monitoring of cell shrinkage, we measured the effect of our treatment on lactate dehydrogenase (LDH) release to the medium. Over a time course of 24 hours, treatment with 1 µM py-2 significantly increased the release of LDH in cells maintained in KH buffer without glucose, in a way that strongly mirrored the results obtained by flow cytometry. Again, inhibition of cPLA$_2$α had no toxic effect on cells kept in culture medium (Figure 23, panel B).

We had previously established that silenced expression of CERK had a precluding effect on lipid droplet biogenesis. Using that approach as an alternative to pharmacological inhibition of cPLA$_2$α, we transfected LN18 cells with siRNA designed against CERK or a control siRNA and treated them with KH buffer without glucose or culture medium. Consistently, down-regulation of CERK accelerated death of cells kept in KH buffer without glucose as compared to control siRNA, but had no effect on cells kept in culture medium (Figure 23, panel C).

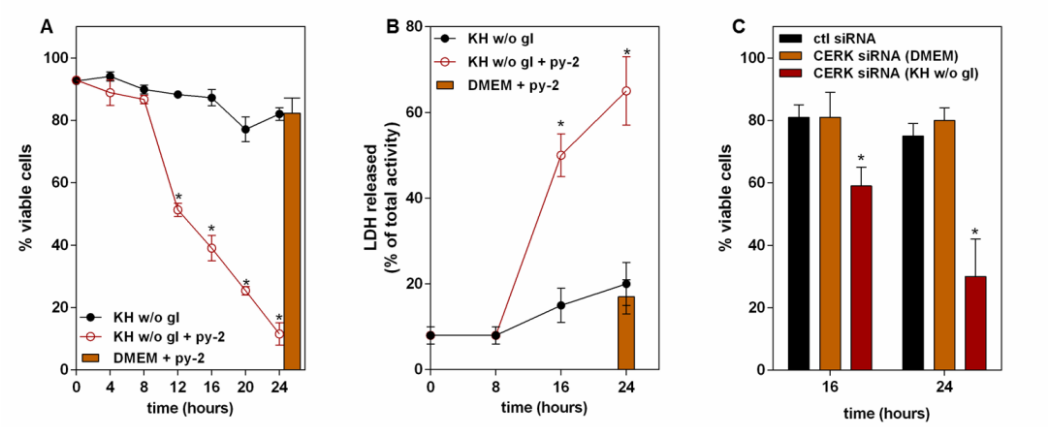

Figure 23*. *Inhibition of lipid droplet formation induces death of nutrient-deprived cells.

*A, LN18 cells were maintained in KH buffer without glucose in the absence (solid symbols) or presence (open symbols) of 1 µM py-2. At the indicated times, cells were harvested, and percentage viability was determined by flow cytometry. Gray bar, viability of cells in DMEM with 1 µM py-2 during 24 h. Inclusion of 1 µM py-2 accelerated the death of nutrient-deprived cells but was not toxic for cells in culture medium. Results are means ± SEM of six independent experiments carried out with duplicate determinations. B, similar results were obtained by determination of LDH activity released to the medium. Results are means SEM. of two independent experiments carried out with quadruplicate determinations. *, significantly different from KH buffer without glucose. C, down-regulation of CERK accelerated death of cells kept in KH buffer without glucose (open bars) as compared with control siRNA (solid bars) but had no effect on cells kept in DMEM (gray bars). Results are means ± SEM of two independent experiments carried out with triplicate determinations. *, significantly different from control siRNA.*

To establish if the correlation between the ability to synthesize lipid droplets and cell survival to starvation was extensive to different cell types, we treated serum-starved human HeLa cells, primary rat astrocytes and hamster CHO-K1 cells with KH buffer without glucose, in the presence or absence of 1 µM py-2. Cell viability was assessed by flow cytometry (Figure 24). Death of starved CHO-K1 and HeLa cells proceeded at a faster pace than that observed in LN18 cells (panels A and B), whereas astrocytes maintained viability longer (panel C). Again, py-2 significantly accelerated death in all cell types under starvation, but it did not affect viability in culture medium.

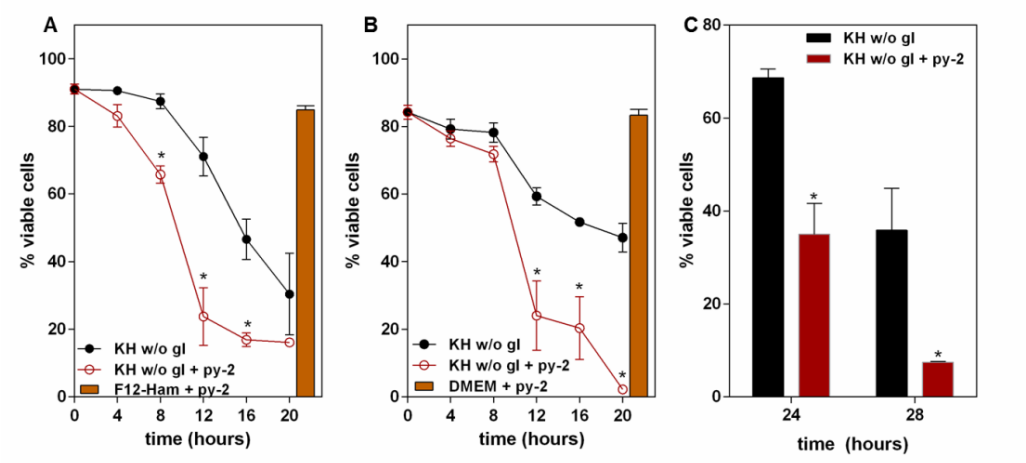

Figure 24. ***Inhibition of lipid droplet biogenesis accelerates death in all cell types tested***

*Hamster CHO cells (A), human HeLa cells (B) and primary rat astrocytes (C) were maintained in FBS-free medium and switched to KH buffer without glucose in the absence (solid symbols) or presence (open symbols) of 1 µM py-2. Inhibition of cPLA2α consistently triggered a significant decrease in cell survival to starvation, but had no effect on cells maintained in culture medium. Results are means ± SEM of 3 (A and B) or two (C) experiments carried out with duplicates. *, significantly different to KH buffer w/o glucose.*

These results show that the ability to form lipid droplets strongly correlates with survival to starvation in all cell types tested. The dramatic effect of $cPLA_2\alpha$ inhibition on nutrient-deprived cells contrasts with the complete lack of toxicity on cells maintained in culture medium.

These findings support our hypothesis that starvation-triggered lipid droplet formation is a cell survival strategy, possibly aimed at supplying catabolic fuel. The bell-shaped profile of lipid droplet occurrence over time (seen on Figure 19, panel A) suggests an ongoing process of biogenesis and mobilization that seems relevant for cell survival, given the toxic effects of py-

2 and CERK knockdown, and is in keeping with a possible catabolic use of lipid droplets generated in response to starvation.

4. Cell death during complete nutrient deprivation is associated to lipid droplet depletion

As a first approach to tackle the possible use of starvation-triggered lipid droplets as catabolic fuel, we loaded LN18 cells with lipid droplets using a 16-h treatment with exogenous lipid in DMEM (10% FBS and 100 μM sodium oleate), reasoning that lipid droplet-preloaded cells should be able to survive nutrient deprivation longer than cells that were depleted of lipid droplets at the beginning of the treatment. Flow cytometry analysis evidenced that LN18 cells that had been depleted of lipid droplets before treatment died fast between 24 and 32 hours. Preloading with lipid droplets significantly increased the survival of cells to complete nutrient deprivation (Figure 25, panel A). The same protective effect of lipid droplet preloading was observed in CHO and HeLa cells (not shown). These results agree with reports that oleic acid preconditioning increases survival of PC12 cells to starvation (Khatchadourian and Maysinger, 2009).

If cell viability during starvation is sustained by the catabolic use of lipid droplets, conceivably cell death should take place after lipid droplet depletion. To test that idea, serum-starved LN18 cells were treated with KH buffer without glucose and harvested over a time-course. After staining with Nile red, cells were analyzed by flow cytometry. As shown previously, flow cytometry allows discriminating viable and dead cells by their distinct distribution in SS/FS plots. This way, viable and dead Nile red-stained cells from the same sample can be recognized and gated separately to quantify lipid droplet occurrence. Panel B represents the quantification of lipid droplets in viable and dead LN18 cells from the same sample, over a time-course of 24 hours. At all treatment times, dead cells were consistently depleted of lipid droplets as compared to viable cells.

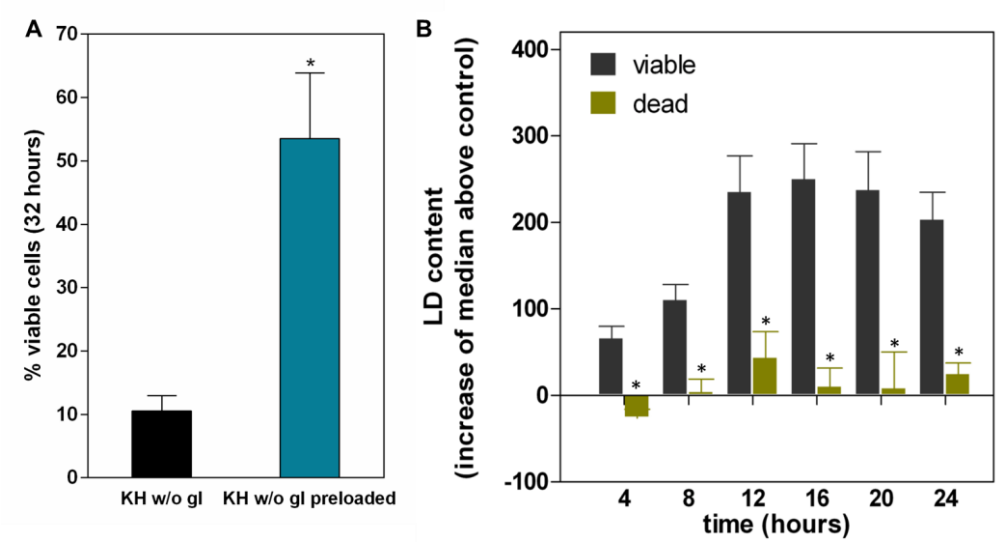

Figure 25. ***Preloading with lipid droplets prolongs survival to starvation. Cells surviving nutrient deprivation contain significantly more lipid droplets than dead cellS.***

*A, LN18 cells were maintained overnight in FBS-free DMEM to ensure depletion of lipid droplets (black bar) or DMEM supplemented with 10% FBS and 100 µM sodium oleate (blue bar) prior to their treatment with KH buffer without glucose for 32 h. Cells devoid of lipid droplets before starvation died faster than those that had been preloaded with lipid droplets. Results are means ±SEM (error bars) of three independent experiments carried out with duplicate determinations. *, significantly different from cells depleted of lipid droplets before treatment. B, serum-starved LN18 cells were maintained in KH buffer without glucose for the times indicated and then stained with Nile red, and lipid droplet content in viable (black bars) and dead (green bars) cell populations was assessed by flow cytometry. Viable and dead cell populations in Nile red-stained samples were gated in SS/FS plots, and their lipid droplet content was determined after the median values of the FL1 event distributions. Results are expressed as FL1 median values above that of control samples devoid of lipid droplets, maintained overnight in culture medium without FBS, and are means ±SEM (error bars) of five independent experiments carried out with duplicate determinations. *, significantly different from viable cells.*

To confirm the correlation between viability and lipid droplet content, we repeated the experiment in CHO K1, HeLa and primary rat astrocytes (Figure 26, panels A, B and C respectively). Serum-starved cells were treated with KH buffer without glucose over a time-course and stained with Nile red for flow cytometry analysis. In all cases, the lipid droplet content of dead cells was significantly lower than that of viable cells, regardless of the treatment time.

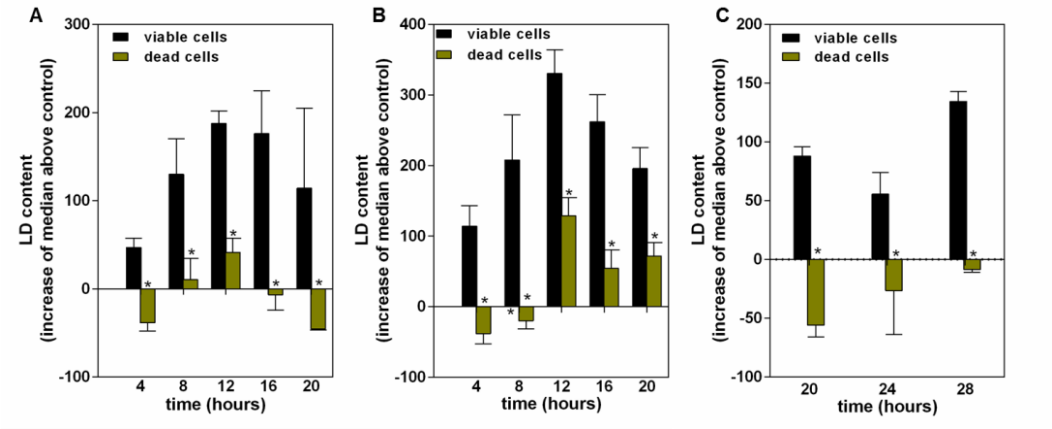

Figure 26. ***The correlation between lipid droplet content and survival to starvation is consistent in all cell types tested***

*CHO K1 (A), HeLa (B) and rat astrocytes (C) were deprived of serum overnight and treated with KH buffer without glucose. Lipid droplet content was measured separately in viable and dead cells by flow cytometry. Regardless of the cell type or treatment time, cells surviving starvation contained significantly more lipid droplets than dead cells. Results are expressed as FL1 median values above that of control samples devoid of lipid droplets, maintained overnight in culture medium without FBS, and are means ±SEM (error bars) of three (A, B) or two independent experiments carried out with duplicate determinations. *, significantly different from viable cells.*

So far, we have confirmed that lipid droplet biogenesis is a conserved response to complete nutrient deprivation, which strongly correlates with the ability of cells to survive starvation. In all cell types, lipid droplets occur in a bell-shaped distribution over time, which is in keeping with a possible process of lipid droplet mobilization for use as catabolic fuel. Consistently, death is associated with lipid droplet depletion, and can be postponed by preloading with lipid droplets before treatment with KH without glucose.

Taken together, our results strongly suggest that lipid droplet biogenesis induced by starvation is a conserved response aimed at providing catabolic substrates to support cell survival.

5. Nutrient deprivation induces β-oxidation of fatty acids, in a process dependent on lipid droplet biogenesis.

As discussed in the introduction, one of the possible fates of fatty acids released by lipolysis is to be oxidized in the mitochondria for energy generation. To test our hypothesis that lipid droplets induced by stress are mobilized for energetic purposes, we first addressed whether complete nutrient deprivation induced lipid droplet-dependent β-oxidation of fatty acids.

To that purpose, we labeled endogenous lipids by incubating LN18 cells with 1µCi/mL [^{3}H]palmitic acid in serum-free culture medium supplemented with 0,5% delipidated bovine serum albumin (BSA). The final concentration of the fatty acid (10-30 nM) was low enough to avoid lipid droplet biogenesis (Gubern et al., 2008), which was further precluded by the absence of lipid sources in the medium. After 24 hours of incubation, cells were thoroughly washed with BSA-containing culture medium and PBS, to ensure complete elimination of extracellular [^{3}H]palmitic acid, and switched to KH buffer without glucose or serum-free culture medium. β-oxidation was monitored using the generation of [^{3}H]water as an index of fatty acid oxidation (Djouadi et al., 2003). Figure 27, panel A shows the result of a representative experiment. LN18 cells treated with KH buffer without glucose released [^{3}H]water in a manner that was sensitive to a 30 µM concentration of etomoxir (EX). EX is an irreversible inhibitor of carnitine palmitoyltransferase (CPT1), widely used to pharmacologically block β-oxidation (Schlaepfer et al., 2014). The sensitivity of starvation-triggered release of [^{3}H]water to EX confirmed that [^{3}H]water measurement was a valid way to quantify β-oxidation. [^{3}H]water generation by cells maintained in culture medium was similar to that in cells where β-oxidation was inhibited with EX, showing that nutrient deprivation did induce the oxidation of fatty acids. In agreement with this, fatty acid oxidation was associated with increased expression of CPT1A in cells treated with KH buffer without glucose (Figure 27, panel A, inset).

Nutrient deprivation also stimulated fatty acid oxidation in CHO K1 and HeLa cells (Figure 27, panels B and C). More importantly, inhibition of lipid droplet biogenesis with py-2 decreased β-oxidation to a level close to that defined by EX (panels A-C). To exclude the possibility that this effect was secondary to cell death, we performed the experiments within a time frame in which cell viability under complete nutrient deprivation was not yet compromised. Thus, LN18 cells, which maintain viability longer, were treated for a maximum of 7 hours, whereas HeLa and CHO-K1 cells, which die faster, were treated for 4 hours.

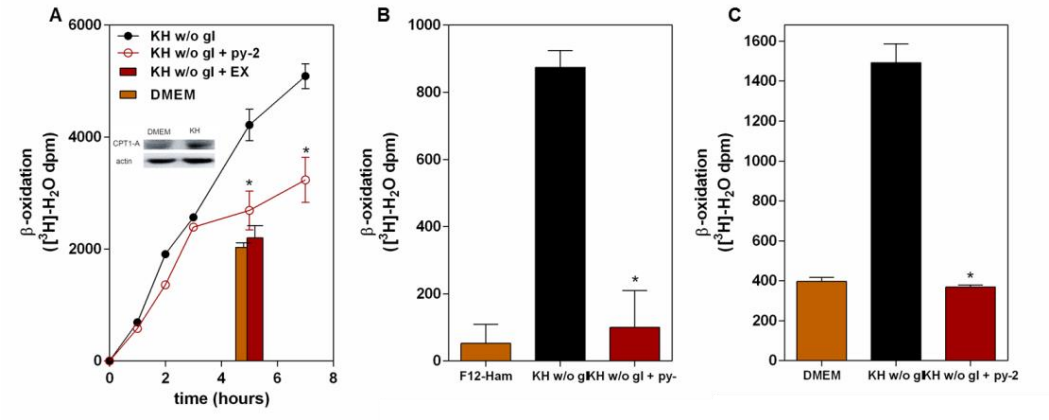

Figure 27. ***Complete nutrient deprivation induces lipid droplet-dependent β-oxidation of fatty acids.***

*A, LN18 cells were prelabeled overnight with [^{3}H]palmitic acid prior to their treatment with DMEM (gray bar) or KH without glucose in the absence (solid symbols) or presence of 1 μM py-2 (open symbols) or 30 μM EX (open bar). β-oxidation was monitored after the generation of [^{3}H]water. The inset shows increased expression of CPT1A after 16 h of starvation. B and C, [^{3}H]palmitic acid-prelabeled CHO-K1 (B) or HeLa (C) cells were treated for 4h with culture medium (gray bar) or KH buffer without glucose in the absence (solid bar) or presence of 1 μM py-2 (open bar). β-oxidation was defined as EX-sensitive production of [^{3}H]water. In all cell types, complete nutrient deprivation stimulated β-oxidation, in a manner that was strictly dependent on lipid droplet biogenesis. Results are means ± SEM (error bars) of an experiment carried out with quadruplicate determinations, and are representative of four (A) or three (B and C) independent experiments with similar outcome. *, significantly different from KH buffer without glucose.*

Labeling with [^{3}H]palmitic acid in conditions that do not lead to lipid droplet formation allows to trace the incorporation of the fatty acid into endogenous lipid components. To confirm that starvation-triggered β-oxidation was preceded by synthesis of triacylglycerol (TAG) from endogenous fatty acid sources, we prelabeled LN18 cells with [^{3}H]palmitic acid following the protocol described above. After 24 hours, cells were switched to serum-free culture medium or KH without glucose, in the presence or absence of EX. After recovering the cellular supernatant to measure β-oxidation, lipids were extracted following the protocol proposed by Bligh and Dyer (Bligh and Dyer, 1959) and the major lipid species were separated by high performance thin layer chromatography. Identification of phospholipids and TAG was achieved by co-migration with 1-palmitoyl-2-oleoyl-phosphatdylcholine and tripalmitin, respectively. The incorporation of [^{3}H]palmitic acid to each lipid species was quantified after scraping radioactive lipids into scintillation vials.

Analysis of the major lipid species revealed that [^{3}H]palmitic acid went mainly to phospholipids (Figure 28, panel A), and nutrient deprivation induced a small but non-significant decrease. As expected, nutrient deprivation induced TAG accumulation that was

potentiated by the inhibition of β-oxidation with EX (Figure 28, panel B). Confirming our previous results, complete nutrient deprivation triggered an increase in β-oxidation as measured by the release of [^{3}H]water, which was completely abrogated by EX (Figure 28, panel C).

These results were in keeping with our hypothesis that stress triggers the formation of lipid droplets containing TAG synthesized from an endogenous fatty acid moiety, which are subsequently degraded to fuel β-oxidation. Panel D, which shows the aggregated values of [^{3}H]TAG and [^{3}H]water, further illustrates this idea. Here, we compared the combined contribution of [^{3}H]palmitic acid to radioactivity present in [^{3}H]water (as a measure of β-oxidation) and [^{3}H]TAG. The inhibition of β-oxidation with EX resulted in an increased accumulation of [^{3}H]TAG. The smaller accumulation of [^{3}H]TAG induced by KH buffer without glucose alone reflected an ongoing process of degradation of [^{3}H]TAG to fuel β-oxidation.

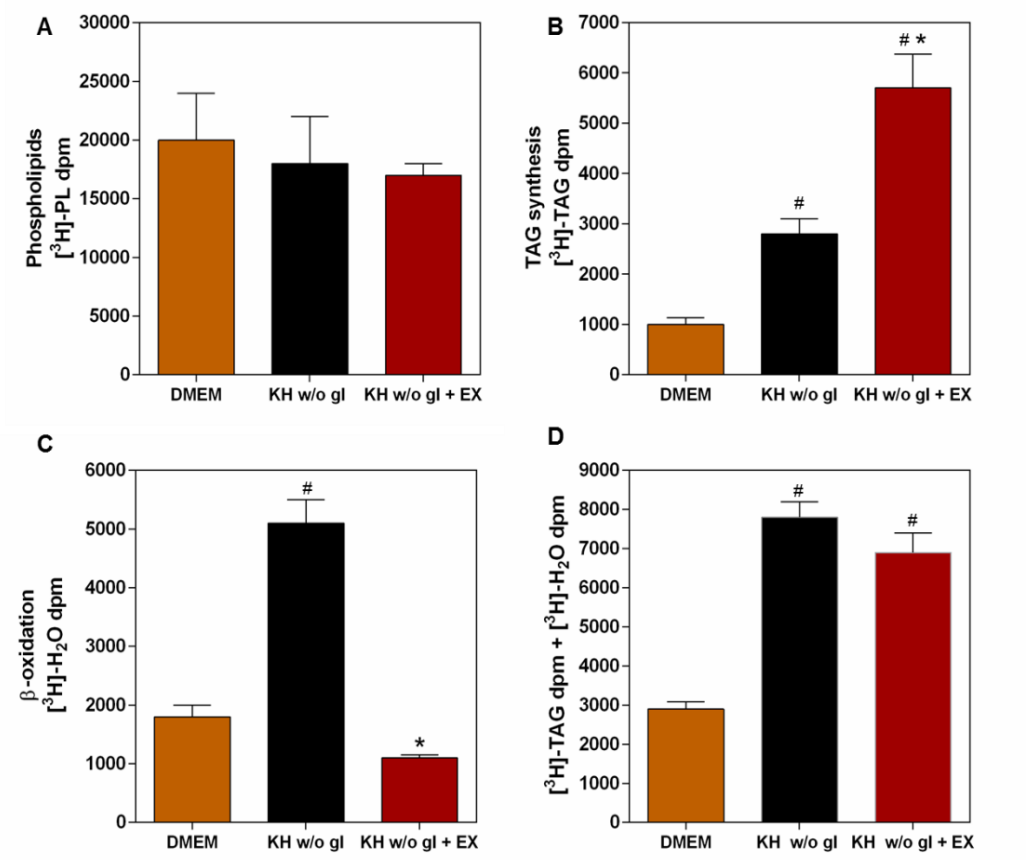

***Figure 28.* Complete nutrient deprivation triggers TAG synthesis from endogenous fatty acid moieties, which fuel β-oxidation.**

*[^{3}H]palmitate-prelabeled LN18 cells were maintained in culture medium (gray bars) or KH without glucose in the absence (solid bars)or presence of 30 μM EX (open bars). After 8 hours, lipids were extracted and separated by high performance thin layer chromatography, and radioactivity in phospholipids (PL) and TAG was quantified. A, nutrient deprivation induced a small but not significant decrease in phospholipid content. B, nutrient deprivation induced TAG accumulation that was potentiated by inhibition of β-oxidation with EX. C, nutrient deprivation stimulated the generation of [^{3}H]water as an index of β-oxidation, which was inhibited by EX. G, aggregated values of [^{3}H]TAG + [^{3}H]water, illustrating that nutrient deprivation induced a process of lipogenesis that led to the oxidation of fatty acids. Results are means ± SEM of one experiment with quadruplicate determinations that was repeated twice with a similar outcome. *, significantly different from KH without glucose; #, significantly different from DMEM.*

Together, these results suggest that survival of nutrient-deprived cells is sustained by a process of TAG synthesis and lipid droplet formation, and their subsequent mobilization to fuel fatty acid oxidation. Given that in this situation TAG are synthesized using fatty acids from endogenous lipid moieties, the whole process could be characterized as a lipidic counterpart of autophagy, whereby fatty acids trapped in structural functions are reused for TAG synthesis and packaged into lipid droplet for energetic purposes.

6. Survival of nutrient-deprived cells is sustained by lipid droplet mobilization and β-oxidation of fatty acids

If lipid droplets exert their cytoprotective role by fueling β-oxidation, its inhibition with EX should have a similar effect on cell survival as that of blocking lipid droplet biogenesis with py-2.

As a first approach to test this idea, we treated serum-starved HeLa cells with KH without glucose containing py-2 or EX for 5 and 10 hours and stained them with PI and BODIPY 493/503 for flow cytometry analysis of cell death and lipid droplet occurrence (Figure 29). Inhibition of lipid droplet biogenesis (panels B and C) led to an increase of PI-positive (dead) cells over time, as compared to control cells maintained in FBS-free culture medium (panels A and D). As we expected, inhibition of β-oxidation with EX had a similar effect on cell survival (panels E and F). Interestingly, inhibition of β-oxidation led to the accumulation of lipid droplets in dead cells, as evidenced by the stronger BODIPY fluorescence observed in FL1/FL3 plots

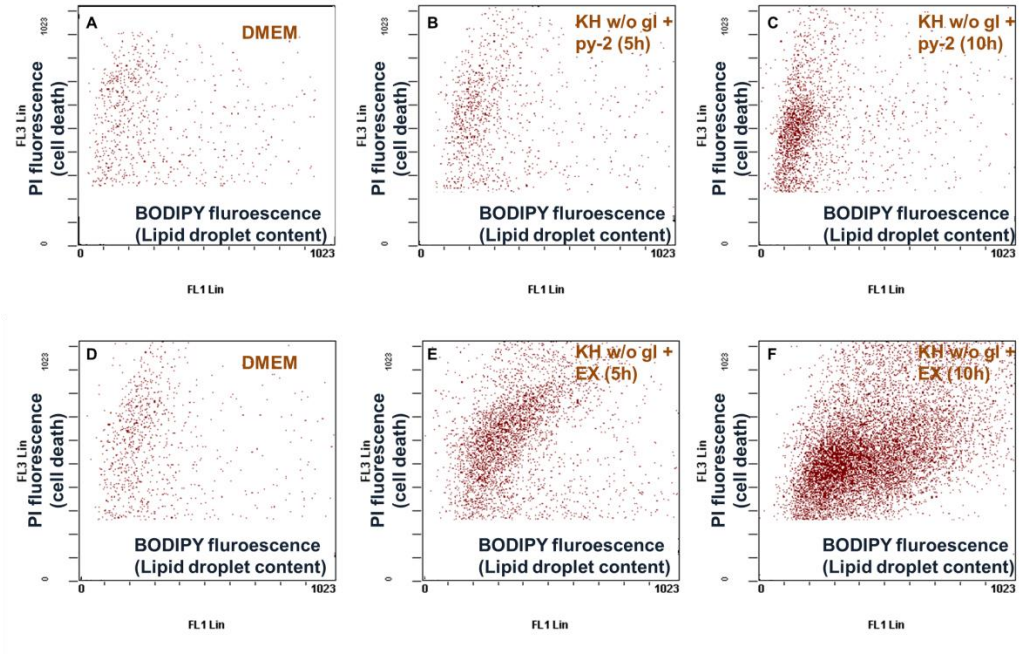

Figure 29. ***Inhibition of lipid droplet biogenesis or β-oxidation accelerates death of nutrient-deprived HeLa cells***

HeLa cells were deprived of serum overnight and treated with serum-free culture medium (A,D), KH w/o glucose + py-2 (B,C) or KH w/o glucose + EX (E, F) for 5 or 10 hours. This figure shows the event distribution of dead cells for each treatment in terms of PI fluroescence (FL3) and lipid droplet occurrence (FL1). Treatment with py-2 led to the accumulation of cells in the PI-positive (dead) population, which was devoid of lipid droplets (B,C). Inhibition of β-oxidation with EX was also toxic for nutrient-deprived cells (E, F), and induced accumulation of lipid droplets on PI-positive cells, as evidenced by the right shift of the FL1 BODIPY signal.

To further characterize the observed toxic effect of β-oxidation inhibition on nutrient-deprived cells, we treated serum-starved HeLa cells with KH buffer without glucose in the absence or presence of EX, and stained them with PI for flow cytometry analysis (Figure 30). After an 8 hour treatment, cells treated with KH buffer without glucose were mostly found in the viable (PI-impermeant) population (panel A). Co-treatment with EX strongly induced the accumulation of cells on the PI-positive (dead) population (panel B). A time-course study of viability evidenced that EX dramatically accelerated death of nutrient-deprived cells, but had no effect on cells maintained in serum-free culture medium (panel C).

Insets to panels A and B show the event distribution of dead cells in each sample in terms of PI fluorescence and lipid droplet content (expressed as the BODIPY 493/503 fluorescence emission in FL1). In cells treated with KH buffer without glucose, dead cells appeared to be devoid of lipid droplets, as evidenced by the low BODIPY fluorescence (panel A, inset), and

in keeping with our previous observations. However, treatment with EX induced the accumulation of lipid droplets in the dead cell population (panel B, inset).

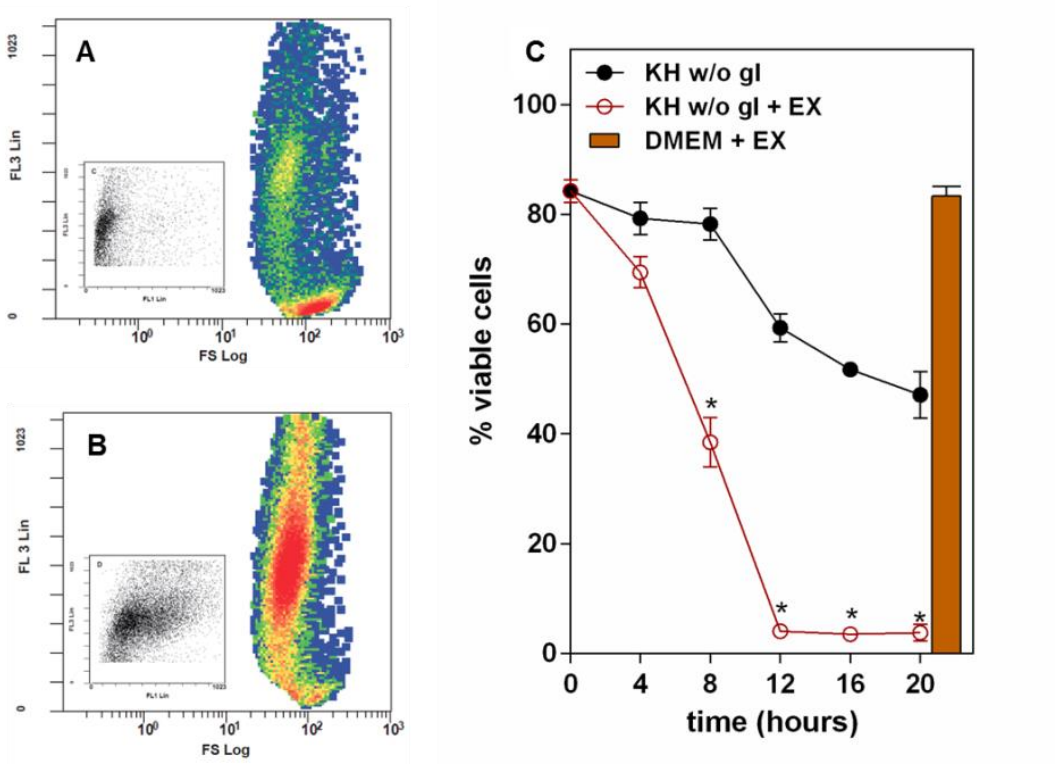

Figure 30. ***Inhibition of β-oxidation with EX accelerates death and induces lipid droplet accumulation in nutrient-deprived HeLa cells, but it is not toxic for cells maintained in DMEM***

*HeLa cells were deprived of serum overnight and treated with KH buffer w/o glucose in the absence (A) or presence (B) of 30 μM EX. Flow cytometry analysis of cells stained with PI evidenced that, at 8 hours of treatment, EX greatly increased the appearance of dead (PI-positive) cells. Insets to panels A and B show the distribution of dead cells in each sample in terms of PI emission and lipid droplet content (BODIPY 493/503 fluorescence). Cells treated with KH buffer without glucose in the presence of EX died full of lipid droplets (panel B, inset), as opposed to those treated with KH buffer without glucose alone (panel A, inset). C, a time-course study of cell survival showed that treatment with EX dramatically accelerates death of nutrient-deprived cells, but has no toxic effect on cells maintained in serum-free DMEM. Results are means ± SEM of three independent experiments carried out with duplicate determinations. *, significantly different than KH buffer w/o glucose.*

As pointed out previously, starvation-induced cell death consistently takes place after lipid droplet depletion. Therefore, EX-induced accumulation of lipid droplets in dead cells is in keeping with the need for their mobilization to fuel β-oxidation. These preliminary findings, together with the strong potentiation of starvation-triggered death by EX, seemed to support our hypothesis that lipid droplets promote survival by fueling β-oxidation.

Additional experiments were carried out to confirm this hypothesis. Based on our previous observations, LN18 and CHO K1 also exhibit increased lipid droplet-dependent β-oxidation when kept in KH buffer without glucose. To assess the effect of inhibition of β-oxidation on their survival and lipid droplet occurrence, LN18 and CHO K1 cells were deprived of serum overnight and treated with serum free culture medium or KH buffer without glucose, in the absence or presence of 30 µM EX. Cells were harvested over a time course of 24 or 20 hours, respectively, and stained with Nile red for flow cytometry analysis of cell viability and lipid droplet occurrence. Figure 31 shows that death of starved LN18 cells was strongly accelerated by treatment with EX (panel A), in a way that mirrored the effect of lipid droplet inhibition in the same conditions (shown in Figure 23, panel A). However, survival of LN18 cells maintained in serum-free culture medium was not affected by EX, in agreement with our observations that these conditions do not induce β-oxidation, and in keeping with the lack of toxicity of lipid droplet inhibition. Moreover, treatment with EX induced a very significant overall accumulation of lipid droplets in nutrient deprived cells (Figure 31, panel B), which was apparent in both viable (panel C) and dead cells (panel D).

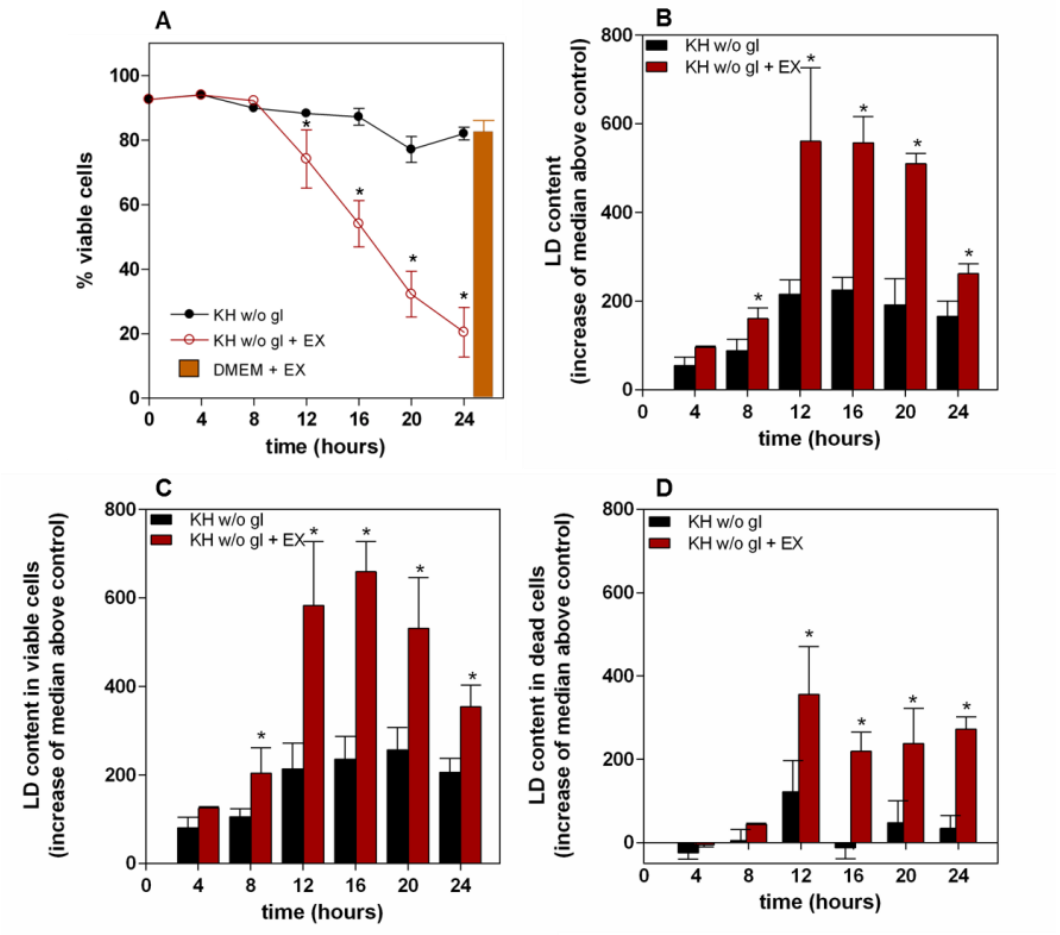

***Figure 31.* Inhibition of β-oxidation with EX accelerates death and induces lipid droplet accumulation in nutrient-deprived LN18 cells**

*Treatment with EX accelerated death of nutrient deprived LN18 cells (A) but had no effect on control. EX induced overall accumulation (B) of lipid droplets, which was apparent on viable (C) and dead (D) cells. Results are means ± SEM (error bars) of six independent experiments carried out with duplicate determinations. *, significantly different than KH w/o gl.*

Death of starved CHO-K1 cells proceeded at a faster pace than that of LN18 cells, and was significantly accelerated by treatment with EX (Figure 32, panel A). Consistently, inhibition of β-oxidation had no effect on cells maintained in serum-free culture medium, and triggered an important overall accumulation of lipid droplets (panel B) which was apparent in both viable and dead cells (panels C and D, respectively).

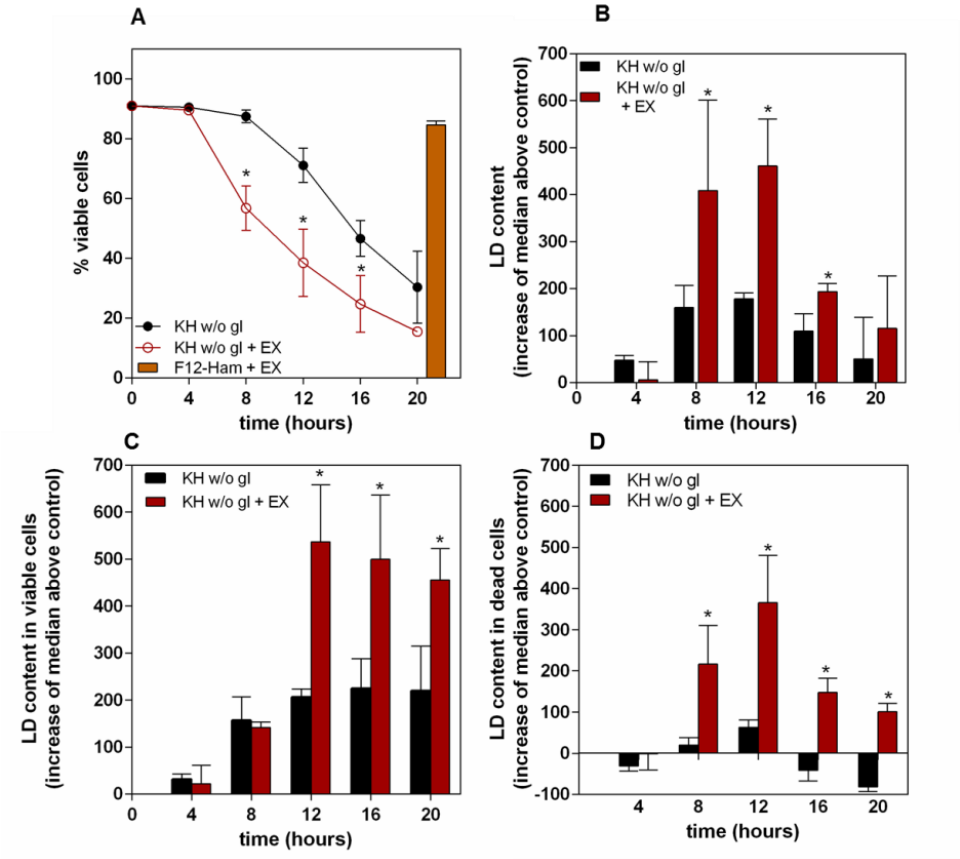

***Figure 32.* Inhibition of β-oxidation with EX accelerates death and induces lipid droplet accumulation in nutrient-deprived CHO-K1 cells**

*Inhibition of β-oxidation with EX had the same effect on CHO-K1 cells as on HeLa and LN18 cells. Thus, EX accelerated death of nutrient-deprived cells, but not of those kept in serum-free culture medium (A). EX also induced accumulation of lipid droplets in nutrient-deprived cells (B), which could be observed in both viable (C) and dead cells (D). Results are means ± SEM of 3 independent experiments carried out with duplicate determinations. *, significantly different than KH w/o gl.*

We had previously observed that LN18 cells that had been loaded with lipid droplets before starvation survived longer than those that were depleted before treatment. This is arguably due to the presence of an already existing lipid droplet reservoir which cells can mobilize as a response to starvation, retarding their need to synthesize new TAG and lipid droplets. We therefore reasoned that lipid droplet preloading would significantly extend survival even if the synthesis of new starvation-triggered lipid droplets was inhibited with py-2. However, the protective effect of lipid droplet preloading should be abrogated by inhibition of β-oxidation, since cells would be unable to use the preexisting lipid droplet reservoir.

To test this idea, LN18 cells were either deprived of serum or treated with FBS supplemented with 100 µM sodium oleate overnight. Cells were then treated for 32 hours with KH buffer without glucose, in the absence or presence of py-2 and EX. (Figure 33). As we had previously observed, nutrient-deprived cells that had been loaded with lipid droplets before treatment survived significantly more than those that had been depleted. This protective effect was maintained even in the presence of py-2, but completely abrogated by the inhibition of β-oxidation with EX.

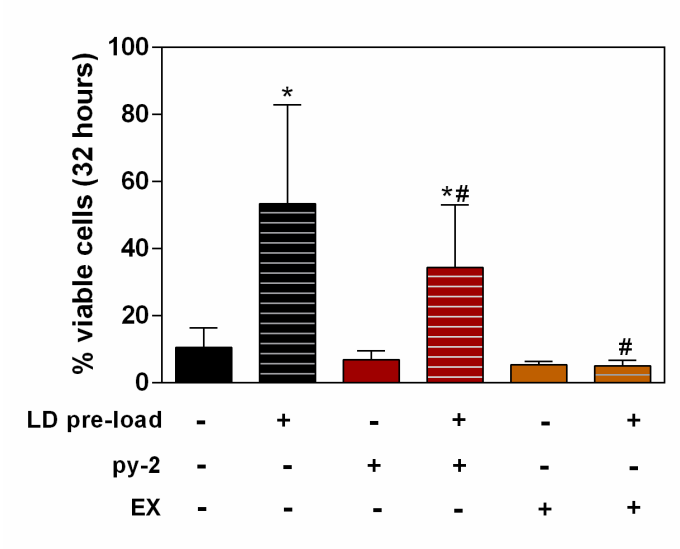

Figure 33. The protective effect exerted by lipid droplet pre-loading before starvation requires β-oxidation

LN18 cells were depleted (solid bars) or preloaded (stripped bars) with lipid droplets overnight, before a 32 hour treatment with KH w/o gl in the absence (black bars) or presence of py-2 (red bars) or EX (orange bars). Lipid droplet preloading extended the survival of cells maintained in KH w/o glucose (black bars) even in the absence of new, starvation triggered synthesis of lipid droplets (red bars). Lipid droplet preloading was still protective in cells treated with KH w/o glucose + py-2. However, py-2 had a significant toxic effect on preloaded cells as compared to preloaded cells maintained in KH w/o glucose alone, arguably due to their inability to synthesize new lipid droplets after the preexisting reservoir was consumed. Inhibition of β-oxidation with EX (orange bars) completely abrogated the protective effect of lipid droplet preloading. Results are means ± SEM of three independent

*experiments carried out with duplicate determinations. *, significantly different from lipid droplet-depleted cells for the same treatment; #, significantly different from lipid droplet-preloaded KH w/o glucose.*

The results presented so far show that all cell types tested respond to complete nutrient deprivation by synthesizing lipid droplets, in a process that requires cPLA2α activity. Under these conditions, survival becomes strictly dependent on the ability of cells to synthesize lipid droplets, and cell death is consistently associated with lipid droplet depletion. Lipid droplet occurrence over time has a bell-shaped distribution that suggests an ongoing process of formation and catabolism. Previous results from our group have shown that stress-triggered lipid droplet biogenesis is preceded by synthesis of TAG from fatty acids released from phospholipid moieties (Gubern et al., 2009b). In agreement with that, nutrient-deprived cells exhibit enhanced TAG synthesis from endogenous fatty acid sources. Starvation-triggered TAG synthesis is mirrored by an increase in β-oxidation rates, and inhibition of β-oxidation with EX leads to further TAG accumulation. In keeping, EX induces a very significant accumulation of lipid droplets in both viable and dead cells, and, more importantly, dramatically accelerates death of nutrient-deprived cells, in a way that resembles the toxic effects of blocking lipid droplet biogenesis.

Taken together, these results strongly support our hypothesis that starvation-triggered lipid droplet biogenesis is a survival response, aimed at providing fuel for β-oxidation in the mitochondria.

7. Autophagy is not involved in the mobilization of starvation-triggered lipid droplets for β-oxidation

As discussed in the introduction, recent findings have led to identify the process of "lipophagy", which is defined as the selective sequestration of lipid droplets into autophagosomes triggered by starvation, and their delivery to lysosomes, where TAG are hydrolyzed by acidic lipases, resulting in the release of free fatty acids back to the cytosol. This process was first identified in cultured hepatocytes and liver *in vivo* (Singh et al., 2009), where it appears to be very prevalent (reviewed by Czaja et al., 2013). The authors of the first study reported that lipid droplet proteins and TAG were found in autophagosomes under basal conditions, along with cytosolic components, but prolonged starvation led to preferential sequestration of lipid droplets. Under those circumstances, inhibition of autophagy led to a reduced TAG breakdown (measured by the decrease of β-oxidation rates) and the accumulation of lipid droplets (Singh et al., 2009). These findings have been confirmed by others in hepatocytes and other cell types, such as neurons, fibroblasts or stellate cells (reviewed by Liu and Czaja, 2013)

Studies on lipophagy are usually performed by loading cells with lipid droplets before starvation (by supplementing the culture medium with FBS or fatty acids), and monitoring the effect of autophagy modulation on lipid droplet turnover and β-oxidation rates (reviewed by Liu and Czaja, 2013). However, the mechanism by which stress-triggered lipid droplets are mobilized is unknown. Given the fact that nutrient deprivation is a powerful stimulus in terms of induction of autophagy, we hypothesized that lipophagy might be involved in our system, mediating the hydrolysis of lipid droplet TAG to release fatty acids for mitochondrial oxidation.

As we expected, treatment of LN18 cells with KH buffer without glucose induced the appearance of autophagosomes (Figure 34, panel A) and microtubule-associated protein light chain 3 (LC3)-I conversion to LC3-II (panel B), as well as the formation of LC3 puncta in the cytosol (panel C), all of which are indicative of autophagy (Tanida et al., 2008; Barth et al., 2010). The autophagy inhibitor 3-methyladenine (3-MA) blocked the conversion from LC3-I to LC3-II and the appearance of LC3 puncta (panels B and D, respectively).

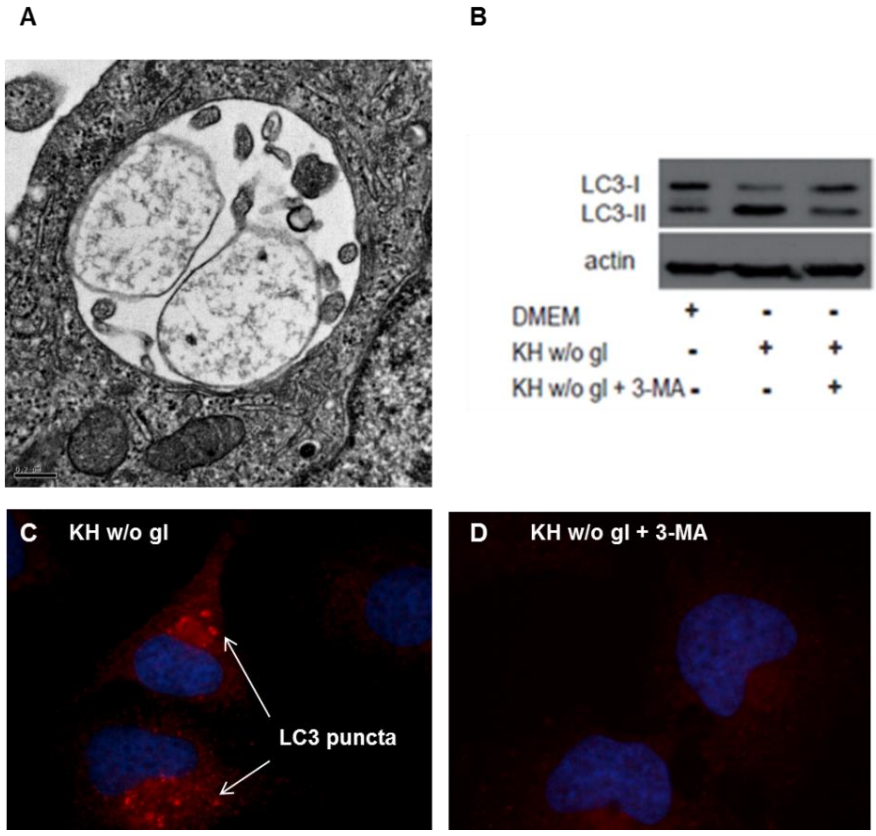

Figure 34. ***Treatment with KH buffer without glucose induces autophagy in LN18 cells.***

A, electronic microscope image of a late autophagosome after 16 hours of treatment. B, treatment with KH buffer without glucose triggered the conversion of LC3-II to LC3-II, as well as the formation of LC3 puncta in the cytosol (C), both of which are indicative of autophagy, and sensitive to 10 mM of the autophagy inhibitor 3-MA (B, C).

Once we had established that our treatment induced autophagy, we aimed to study the involvement of the autophagic machinery on lipid droplet mobilization. We reasoned that, if autophagy was an upstream event necessary to release fatty acids for β-oxidation, its inhibition should result on a decrease of starvation-triggered β-oxidation. Since we had previously established that lipid droplet-fueled β-oxidation is necessary for survival to complete nutrient deprivation, inhibition of autophagy should conceivably have a toxic effect, similar to that observed when blocking lipid droplet formation or β-oxidation.

As a first approach to test that hypothesis, LN-18 cells were deprived of serum overnight and switched to KH buffer without glucose or serum-free culture medium and in the absence or presence of 10 mM 3-MA. That concentration was high enough to inhibit autophagy, as monitored by LC3-I/LC3-II conversion (as shown in Figure 34, panel B), but low enough to be non-toxic for control cells maintained in culture medium (Figure 35, panel A). Cell survival and lipid droplet content were monitored by flow cytometry over a time-course of 32 hours.

As we had observed previously, LN18 cells treated with KH buffer without glucose maintained viability for 24 hours, and died rapidly thereafter. Surprisingly, inhibition of autophagy with 3-MA was not toxic for nutrient-deprived cells but, instead, significantly extended their survival (Figure 35, panel A). Flow cytometry revealed that inhibition of autophagy resulted in a small but significant accumulation of lipid droplets, which became more apparent at long treatment times (panel B).

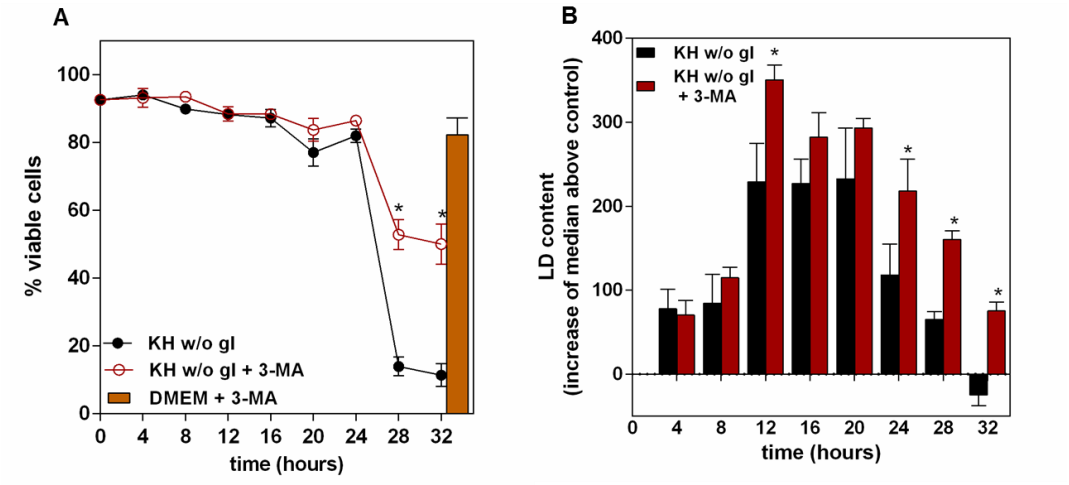

Figure 35. ***Inhibition of autophagy with 3-MA extends survival of nutrient-deprived LN18 cells and has no effect on β-oxidation***

*A, LN18 cells were maintained for 32 hours on KH buffer w/o glucose in the absence (black symbols) or presence (red symbols) of 10 mM 3-MA. Survival was assessed by flow cytometry, evidencing that 3-MA significantly extended survival of nutrient-deprived cells, and was not toxic for control cells maintained in culture medium (orange bar). B, inhibition of autophagy with 3-MA resulted in a small but significant accumulation of LD, which became more apparent at long treatment times. Results are means ± SEM of 3 independent experiments carried out with duplicate determinations. *, significantly different from KH w/o gl.*

The protective effect of 3-MA on nutrient-deprived cells seemed incompatible with an involvement of the autophagic machinery on lipid droplet hydrolysis leading to β-oxidation. Also, the small increase of lipid droplet content in cells treated with 3-MA contrasted with the striking effect of blocking β-oxidation with EX. We therefore concluded that nutrient deprived cells were still able to utilize lipid droplet TAG for β-oxidation in the absence of autophagy.

To confirm our conclusion, we labeled LN18 cells with 1μCi/mL [^{3}H]palmitic acid overnight, and switched them to DMEM or KH buffer without glucose in the absence or presence of 3-MA or EX. Treatment with KH buffer without glucose induced β-oxidation, measured as the EX-sensitive release of [^{3}H]water. As we expected, treatment with 3-MA did not affect β-

oxidation (Figure 36, panel A). Further, fluorescence microscopy analysis of cells stained with BODIPY 493/503 and LysoTracker Red (a widely used lysosome marker) failed to reveal colocalization of starvation-triggered lipid droplets with lysosomes, which is a hallmark of lipophagy (Singh et al., 2009) (panels B and C).

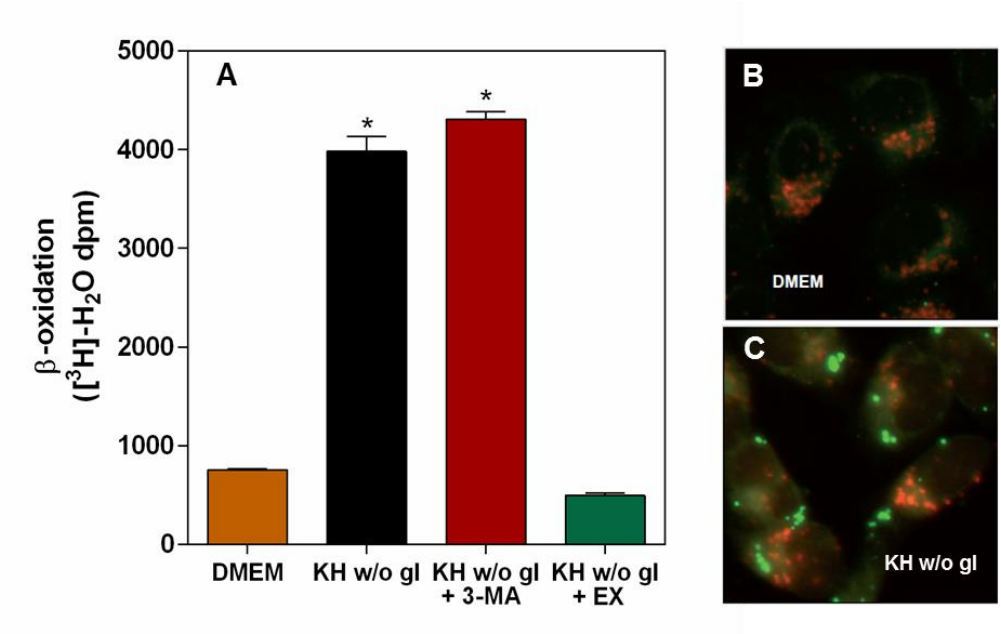

Figure 36. Inhibition of autophagy with 3-MA does not preclude β-oxidation in nutrient-deprived cells. Starvation-triggered lipid droplets do not colocalize with lysosomes.

*A, LN18 cells pre-labeled with [^{3}H]palmitic acid were treated with DMEM or KH w/o glucose in the absence or presence of 10 mM 3-MA or 30 µM EX. Treatment with KH w/o glucose induced β-oxidation, as measured by the EX-sensitive release of [^{3}H]water to the medium. Treatment with 3-MA did not preclude β-oxidation. Results are means ± SEM of one experiment with quadruplicate determinations that was repeated twice with a similar outcome. *, significantly different from DMEM. B and C, LN18 cells were maintained in FBS-free culture medium overnight before treatment with FBS-free DMEM (B) or KH w/o gl (C). Co-staining with BODIPY (green) and LysoTracker Red revealed that serum-starved cells were devoid of lipid droplets (B). Treatment with KH w/o glucose induced the appearance of lipid droplets, which did not colocalize with lysosomes (C)*

Taken together, these findings suggested that autophagy is not involved in the mobilization of starvation-triggered lipid droplets for β-oxidation.

An important drawback in autophagy research is the lack of specific autophagy inhibitors. 3-MA inhibits autophagy at an early stage, by blocking autophagosome formation via the inhibition of type III Phosphatidylinositol 3-kinases (PI-3K). However, at high concentrations, 3-MA can target other kinases and affect different cellular processes, such as glycogen metabolism, lysosomal acidification or endocytosis (Mizushima et al., 2010). Therefore, we searched for a more specific approach to target autophagy and ensure the relevance of our observations. As an alternative to inhibiting autophagy with 3-MA, we used mouse embryonic

fibroblasts (MEF) with knockout of the autophagy related gene Atg5 (henceforth Atg5 KO MEF). This cell line is commonly used as a model to study the functions of autophagy (Chen et al., 2012; Lin et al., 2014), since Atg5 knockout is a highly specific method to ensure autophagy deficiency (Mizushima et al., 2001).

Our first step was to determine the time necessary for Atg5 KO and wild type MEF cells to achieve lipid droplet depletion when switched to FBS-free culture medium. This was the first feature we studied for every new cell type, since we needed to ensure that lipid droplets arose exclusively as a result of stress due to complete nutrient deprivation. In the case of LN18, CHO K1, HeLa and rat astrocytes, lipid droplet depletion was achieved by an overnight treatment (16-18 hours) with serum-free culture medium, although shorter treatments were sufficient in the case of CHO K1 and LN18 cells.

Wild type (wt) and Atg5 KO MEF cells were cultured in DMEM supplemented with 10% FBS, and switched to FBS-free DMEM. At different times, cells were harvested and stained with Nile red for flow cytometry assessment of lipid droplet content. We observed that Nile red fluorescence emission on wt MEF decreased rapidly, and stabilized around 200 arbitrary units (a.u) in 24 hours. However, Atg5 KO MEF contained significantly more lipid droplets, as evidenced by their higher Nile red fluorescence emission, and required a 48 hour treatment with serum-free DMEM to achieve complete lipid droplet depletion (Figure 37, panel A). Throughout the treatment, there were no significant differences in the survival of wt and Atg5 KO cells (panel B)

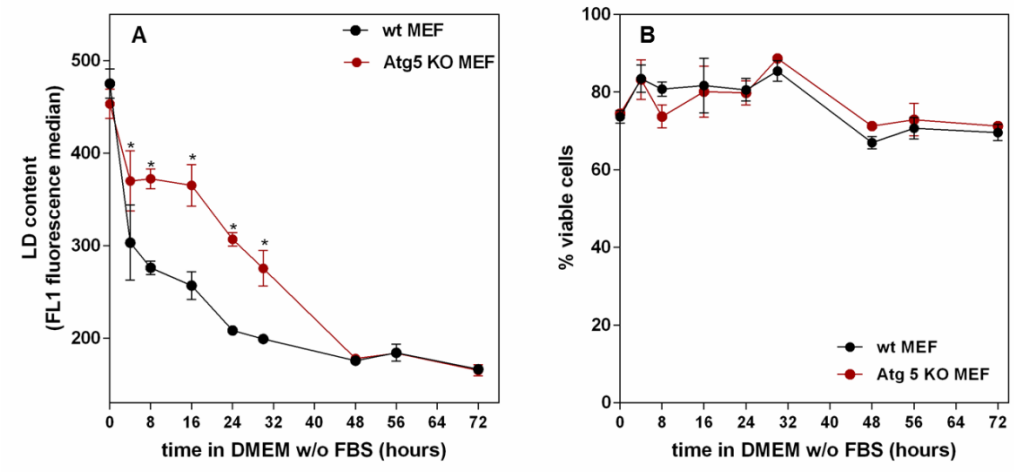

Figure 37. ***Lipid droplet depletion is slower in autophagy-deficient Atg5 KO MEF as compared to wt MEF.***

A, wt and Atg5 KO MEF cells were cultured in complete DMEM and switched to FBS-free DMEM to monitor lipid droplet depletion. wt MEF achieved complete lipid droplet depletion in 24 hours, with FL1 fluorescence values stabilizing around 200 arbitrary units. Autophagy-deficient Atg5 KO MEF cells required twice that time (48 hours)

*to achieve complete lipid droplet depletion. B, flow cytometry monitoring of cell viability revealed no significant differences in the survival of wt and Atg5 KO cells. Results are means ± SEM of three independent experiments carried out with duplicate determinations. *, significantly different from wt.*

The fact that autophagy-deficient MEF cells required twice as much time as their wt counterparts to achieve complete lipid droplet depletion suggested that the autophagic machinery is involved in the process. We observed a similar effect in LN18 cells, where inhibition of autophagy with 3-MA caused a significant delay on lipid droplet depletion when cells were switched from complete to serum-free culture medium. In this case, lipid droplet depletion proceeded at a faster pace, and was achieved after 8 hours of treatment with serum-free DMEM. However, the presence of 5 mM 3-MA caused a 4-hour lag (Figure 38).

Interestingly, autophagy deficiency or inhibition did not completely block lipid droplet depletion, but rather, caused a significant delay. These findings suggest that, whereas autophagy might participate in the process of lipid droplet mobilization, it is not the sole mechanism involved.

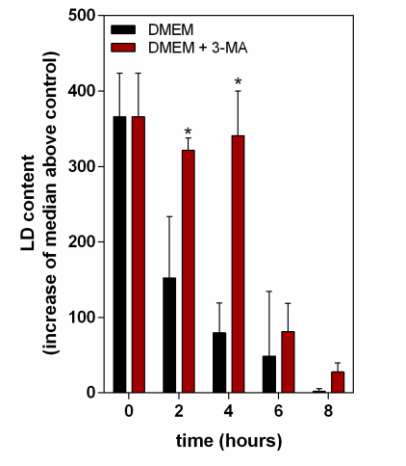

***Figure 38.* Inhibition of autophagy with 3-MA delays lipid droplet depletion.**
*LN18 cells were switched from complete to serum-free DMEM in the absence (black bars) or presence (red bars) of 3-MA. Inhibition of autophagy significantly delayed lipid droplet depletion. Results are means ± SEM of two independent experiments carried out with duplicate determinations. *, significantly different than DMEM.*

We had previously established that lipid droplet-fueled β-oxidation sustained cell survival to complete nutrient deprivation, in a process that was not affected by inhibition of autophagy with 3-MA. Indeed, cells treated with KH buffer without glucose in the presence of 3-MA survived longer than those treated with KH buffer without glucose alone. To establish if a deficiency in autophagy was consistently protective under complete nutrient deprivation, we maintained wt and Atg5 KO MEF cells in serum-free DMEM for 48 hours (a treatment time that we had established as sufficient for both cell types to achieve complete lipid droplet depletion, as shown in Figure 35, panel A). We then switched the cells to KH buffer without glucose and harvested them over a time-course of 24 hours for flow cytometry analysis of

lipid droplet content and cell viability (Figure 39). We observed that death in wt MEF cells proceeded at a faster pace, and after a 24 hour treatment only 25% of the population remained viable. Atg5 KO MEF cells survived complete nutrient deprivation longer, with 50% of the cells maintaining viability after a 24 hour treatment (panel A). These findings were consistent with the protective effect of autophagy inhibition observed in LN18 cells (shown in Figure 33, panel A).

Both wt and Atg5 KO MEF synthesized lipid droplets as a result of complete nutrient deprivation. As in all cell types tested, lipid droplet occurrence over time had a bell-shaped distribution, suggesting an ongoing process of formation and catabolism (Figure 39, panel B), and autophagy-deficient Atg5 KO cells exhibited an overall increase in lipid droplet content.

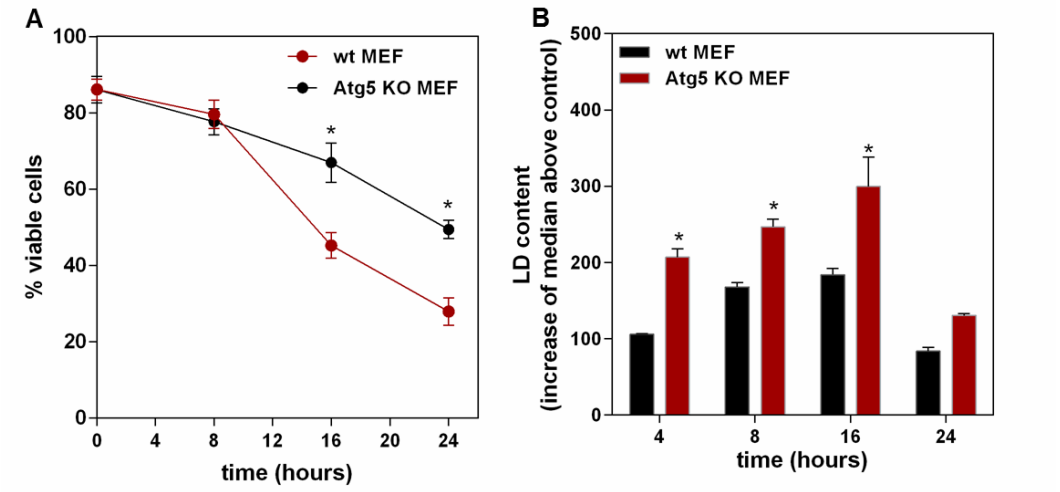

Figure 39. Autophagy-deficient Atg5 KO MEF cells survive nutrient deprivation longer than wt MEF, and contain significantly more starvation-triggered lipid droplets

*Wt and Atg5 KO MEF cells were maintained in serum-free DMEM for 48 hours and switched to KH buffer without glucose. A, flow cytometry analysis revealed that Atg5 KO cells survived starvation longer than wt. B, both wt and Atg5 KO cells synthesized lipid droplets as a response to complete nutrient deprivation. Lipid droplet content had a bell-shaped distribution over time, consistent with an ongoing process of biogenesis and catabolism. Atg5 KO cells contained significantly more lipid droplets than wt. Results are means ± SEM of three independent experiments carried out with duplicate determinations. *, significantly different than wt MEF.*

In order to study the effect of autophagy deficiency on starvation-triggered β-oxidation, we depleted wt and Atg5 KO MEF cells of lipid droplets and labeled them with [^{3}H]palmitic acid before switching them to DMEM or KH buffer without glucose. Complete nutrient deprivation increased the release of [^{3}H]water in both wt and Atg5 KO MEF cells (Figure 40).

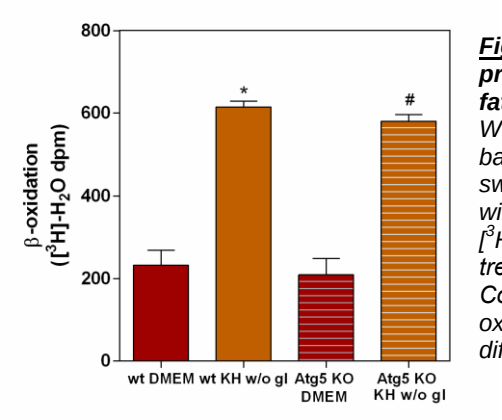

***Figure 40*. Autophagy deficiency does not preclude starvation-triggered β-oxidation of fatty acids.**
*Wt (solid bars) and Atg5 KO MEF cells (stripped bars) were labeled with [^{3}H]palmitic acid and switched to DMEM (red bars) or KH buffer without glucose (orange bars). The release of [^{3}H]water was measured after a 7 hour treatment as an indicator of of β-oxidation. Complete nutrient deprivation triggered β-oxidation in both cell types. *, significantly different from DMEM.*

Taken together, our results show that the selective delivery of lipid droplets to lysosomes triggered by starvation (or lipophagy) is not necessary as an upstream event leading to lipid droplet-fueled β-oxidation of fatty acids. Our results do not completely rule out the involvement of autophagy in lipid droplet mobilization, a process that could account for the observed accumulation of lipid droplets in Atg5 KO MEF or LN18 cells treated with 3-MA. However, the lack of toxicity of autophagy inhibition or deficiency, as well as the sustained induction of lipid droplet-fueled β-oxidation, indicates the presence of an alternative, autophagy-independent mechanism of lipolysis that results in the release of fatty acids for mitochondrial oxidation.

8. Perilipins 2 and 3 are not involved in the regulation of lipolysis of starvation-triggered lipid droplets

As mentioned in the introduction, the process of lipolysis in non-adipose tissues is poorly understood. However, different lines of evidence point at a role for the perilipin family of lipid droplet proteins in the regulation of lipolysis. Perilipins have been shown to promote TAG accumulation, and to participate in the regulation of the activity of cytosolic lipases (reviewed by Khor et al., 2013).

We hypothesized that lipid droplet lipolysis leading to mitochondrial oxidation of fatty acids was an autophagy-independent process, likely catalyzed by cytosolic lipases, and regulated by members of the perilipin family. Perilipins 2 and 3 are ubiquitously expressed (as opposed to perilipins 4 and 5, whose expression is restricted to white adipose tissue or highly oxidative tissues, respectively). Therefore, we used siRNA designed against perilipins 2 and 3 to study their function in the regulation of lipid droplet lipolysis in our system. To avoid a

possible functional compensation (Sztalryd et al., 2006; Bell et al., 2008), we simultaneously silenced the expression of both perilipins in LN18 cells.

LN18 cells maintained in KH buffer without glucose expressed perilipins 2 and 3, and treatment with siRNA designed against each perilipin successfully reduced their expression (Figure 41, panel A). Silenced expression of perilipins 2 and 3 did not preclude lipid droplet formation triggered by complete nutrient deprivation, as evidenced by fluorescence microscopy of Nile red stained cells (panels B and C), but lipid droplets were clearly bigger when both perilipins were down-regulated (panel C). This probably reflects a fusion process, aimed at reducing surface area contact with the aqueous cytosol in the absence of the surfactant properties of perilipins (Bell et al., 2008).

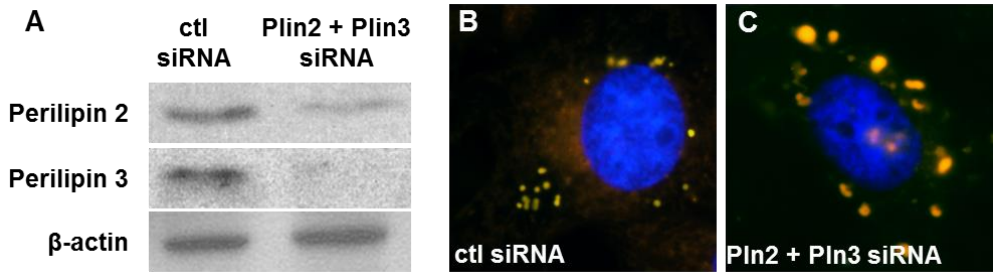

Figure 41. Silenced expression of perilipins 2 and 3 does not preclude starvation-triggered lipid droplet formation

LN18 cells were treated with control siRNA or siRNA designed against perilipin 2 and perilipin 3. A, LN18 cells treated with KH w/o glucose expressed perilipins 2 and 3, and their expression was successfully reduced by simultaneous treatment with siRNA against both proteins. B,C; LN18 were transfected with control siRNA (B) or siRNA designed against perilipins 2 and 3, deprived of serum overnight and switched to KH w/o glucose for 16 hours. Silenced expression of both perilipins did not preclude lipid droplet formation (C), but resulted in the appearance of clearly bigger lipid droplets as compared to cells transfected with control siRNA (B).

Perilipins 2 and 3 promote TAG accumulation in lipid droplets by regulating the access of cytosolic lipases to the lipid droplet core (reviewed by Ducharme and Bickel, 2008) . Therefore, we reasoned that their silencing should facilitate the access of cytosolic lipases to their substrates, resulting in a significant increase of fatty acids available for starvation-triggered β-oxidation. To test this hypothesis, we treated LN18 cells with control siRNA or siRNA designed against perilipins 2 and 3, and labeled them overnight with [^{3}H]palmitic acid in the absence of an external lipid source. We then switched cells to DMEM or KH buffer without glucose, and measured β-oxidation after the release of [^{3}H]water.

Contrary to our expectations, joint silencing of perilipins 2 and 3 had no significant effect on β-oxidation, which proceeded at the same rate as in cells treated with control siRNA (Figure

42, panel A). Consistently, flow cytometry monitoring of cell viability showed that silenced expression of perilipins 2 and 3 had no significant effect on the survival of LN18 cells to complete nutrient deprivation (panel B), or the overall lipid droplet content (panel C).

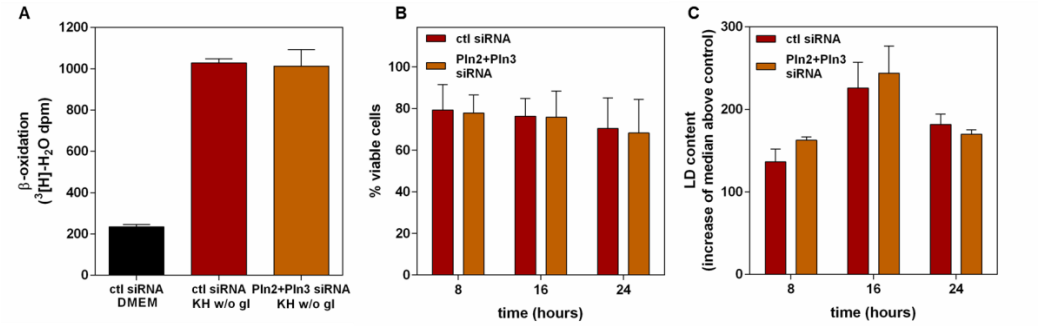

Figure 42. ***Silenced expression of perilipins 2 and 3 has no effect on cell survival to nutrient deprivation, overall lipid droplet content or starvation-triggered β-oxidation.***

A, LN18 cells with silenced expression of perilipins 2 and 3, or control, were labeled with [^{3}H]palmitic acid overnight and switched to DMEM or KH buffer without glucose. Treatment with KH without glucose induced β-oxidation, measured as the release of [^{3}H]water, and silenced expression of both perilipins had no significant effect. B,C, LN18 cells were treated with siRNA designed against perilipins 2 and 3 or control siRNA, deprived of serum overnight, and switched to KH buffer w/o glucose. Cell survival (A) and overall lipid droplet content (B) were not affected by the absence of both perilipins. Results are means ± SEM of three independent experiments carried out with duplicate determinations (B,C) or means ± SEM of a representative experiment carried out with quadruplicate determinations that was repeated twice with a similar outcome (A)

Other groups had reported normal levels of β-oxidation in hepatocytes from perilipin 2 null mice, even in the absence of functional compensation by perilipin 3 (Chang et al., 2006; Imai et al., 2007). In those cases, however, the results could be explained by the presence of perilipin 5 in hepatocytes (Bell et al., 2008). As mentioned above, the expression of perilipin 5 is restricted to tissues with high oxidative demands (such as liver, skeletal muscle and heart), where it has been reported to promote both TAG accumulation and fatty acid oxidation (Kuramoto et al., 2012; Bosma et al., 2012). Given the fact that silenced expression of perilipins 2 and 3 had no significant effect on β-oxidation levels and overall lipid droplet content, it was tempting to hypothesize that complete nutrient deprivation might induce perilipin 5 expression, to participate in the regulation of lipid droplet turnover and mitochondrial oxidation.

However, our attempts to study a possible role for perilipin 5 in our model were hindered by the unavailability of good commercial antibodies. Figure 43 shows a representative example of an immunoblot for perilipin 5, using an antibody purchased from COMPAÑÍA. Samples were lysates from LN18 cells treated over a time course with KH buffer without glucose, and whole tissue-rat heart lysates, which had been proposed by the manufacturer as a good

positive control for perilipin 5. The antibody detected multiple bands between 100 and 37 KDa in all our samples, including the positive controls. The bands closer to the predicted molecular weight for perilipin 5 (≈ 50 KDa, Wolins et al., 2006) have been highlighted in red. The presence of multiple bands in our positive controls could not be avoided by lowering sample or antibody concentrations (not shown), and hampered the interpretation of the results.

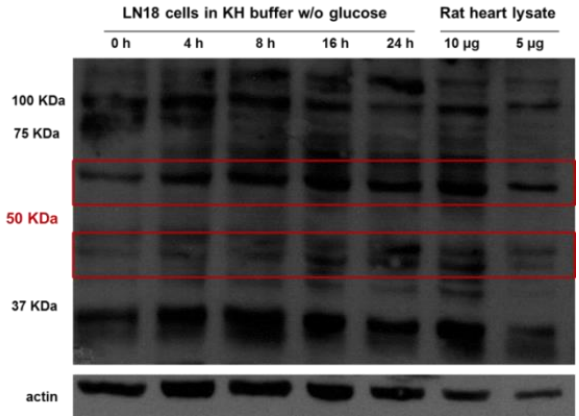

Figure 43. Immunoblot for perilipin 5

A guinea pig anti-perilipin 5 antibody purchased from COMPAÑÍA detected multiple bands between 37 and 100 KDa in lysates from LN18 cells treated over a time course with KH without glucose, and whole-tissue hart lysates that were used as control. The bands closer to the predicted molecular weight for perilipin 5 have been highlighted in red, and exhibit an increased intensity at longer treatments with KH buffer without glucose. However, the presence of multiple bands in the controls hampered the interpretation of the results.

A perilipin 5 antiserum (kindly provided to us by Dr John T. Tansey, from Otterbein University, Ohio) yielded similar results (not shown). As an alternative approach, we used the antiserum to attempt perilipin 5 detection by immunocytochemistry. To that end, we transfected LN18 cells with siRNA designed against perilipin 5 or control siRNA, and induced the formation of lipid droplets by a 16 hour treatment with KH buffer without glucose, or DMEM supplemented with 10% FBS. Treatment with KH buffer without glucose induced the appearance of puncta in the cytosol (Figure 44, panel A), which was sensitive to siRNA designed against perilipin 5 (panel B). However, when cells were maintained in DMEM + FBS, the antiserum did not detect cytosolic puncta (panels C and D).

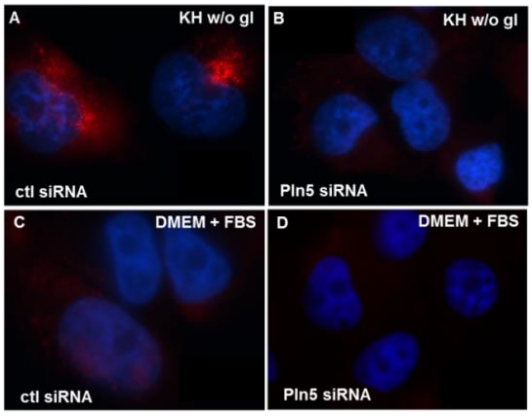

Figure 44. a perilipin 5 antiserum detects cytosolic puncta, which are sensitive to siRNA designed against perilipin 5, in cells treated with KH buffer without glucose
Immunocytochemistry assays revealed the appearance of cytosolic puncta that were detected by a perilipin 5 antiserum in cells treated with KH w/o glucose (panel A), but not in cells treated with DMEM + FBS (panels C and D), The signal was sensitive to transfection with siRNA designed against perilipin 5 (panel B).

LN18 cells transfected with siRNA designed against perilipin 5 died significantly more than control during a 16 hour treatment with KH without glucose (Figure 45, panel A). Perilipin 5 siRNA also induced a significant increase in starvation-triggered β-oxidation as compared to control siRNA (panel B).

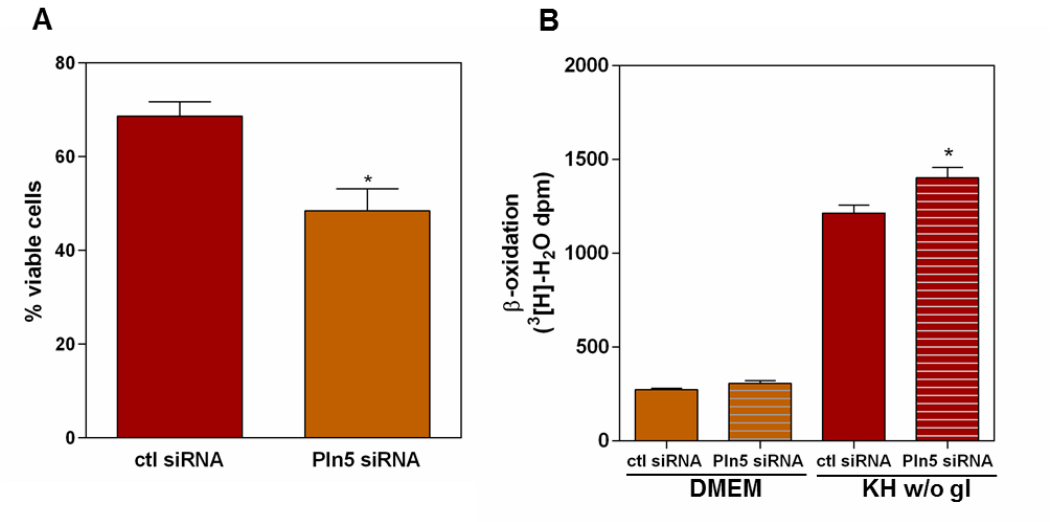

***Figure 45*. siRNA designed against perilipin 5 accelerates death and increases β-oxidation in starved cells.**

*A, LN18 cells were transfected with siRNA directed against perilipin 5, or control siRNA, and treated with KH buffer w/o glucose for 16 hours. Perilipin 5 siRNA caused a significant increase of cell death. Results are means ± SEM of three independent experiments carried out with duplicate determinations. *, significantly different from control siRNA. B, LN18 cells were transfected with perilipin 5 or control siRNA, and labeled with [^{3}H]palmitate for analysis of β-oxidation. SiRNA designed against perilipin 5 caused a significant increase in the release of [^{3}H]water triggered by complete nutrient deprivation. Results are means ± SEM of an experiment carried out with quadruplicate determinations, which was repeated twice with a similar outcome. *, significantly different from control siRNA*

These preliminary findings were in keeping with observations made in perilipin 5 *null* mice, which exhibit increased β-oxidation levels and subsequent decline of heart function due to the accumulation of reactive oxygen species (Kuramoto et al., 2012). However, our inability to monitor perilipin 5 expression by western blot did not allow making a reliable interpretation of the results.

The results presented in this section gather our attempts to understand the process of lipid droplet lipolysis that precedes starvation-triggered β-oxidation. Although we were unable to determine the mechanisms involved, our experiments yielded some interesting results.

When cells were switched from FBS-containing to FBS-free medium, inhibition or deficiency of autophagy caused a very significant delay on lipid droplet depletion. These findings agreed with observations made by others that starvation induces the selective sequestration

of lipid droplets into autophagosomes for lysosomal degradation (or “lipophagy”, reviewed by Christian et al., 2013). However, in the absence of autophagy, starvation-triggered lipid droplet occurrence over time maintained the bell-shaped distribution associated with an ongoing process of biogenesis and catabolism, and lipid droplets were still able to fuel β-oxidation and sustain cell survival.

Further, immunocytochemistry analysis revealed the appearance of cytosolic puncta that were detected by a perilipin 5 antiserum, and sensitive to treatment with siRNA designed against perilipin 5. Those puncta only arose when cells where treated with KH buffer without glucose, and where absent in cells maintained in culture medium with FBS. As explained above, our failure to reliably monitor perilipin 5 induction or silencing by immunoblot hindered our interpretation of these results. However, it is tempting to hypothesize that different regulatory mechanisms are at play when lipid droplets arise as a result of lipid availability or complete nutrient deprivation.

9. ACSL in the biogenesis and mobilization of starvation- and FBS-triggered lipid droplets

Collectively, the results presented so far reveal clear differences in the biology of lipid droplets induced by lipid availability or stress due to complete nutrient deprivation.

When confronted with an external lipid source, cells synthesize lipid droplets to avoid the toxic effects of excessive lipids in the cytosol, and to create an energy reservoir in case of need. However, we have shown that starvation-triggered lipid droplet formation is a survival response, whereby cells recycle fatty acids from structural moieties to use them as metabolic fuel through mitochondrial oxidation.

These findings, along with the observations made in the previous section, suggest that processes of lipid droplet formation and catabolism serve different functions, and are likely governed by different mechanisms, when they are induced by lipid availability or stress due to complete nutrient deprivation.

To further address this idea, we decided to study the process of fatty acid activation that precedes TAG synthesis and mitochondrial β-oxidation. As explained in the introduction, all pathways of fatty acid metabolism require the acyl-coenzyme A synthetase (ACS)–mediated conversion of fatty acids to acyl-CoAs. The presence of 26 distinct genes for ACS in the

human genome has led to hypothesize that each ACS has a unique role, directing the acyl-CoA product to a specific metabolic fate (Watkins et al., 2007).

Of the 5 isoforms of ACSL, three of them (ACSL1, 3 and 4) have been found in association with lipid droplets (reviewed by Mashek et al., 2010), and their competitive inhibitor Triacsin C has been reported to block neutral lipid synthesis and lipid droplet formation as a response to an external lipid influx (Igal et al., 1997; Fujimoto et al., 2007; Ujimoto et al., 2006; Liefhebber et al., 2014). In fact, Triacsin C is considered to be a potent inhibitor of lipid droplet biogenesis (Zou et al., 2014).

Taking these ideas into account, we hypothesized that the processes of lipid droplet formation and lipid droplet-fueled β-oxidation were initiated by different ACSL isoforms when triggered by lipid availability, or stress due to complete nutrient deprivation.

As a first approach, we treated LN18 cells with DMEM supplemented with FBS, and added [^{3}H]palmitic acid to measure fatty acid incorporation into TAG in the absence or presence of 10 μM Triacsin C. After an 8-hour treatment, cellular lipids were extracted as described (Bligh and Dyer, 1959), and separated by high performance thin layer chromatography. As expected, treatment with FBS induced de novo TAG synthesis, which was completely abrogated by inhibition of ACSL1, 3 and 4 with Triacsin C (figure 46).

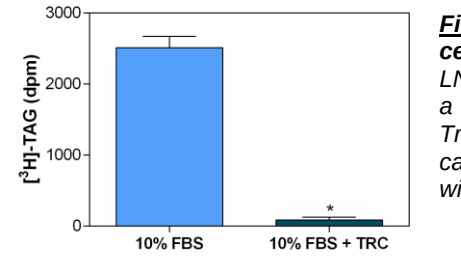

Figure 46 Treatment with Triacsin C abrogates TAG synthesis in cells treated with DMEM + FBS
*LN18 cells maintained in DMEM + FBS synthesized TAG (black bar) in a process that was completely abrogated by ACSL inhibition with Triacsin C (blue bar). Results are means ± SEM of an experiment carried out with quadruplicate determinations, which was repeated twice with a similar outcome. *. Significantly different from DMEM + FBS*

Once we had confirmed that Triacsin C blocked TAG synthesis in cells treated with DMEM + FBS, we aimed to study its effects on lipid droplet biogenesis. To that effect, we deprived LN18 cells of serum overnight and switched them to culture medium supplemented with FBS, or KH buffer without glucose, in the presence or absence of 10 μM Triacsin C (Figure 47). As expected, both FBS and KH buffer without glucose induced the appearance of lipid droplets (panels A and C, respectively), and Triacsin C precluded lipid droplet formation in cells maintained in FBS-containing medium (panel B). However, the drug did not affect the ability of nutrient-deprived cells to synthesize lipid droplets (panel D).

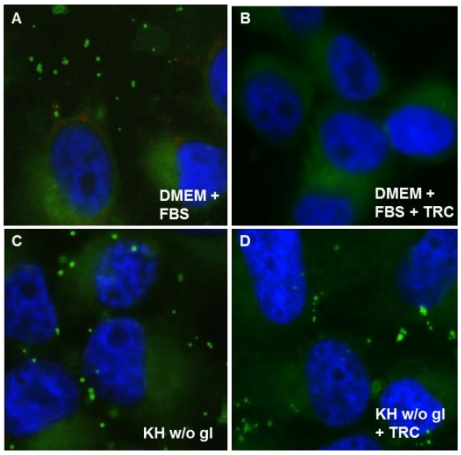

Figure 47. Treatment with Triacsin C inhibits lipid droplet biogenesis triggered by FBS, but not by KH buffer without glucose.
LN18 cells were deprived of serum overnight, and switched to DMEM + FBS, or KH buffer without glucose, in the absence or presence of Triacsin C Fluorescence microscopy of cells stained with BODIPY493/503 revealed that both FBS (A) and KH w/o glucose (C) induced the formation of lipid droplets, which was inhibited by Triacsin C in cells maintained in DMEM + FBS (B). However, treatment with Triacsin C did not block starvation-triggered lipid droplet formation (D)

Flow cytometry analysis of LN18 cells treated for 16 hours with increasing concentrations of Triacsin C further supported these finding (Figure 48). A 2,5 µM concentration of Triacsin C was sufficient to significantly reduce lipid droplet occurrence in cells maintained in DMEM + 10% FBS (panel A). However, increasing concentrations of the drug failed to preclude starvation-triggered lipid droplet formation (panel B).

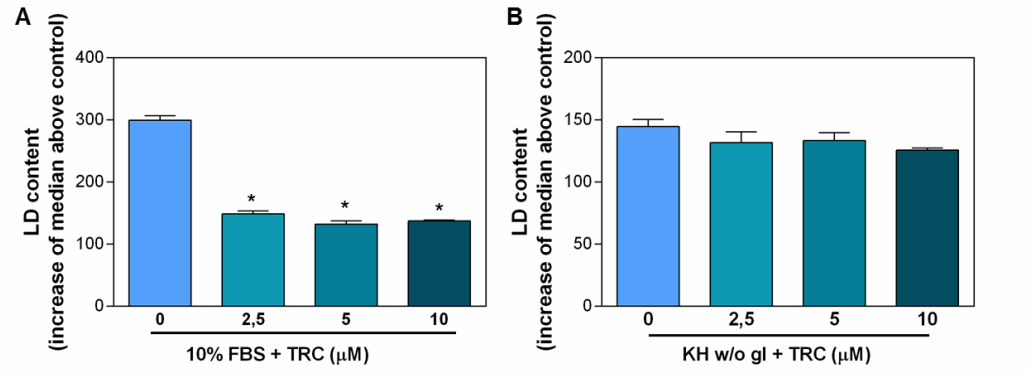

Figure 48. Treatment with Triacsin C inhibits lipid droplet biogenesis triggered by FBS, but not by KH buffer without glucose.

*LN18 cells were deprived of serum overnight, and switched to DMEM + FBS, or KH buffer without glucose, in the absence or presence of increasing concentrations of Triacsin C. At all concentrations, Triacsin C significantly reduced lipid droplet occurrence in cells maintained in DMEM + FBS (A). However, the drug had no effect on lipid droplet biogenesis triggered by complete nutrient deprivation (B). Results are means ± SEM of three independent experiments carried out with duplicate determinations. *, significantly different from DMEM + FBS.*

These findings supported our hypothesis that lipid droplet biogenesis is initiated by different ACSL isoforms when triggered by an external lipid source, or stress due to complete nutrient deprivation.

To further characterize the effect of ACLS1, 3 and 4 inhibition with Triacsin C, LN18 cells were deprived of serum overnight and switched to FBS-containing DMEM, or KH buffer without glucose, and in the absence or presence of 5 μM Triacsin C. Cells were harvested over a time-course of 24 hours for flow cytometry analysis of viability (Figure 49). Cells treated with DMEM + FBS or KH buffer without glucose maintained viability for 24 hours (solid bars). Triacsin C did not affect survival of cells in DMEM + FBS, but significantly accelerated death of nutrient-deprived cells.

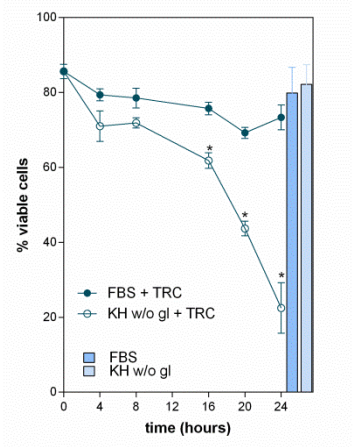

Figure 49. Treatment with Triacsin C accelerates death of nutrient-deprived cells.

*LN18 cells were deprived of serum overnight, and switched to DMEM + FBS, or KH buffer without glucose, in the absence or presence of Triacsin C Flow cytometry analysis of viability revealed that cells treated with DMEM + FBS or KH buffer w/o glucose maintained viability for 24 hours (solid bars). Treatment with Triacsin C had no effect on cells maintained in DMEM + FBS (solid symbols), but significantly accelerated death of nutrient-deprived cells (open symbols). Results are means ± SEM of three independent experiments carried out with duplicate determinations. *, significantly different from FBS + Triacsin C (TRC).*

Since nutrient-deprived cells were still able to synthesize lipid droplets in the presence of Triacsin C, we reasoned that the toxic effect of the drug was due to their inability to use lipid droplets to fuel fatty acid oxidation. To test that idea, we deprived LN18 cells of serum overnight and labeled them with [^{3}H]palmitic acid. Cells were treated for 5 hours with DMEM or KH buffer without glucose in the absence or presence of increasing concentrations of Triacsin C (Figure 50). The treatment time was reduced from the usual 7 hours due to the perceivable (although not significant) decrease of viability at short treatment times (see Figure 49).

As we expected, Triacsin C precluded β-oxidation at all the concentrations employed, reducing the emission of [^{3}H]water to the levels obtained by inhibiting β-oxidation with EX.

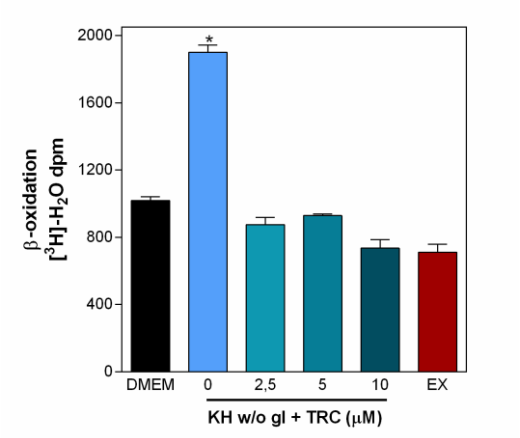

Figure 50. Treatment with Triacsin C precludes starvation-triggered β-oxidation
*LN18 cells were labeled with [^{3}H]palmitic acid and treated with DMEM or KH w/o glucose in the absence (light blue bar) or presence of increasing concentrations of Triacsin C (blue bars) or 30 μM EX (red bar). B-oxidation, measured as the EX-sensitive release of [^{3}H]water, was significantly potentiated by KH w/o glucose, and completely abrogated by treatment with Triacsin C. Results are means ± SEM of an experiment carried out with quadruplicate determinations and repeated twice with a similar outcome. *, significantly different from DMEM.*

Taken together, the results presented so far show that inhibition of ACSL1, 3 and 4 with Triacsin C has different effects on cells treated with FBS-containing DMEM or KH buffer without glucose. Triacsin C completely abrogated TAG synthesis and lipid droplet biogenesis induced by lipid availability, but did not preclude lipid droplet formation triggered by complete nutrient deprivation. However, inhibition of ACSL1, 3 and 4 had a toxic effect on cells treated with KH buffer without glucose. This argued for a role of those ACSL in the activation of fatty acids that precedes mitochondrial oxidation. Consistently, their inhibition with Triacsin C completely abrogated starvation-induced β-oxidation.

We had previously observed that, during complete nutrient deprivation, inhibition of β-oxidation with EX caused a very significant accumulation of lipid droplets, which was apparent in both viable and dead cells, and mirrored by an increase on TAG content. However, treatment with Triacsin C failed to induce lipid droplet accumulation (as shown in Figure 48).

To study the effect of Triacsin C on TAG synthesis triggered by starvation, we labeled serum-starved LN18 cells with [^{3}H]palmitic acid and switched them to DMEM or KH buffer without glucose in the absence or presence of Triacsin C or EX. After a 5 hour treatment, cellular lipids were extracted and separated by high performance thin layer chromatography (Figure 51).

Treatment with KH without glucose strongly induced the synthesis of TAG as compared to cells treated with serum-free DMEM, confirming our previous observations (panel A). Treatment with EX (red bar) induced a significant further accumulation of TAG, in agreement with our previous observations (shown in Figure 26). Importantly, treatment with Triacsin C did not block TAG synthesis. However, we observed a significant Triacsin C-induced

accumulation of non-esterified fatty acids (panel B), as compared to cells treated with KH buffer without glucose alone, or in the presence of EX.

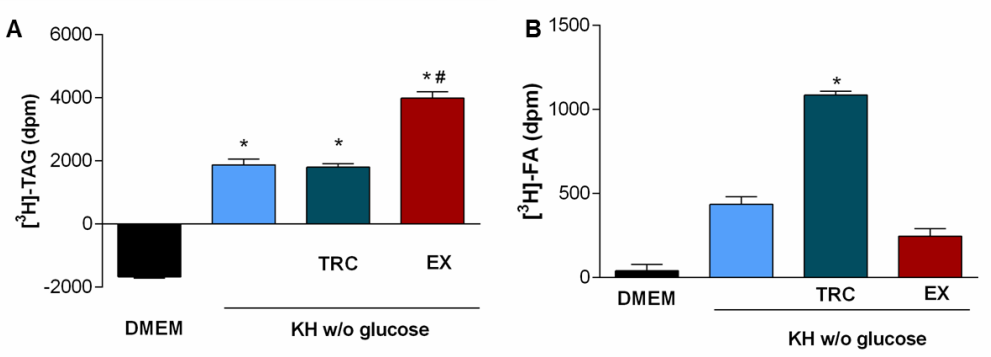

Figure 51. ***Treatment with Triacsin C induces the accumulation of non-esterified fatty acids.***

*LN18 cells were labeled with [^{3}H]palmitic acid and treated with DMEM (black bars) or KH w/o glucose in the absence (light blue bars) or presence of increasing concentrations of Triacsin C (blue bars) or 30 μM EX (red bars).A, treatment with KH buffer without glucose strongly induced TAG synthesis, as compared to cells treated with DMEM, and treatment with EX caused a further significant TAG accumulation. Treatment with Triacsin C did not preclude TAG synthesis. B, Treatment with Triacsin C led to a significant accumulation of non-esterified fatty acids Results are means ± SEM of an experiment carried out with quadruplicate determinations, which was repeated twice with a similar outcome. *, significantly different from DMEM (panel A) or KH buffer without glucose (panel B).$^{\#}$, significantly different from KH buffer without glucose.*

Taken together, our results suggest that, during complete nutrient deprivation, TAG synthesis from endogenous fatty acid moieties is initiated by an isoform of ACSL which is not inhibited by Triacsin C. This is evidenced by the ability of LN18 cells to synthesize both TAG and lipid droplets as a response to starvation in the presence of increasing concentrations of the drug. However, the utilization of fatty acids released from lipid droplet TAG to fuel mitochondrial oxidation is sensitive to treatment with Triacsin C. This is made apparent by the complete abrogation of β-oxidation induced by Triacsin C, as well as the accumulation of non-esterified fatty acids, and explains the toxicity of the drug during complete nutrient deprivation.

FUURE DIRECTIONS

Experiments with siRNAs designed against each of the five ACSL isoforms have been undertaken to elucidate precisely which isoenzymes initiate the crucial processes of starvation-triggered TAG synthesis and β-oxidation.

Silenced expression of ACSL1, 3 or 4 did not affect the ability of LN18 cells to synthesize lipid droplets during a 16 hour treatment with KH buffer without glucose (Figure 52, panel A). However, silencing the enzymes caused a significant decrease of viability (panel B), which was more apparent in cells treated with siRNA designed against ACSL1 and ACSL4 (panel B). The increased toxicity of those siRNAs was mirrored by the significant reduction they induced on starvation-triggered β-oxidation (panel C). Silenced expression of ACSL3, which had a very limited effect on survival to starvation, did not significantly block β-oxidation.

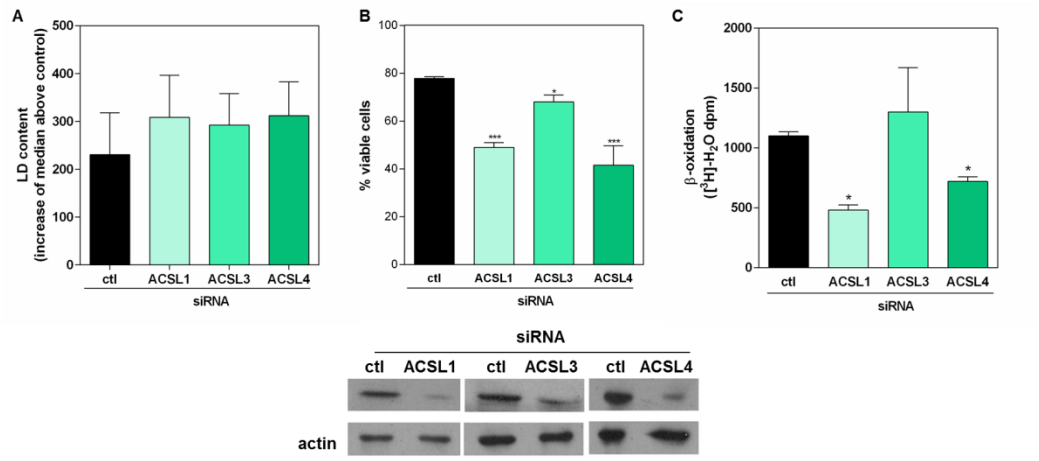

Figure 52. ACSL1 and ACSL4 appear to be the isoforms involved in fatty acid activation leading to mitochondrial oxidation

*LN18 cells were transfected with siRNA designed against ACSL1, 3, 4 or control, deprived of serum overnight, and switched to KH buffer w/o glucose.After a 16 hour treatment, cells were harvested and stained with Nile red for flow cytometry analysis of lipid droplet content and survival. ACSL1, 3 and 4 had no significant effect on lipid droplet content, but caused a significant (ACSL3) or very significant (ACSL1 and ACSL4) decrease of survival to starvation. Results are means ± SEM of two independent experiments carried out with duplicate determinations. *, significantly different from control; **p<0.0001 (different from control). C, LN18 cells transfected with ACSL or control siRNAs were labeled with [^{3}H]palmitic acid and switched to KH buffer without glucose. Complete nutrient deprivation induced the release of [^{3}H]water, which was significantly reduced by silenced expression of ACSL1 and ACSL4, but not ACSL3. Results are means ± SEM of one experiment carried out with quadruplicate determinations. *, significantly different from control.*

Together, this preliminary findings support the hypothesis that ACSL isoforms have sepparate functions, and suggest that ACSL1 and ACSL4 are the isoenzymes responsible for the activation of fatty acids that initiates mitochondrial oxidation triggered by stress.

Further experiments should aim to optimize the silencing of these ACSL, and to study their involvement in TAG synthesis and fatty acid oxidation triggered by an external lipid source.

An article published in 2009 by Mashima et al. reported that extracellular acidosis induced toxicity in human glioma cells, which was precluded by overexpression of ACSL5 and exacerbated by its silencing with siRNA (Mashima et al., 2009). Previous results from our group have shown that acidic pH is one of the signals that triggers TAG synthesis and lipid droplet formation from structural fatty acid moieties (shown in Figure 6 of the introduction, Gubern et al., 2009b). With these ideas in mind, it is tempting to hypothesize that ACSL5 might be the isoenzyme involved in lipid droplet formation triggered by stress.

Our preliminary experiments with siRNA designed against ACSL5 have yielded promising results, showing a significant reduction of lipid droplet content (Figure 53, panel A) and survival to starvation (panel B) in cells treated with KH buffer without glucose. Treatment with siRNA designed against ACSL6 caused a smaller, but significant, reduction of lipid droplet content and survival.

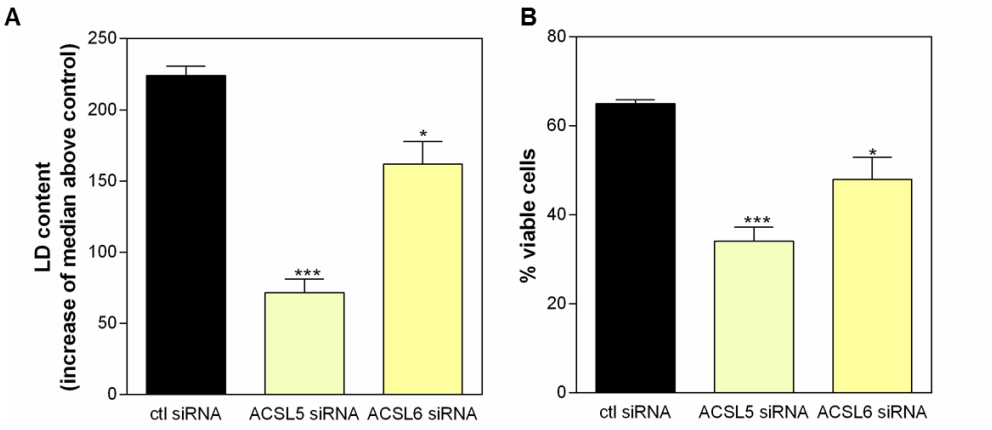

Figure 53 . ACSL5 and ACSL6 appear to be the isoforms involved in fatty acid activation leading to lipid droplet formation

*LN18 cells were transfected with siRNA designed against ACSL15, 6 or control, deprived of serum overnight, and switched to KH buffer w/o glucose.After a 16 hour treatment, cells were harvested and stained with Nile red for flow cytometry analysis of lipid droplet content and survival. Silenced expression of the isoenzymes caused a significant (ACSL6) or very significant (ACSL5) decrease on lipid droplet content (A) and cell survival (C). Results are means ± SEM of two independent experiments carried out with duplicate determinations. *, significantly different from control; ***p<0.0001 (different from control).*

DISCUSSION

Lipid droplet biogenesis induced by complete nutrient deprivation is a survival strategy, aimed at recycling phospholipid-linked fatty acids for energy generation.

The formation of lipid droplets is a hallmark of cellular stress that can be observed from yeast to humans. Lipid droplet biogenesis has been assessed in processes of hypoxia, inflammation, nutrient deprivation or apoptosis (Boren and Brindle, 2012; Jiang et al., 2012; Bozza and Viola, 2010). The formation of lipid droplets in cancer cells is thought to be a stress response to the tumor microenvironment, which is often characterized by conditions of hypoxia/ischemia or acidic pH (Delikatny et al., 1996). The neutral lipids at the core of lipid droplets give raise to NMR-visible signals, which are now routinely used to monitor tumor progression and response to treatment (Zietkowski et al., 2012). Further, lipid droplets are considered to be a hallmark of ischemic but viable tissue (Barba et al., 2009), and it has been observed that lipid droplets accumulate in myocardium surviving an acute coronary occlusion (Straeter-Knowlen et al., 1996).

Taken together, these findings suggest that the ability to synthesize lipid droplets in response to stress is a universal feature. However, very few studies have aimed to identify the underlying mechanisms or physiological significance of this process. Previous results from our group have shown that stress caused by different insults triggered the $iPLA_2$-VIA-mediated release of fatty acids from membrane phospholipids. Those fatty acids were used to synthesize triacylglycerols (TAG), which were subsequently packaged into lipid droplets in a process dependent on $cPLA_2\alpha$ activity (Gubern et al., 2009b). Under these conditions, overexpression of $iPLA_2$-VIA increased TAG synthesis and delayed cell death. The protective effect of increased TAG synthesis was precluded by blocking lipid droplet formation (Gubern et al., 2009b).

These findings, together with the apparent protective effect of lipid droplet formation in ischemia-reperfusion injury (Barba et al., 2009) or neuron survival to starvation (Du et al., 2009), led us to hypothesize that stress-triggered lipid droplet biogenesis is a cell survival strategy. Given the fact that TAG at the core of stress-induced lipid droplets are synthesized from fatty acids released from pre-existing phospholipids, we proposed that, in this situation, lipid droplet formation is a process akin to autophagy, whereby structural lipid components are recycled to TAG for energy production.

To study the physiological role of stress-triggered lipid droplet biogenesis, we selected complete nutrient deprivation as a model for stress induction. Several types of stress had been previously assayed by our group, and they all had been found to induce TAG synthesis

and lipid droplet formation through the same iPLA-VIA/cPLA2α-dependent mechanism. However, complete nutrient deprivation was the strongest stimulus in terms of TAG synthesis and lipid droplet occurrence (Gubern et al., 2009b). Therefore, cells were maintained in serum-free culture medium to deplete FBS-induced lipid droplets, and switched to KH buffer without glucose. This experimental setting was designed to ensure that lipid droplets arose exclusively as a result of our stressor.

Flow cytometry analysis of Nile red-stained cells proved to be an ideal way to simultaneously monitor lipid droplet occurrence and cell survival to complete nutrient deprivation. Forward/Side Scatter plots revealed that cells were divided into two distinct populations, characterized by different size. Only the population composed of smaller cells was permeable to propidium iodide (PI), which allowed us to quantify viable cells based on their size, in the absence of PI co-staining.

We determined that treatment with KH buffer without glucose induced the appearance of lipid droplets, in a manner that was sensitive to inhibition of $cPLA_2\alpha$ with py-2, or silenced expression of the enzyme. In all cell types tested, starvation-triggered lipid droplet occurrence followed a bell-shaped distribution over time.

Separate gating of the two populations in the FS/SS plots revealed that dead cells were consistently depleted of lipid droplets, as compared to viable ones. Inhibition of lipid droplet biogenesis during starvation led to a very significant acceleration of cell death, but had no effect on control cells maintained in serum-free culture medium. Further, the presence of a pre-existing lipid droplet reservoir before starvation (achieved by maintaining cells in culture medium supplemented with FBS and 100 µM oleic acid before switching them to KH buffer without glucose) significantly extended survival to starvation. Together, these findings supported our hypothesis that starvation-triggered lipid droplets had a cell-protective effect.

The bell-shaped profile of lipid droplet occurrence over time suggested an ongoing process of biogenesis and mobilization that seemed relevant for survival to starvation, given the toxic effects of py-2, and was in keeping with a possible catabolic use of lipid droplets triggered by starvation. Indeed, we determined that treatment with KH buffer without glucose induced TAG synthesis from pre-existing fatty acids, and an increase of mitochondrial β-oxidation. Importantly, in all cell types tested, starvation-triggered β-oxidation was precluded by inhibition of lipid droplet biogenesis with py-2.

Pharmacological inhibition of β-oxidation with EX, an irreversible inhibitor of carnitine palmitoyltransferase (CPT1), caused a further accumulation of TAG during nutrient

deprivation, which was mirrored by a very significant increase on lipid droplet content in both viable and dead cells. Importantly, inhibition of β-oxidation caused a dramatic acceleration of cell death during complete nutrient deprivation, but was not toxic for cells maintained in serum-free culture medium. The fact that cells treated with EX died full of lipid droplets was in keeping with a need for their mobilization to fuel β-oxidation. Further evidence was provided by studying the survival of lipid droplet-preloaded cells to a long treatment with KH buffer without glucose. The protective effect of a pre-existing lipid droplet reservoir was completely abrogated by EX.

It has long been known that cancer cells exhibit an aberrant metabolism, which is characterized by an enhanced uptake of glucose and production of lactic acid under aerobic conditions (Kim and Dang, 2006). The tendency of cancer cells to favor aerobic glycolysis instead of the Krebs cycle, which is much more efficient in terms of ATP production, has been proposed to facilitate the production of biomass, and hence tumor growth and progression (Vander Heiden et al., 2009). The study of this feature of cancer cells (known as the Warburg effect), has uncovered that many oncogenes and tumor suppressor genes act as central regulators of cellular metabolism (Kim and Kim, 2013). In this context, the relevance of fatty acid catabolism on cancer cell function has gained increased attention over the last few years (reviewed by Carracedo et al., 2013).

It has been observed that, although aerobic glycolysis is usually enough to sustain cancer cell function (Vander Heiden et al., 2009), certain situations, such as loss of attachment (LOA) to the extracellular matrix, can trigger metabolic stress. Cells undergoing LOA exhibit inhibition of glucose uptake and catabolism, which results in the loss of ATP, NADPH, and increased production of reactive oxygen species (ROS) (Carracedo et al., 2013). Under these circumstances, fatty acid oxidation is critical to provide ATP and prevent LOA-induced cell death (Schafer et al., 2009; Carracedo et al., 2012). Interestingly, the promyelocytic leukaemia (PML) protein has been observed to regulate fatty acid oxidation in a manner dependent on peroxisome proliferator-activated receptors (PPARs). PML increases fatty acid oxidation, and provides a selective advantage to breast cancer cells undergoing metabolic stress. PML is overexpressed in a subset of aggressive breast cancer specimens, and correlates with poor prognosis and activated PPAR signaling (Carracedo et al., 2012).

Further evidence for the relevance of fatty acid oxidation in cancer cell function was provided by Zaugg and coworkers, who reported the identification of carnitine palmitoyltransferase 1C (CPT1C), a brain-specific CPT1 enzyme, as a potential oncogene which may participate in metabolic transformation. Tumor cells constitutively expressing CPT1C showed increased

fatty acid oxidation, ATP production, and resistance to glucose deprivation or hypoxia. Conversely, cancer cells lacking CPT1C produced less ATP and were more sensitive to metabolic stress. CPT1C depletion via siRNA suppressed xenograft tumor growth. In vivo, CPT1C could be induced by hypoxia or glucose deprivation (Zaugg et al., 2011). More recently, Schlaepfer and coworkers reported that pharmacological inhibition of CPT1A with EX resulted in decreased fatty acid oxidation, which was toxic for prostate cancer cells. Treatment of nude mice with EX resulted in decreased xenograft tumor growth (Schlaepfer et al., 2014).

Our results have evidenced that, under complete nutrient deprivation, cell survival becomes strictly dependent on fatty acid oxidation, which is accompanied by an increased expression of CPT1A, and preceded by a process of TAG synthesis from phospholipid-linked fatty acid sources, and their subsequent packaging into lipid droplets. In this regard, similar to the inhibition of β-oxidation with EX, precluding the formation of lipid droplets with py-2 abrogates fatty acid oxidation and accelerates the death of starved cells, but it does not affect the viability of cells that do not depend on fatty acid catabolism.

As mentioned above, complete nutrient deprivation is not the only type of stress that triggers lipid droplet biogenesis from pre-existing fatty acids. Other stressors tested by our group, such as acidic pH, inhibition of fatty acid synthase (FAS) or induction of endoplasmic reticulum stress induced the formation of lipid droplets through the same iPLA-VIA/cPLA$_2$α-dependent mechanism (Gubern et al., 2009b).

Further, it has been observed that lipid droplets arise in tumors as a result of acidic pH, glucose deprivation or hypoxia (reviewed by Delikatny et al., 2011). The presence of lipid droplets correlates with tumor necrosis, and several studies have identified lipid droplets in viable tissue surrounding the necrosis (Freitas et al, 1990; Rémy et al, 1997; Lahrech et al, 2001; Zoula et al, 2001). The accumulation of lipid droplets in viable tumoral cells located at the periphery of necrosis is thought to result from stress induced by the hypoxic state of these cells (Freitas et al, 1990, 1996; Kuesel et al, 1994). Tumor hypoxia has long been considered as a limiting factor in association with poorer outcome after radiotherapy, chemotherapy and surgery (Zoula et al., 2003). Interestingly, a recent report by Trinitato and coworkers identified lipid droplets as a distinctive marker of cancer stem cells in colorectal cancer. Xenotransplantation experiments demonstrated that colorectal cancer stem cells overexpressing lipid droplets retained the highest tumorigenic potential (Tirinato et al., 2014).

In this context, our observations suggest that lipid droplet biogenesis triggered by the stressors present in the tumor microenvironment could offer a metabolic advantage to cancer cells, and that targeting lipid droplet formation might be an attractive therapeutic approach.

Since our model of stress-triggered β-oxidation that sustains cell survival requires a previous step of lipid droplet biogenesis, and its inhibition is only toxic for cells that depend on fatty acid catabolism, it might be worth pursuing further studies to test whether pharmacological inhibition of $cPLA_2\alpha$ with py-2 could prove useful as an adjuvant antitumor therapy to target fatty acid oxidation.

Different mechanisms are involved in the biogenesis and mobilization of lipid droplets triggered by lipid availability, or stress due to complete nutrient deprivation

The life cycle and physiological role of lipid droplets induced by exogenous lipid availability have been extensively studied. Although some steps in the various processes of biogenesis and mobilization remain unknown or controversial, there is general agreement that lipid droplet content arising from the medium has a storing purpose for energy generation and membrane building (reviewed by Beller et al., 2010). On the other hand, our results evidence that lipid droplet biogenesis triggered by starvation is a cell survival strategy, aimed at recycling phospholipid-bound fatty acids for energy generation in the mitochondria.

Our results seem to indicate that this functional diversity is accompanied by differences in the processes that govern lipid droplet biogenesis and mobilization when it is triggered by lipid availability, or stress due to complete nutrient deprivation.

Lipid droplet biogenesis induced by complete nutrient deprivation is insensitive to treatment with Triacsin C

It has long been known that Triacsin C blunts lipid droplet formation, by inhibiting the long-chain acyl-CoA synthases (ACSL) that catalyze the activation of fatty acids required for TAG synthesis (Iorio, 2003; Zou et al., 2014). Of the five isoforms of ACSL, only three (ACSL1, 3 and 4) are sensitive to inhibition by Triacsin C (Fujimoto et al., 2007; Liefhebber et al., 2014).

The existence of several ACSL isoforms has led to hypothesize that they might have different functions, directing their acyl-CoA products towards specific metabolic fates (Watkins et al.,

2007; Ellis et al., 2010). Our observation that starvation-triggered β-oxidation of fatty acids requires the formation of lipid droplets also implies a metabolic channeling, aimed at ensuring that acyl-CoA pools derived from lipid droplet mobilization do not mix with other acyl-CoA pools within the cytosol. Otherwise, neither the synthesis of TAG from acyl-CoA, nor their packaging into lipid droplets would be necessary, and the release of fatty acids from phospholipids by $iPLA_2$-IVA and their activation by ACSL would meet the requirement to fuel mitochondrial oxidation.

Our results evidenced that competitive inhibition of ACSL1, 3 and 4 with Triacsin C had the expected blunting effect on lipid droplet biogenesis when it was induced by an external lipid source. Cells maintained in serum-enriched culture medium exhibited synthesis of TAG and lipid droplet formation, which was blocked by a treatment with 2,5 µM Triacsin C. Importantly, cells maintained in KH buffer without glucose still synthesized TAG and lipid droplets in the presence of increasing (2,5-10 µM) concentrations of Triacsin C.

The observed toxicity of Triacsin C during complete nutrient deprivation suggested that ACSL1, 3 and 4 isoenzymes might be required at a later step, in the activation of fatty acids released from lipid droplets that initiates mitochondrial oxidation. In agreement with that, Triacsin C precluded starvation-induced β-oxidation, and led to the accumulation of non-esterified fatty acids.

These findings support the hypothesis that ACSL isoenzymes exhibit a functional diversity, and show that starvation-triggered TAG synthesis and lipid droplet formation to fuel β-oxidation is likely initiated by Triacsin C-insensitive ACSL. The intervention of those specific ACSL isoforms might ensure the efficient channeling of phospholipid-linked fatty acids released by $iPLA_2$-VIA towards mitochondrial oxidation.

Our preliminary experiments with siRNA directed against each of the ACSL isoenzymes have revealed that ACSL1 and 4 are likely involved in the activation of fatty acids for β-oxidation, whereas ACSL5 and 6 seem to intervene at the step that initiates TAG synthesis. Although the results are still preliminary, and the silencing has not been fully optimized, we have observed that ACSL5 siRNA causes a very significant inhibition of lipid droplet biogenesis induced by starvation, which is mirrored by an increased cell death.

ACSL5 is often overexpressed in glioma cell lines, as well as primary gliomas of grade IV malignancy (Yamashita et al., 2000). In experiments performed on human glioma cell lines, as well as in vivo, Mashima and coworkers observed that ACSL5 promoted cell survival to extracellular acidosis conditions. Using extracellular acidic pH to mimic the stress conditions

of the tumor microenvironment, Mashima et al observed that inhibition of ACSL5 expression significantly reduced cell viability under the acidic state, but did not affect cells under normal conditions. The protective effect of ACSL5 was dependent on its enzymatic activity, and could not be reproduced by an inactive ACSL5 mutant. Further, in vivo treatment with ACSL5 siRNA significantly suppressed the tumorigenic potential of A1207 cells in mice (Mashima et al., 2009).

In this context, it is tempting to hypothesize that ACSL5 might contribute to the tumorigenic potential of glioma cell lines by ensuring an increased channeling of fatty acids towards energy generation, via synthesis of TAG from phospholipid-linked fatty acids, and lipid droplet formation. This channeling could provide a metabolic advantage to glioma cells, and contribute to their adaptation to the tumor microenvironment. In this regard, the results of Mashima and coworkers are similar to those obtained by Schlaepfer et al, who found that inhibition of β-oxidation with EX in nude mice resulted in decreased xenograft tumor growth (Schlaepfer et al., 2014).

Interestingly, survival of glioma cell lines was only dependent on ACSL5 activity under stress, but not for cells that were maintained in normal culture conditions (Mashima et al., 2009). These findings are compatible with our observations that inhibition of lipid droplet biogenesis or β-oxidation is only toxic in starved cells, and has no effect on cells maintained in culture medium.

Future work should aim to optimize the silencing of ACSL isoenzymes, in order to confirm our preliminary results, and to further investigate the functional diversity of ACSL isoenzymes and their involvement in the different steps of stress-triggered lipid droplet biology, regarding the possible selective channeling of phospholipid-linked fatty acids towards β-oxidation in situations of stress.

Autophagy is not involved in the process of lipid droplet lipolysis that precedes starvation-triggered β-oxidation.

Several groups have observed that autophagy participates in lipid catabolism, through the selective sequestration of lipid droplets into autophagosomes and their targeting to lysosomes for degradation. In liver, autophagy participates in constitutive lipid droplet degradation, but autophagy-mediated lipid droplet clearance is augmented in response to external stimuli, such as treatment with fatty acids or starvation (Weidberg et al., 2009; Singh

and Cuervo, 2012; Liu and Czaja, 2013) (Figure 54). The starvation-induced selective targeting of lipid droplets to lysosomes via their sequestration into autophagosomes has been observed in hepatocytes both in vivo and in vitro (Singh et al., 2009; Skop et al., 2012; Schulze et al., 2013; Lee et al., 2014), and in a variety of other cell types, including neurons (Martinez-Vicente et al., 2010; Kaushik et al., 2011) and stellate cells (Hernández-Gea et al., 2012).

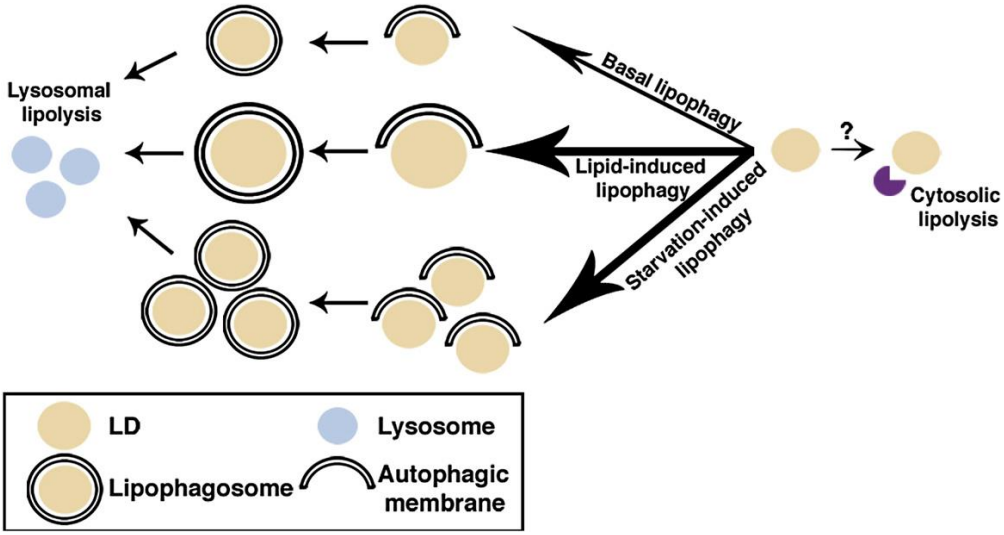

Figure 54. Schematic model for lipophagy (lipid droplet autophagy)

Under normal growth conditions, lipid droplets are degraded at a basal level via the autophagic pathway (top). Elevation in free fatty acids stimulates lipid droplet growth and induces lipid droplet degradation by lipophagy (middle). Under stress conditions, such as starvation, the selective degradation of lipid droplets by lipophagy increases, thus providing cells with needed nutrients (bottom). The role of the cytosolic lipases and a possible crosstalk with the autophagic process, both in basal and stimulated lipolysis, has not been determined (Weidberg et al., 2009)

In agreement with those findings, we observed that when cells were switched from FBS-containing to FBS-free culture medium, inhibition or deficiency of autophagy caused a very significant lag on lipid droplet depletion. However, treatment with 3-methyladenine (3-MA) or knocked down expression of the autophagy related protein Atg5 did not completely prevent lipid droplet clearance, which was finally achieved at longer treatments with serum-free culture medium, probably due to the compensatory action of cytosolic lipases. A recent article by Dupont and coworkers reported similar results. HeLa cells stably expressing a dominant negative mutant of the autophagy related protein Atg2 still achieved lipid droplet depletion after treatment with oleic acid and subsequent serum starvation (Dupont et al., 2014).

Treatment with KH buffer without glucose induced autophagy, but its inhibition or deficiency did not accelerate cell death or preclude lipid droplet-fueled β-oxidation. Lipid droplet occurrence in the absence of autophagy maintained the bell-shaped distribution associated with an ongoing process of biogenesis and catabolism, and β-oxidation proceeded without significant differences from control cells.

A small but significant accumulation of lipid droplets was observed in LN18 cells treated with 3-MA or Atg5 KO MEF cells during a time-course treatment with KH buffer without glucose. However, this effect is not likely to reflect a selective targeting of lipid droplets by the autophagic machinery aimed at providing metabolic fuel, given the lack of effect of autophagy deficiency or inhibition in fatty acid oxidation. Singh and coworkers have reported that lipid droplets are often partially or totally sequestered into autophagosomes in basal conditions, as part of a nonselective “in bulk” process (Singh et al., 2009).

Interestingly, the absence of autophagy significantly prolonged the survival of LN18 and Atg5 KO MEF cells to complete nutrient deprivation, and we observed a similar effect in HeLa and CHO K1 cells (not shown). In this regard, Du and coworkers reported that primary neurons from male and female rats exhibit sex differences in autophagy during nutrient deprivation. When treated with nutrients-free culture medium, neurons underwent a sex-dependent increase in autophagy, which was bigger in male neurons. Female neurons synthesized lipid droplets and exhibited an extended survival to starvation, which was abrogated by inhibition of lipid droplet biogenesis with py-2. Conversely, treatment with 3-MA significantly increased the survival of male neurons to starvation (Du et al., 2009)..

Together, these findings suggest that, in situations of stress due to critical nutrient deprivation, the metabolic channeling of phospholipid-linked fatty acids towards mitochondrial oxidation, via lipid droplet formation, is a more efficient way to generate energy and sustain survival than autophagy. In this context, the nonselective sequestration of lipid droplets by autophagosomes due to an ongoing process of starvation-triggered autophagy would partially prevent the correct channeling of fatty acids to the mitochondria. This would explain the protective effect of autophagy inhibition during starvation, as well as the observed increase in overall lipid droplet content.

Figures 55 and 56 are schematic representations of the processes of lipid droplet biogenesis and catabolism, as we have observed them in cells maintained in culture medium supplemented with FBS (Figure 55) or KH buffer without glucose (Figure 56).

When cells are maintained in FBS-containing culture medium, they synthesize TAG in the endoplasmic reticulum (ER), in a process that requires activation of fatty acids by Triacsin C-sensitive ACSL isoenzymes. Once the nascent lipid droplets have accumulated enough TAG, they are cleaved from the ER in a cPLA$_2$α-dependent manner (Gubern et al., 2008, 2009a; b; Du et al., 2009). In this situation, lipid droplet formation serves the dual purpose of buffering cells from the toxic effects of excessive cytosolic lipids, and generating a reservoir of fatty acids for future use. When lipid droplet-loaded cells are switched to FBS-free medium, lipid droplets are mobilized to release fatty acids for their use in anabolic or catabolic pathways. The significant delay on lipid droplet depletion that results from inhibiting autophagy suggests that the autophagic machinery might be involved in the process. However, complete depletion is achieved through continued serum starvation, evidencing the action of cytosolic lipases (Figure 55).

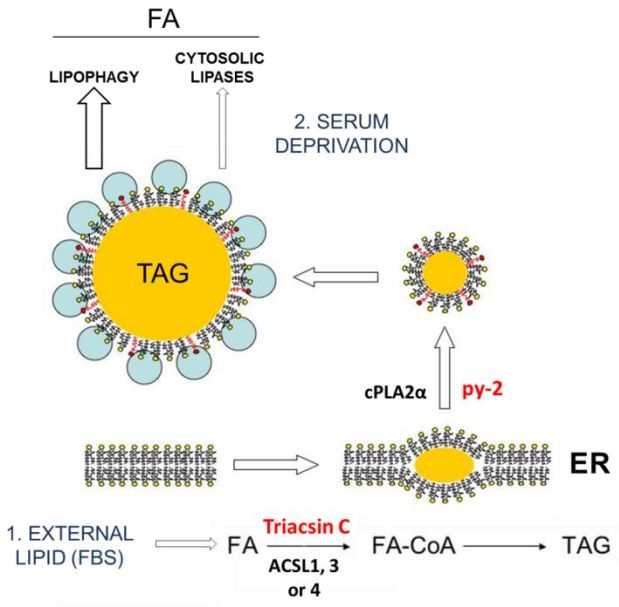

Figure 55. ***FBS-triggered lipid droplet formation and mobilization***

When cells are depleted of lipid droplets, treatment with KH buffer without glucose triggers the release of fatty acids from phospholipids, in a process that requires iPLA$_2$-VIA activity (Gubern et al., 2009b). Those fatty acids are used to synthesize TAG, in a process which is initiated by the Triacsin C-insensitive ACSL isoenzymes 5 or 6. Once the newly synthesized

TAG have accumulated sufficiently, lipid droplets are cleaved from the ER in a cPLA$_2$α-mediated manner. Through a process of lipolysis, which is independent of autophagy and likely catalyzed by cytosolic lipases, fatty acids are released from lipid droplet TAG, and subsequently esterified to CoA A by Triacsin C-sensitive ACSL isoenzymes. The resulting acyl-CoAs are used as substrates for mitochondrial oxidation. . In this situation, lipid droplet biogenesis constitutes a survival response to starvation, aimed at recycling fatty acids from structural moieties for mitochondrial oxidation (Figure 56).

Treatment with EX irreversibly inhibits CPT1A, blocking the entrance of acyl-CoA to the mitochondria and precluding β-oxidation. Starved cells treated with EX exhibited a very significant accumulation of lipid droplets, which was mirrored by an increased TAG content as compared to cells treated with KH buffer without glucose alone. This accumulation was not apparent when β-oxidation was inhibited by blocking fatty acid activation with Triacsin C. A possible explanation is that acyl-CoA unable to access the mitochondrial matrix might be re-esterified into TAG (Edens et al., 1990), contributing to a further lipid droplet accumulation. Conversely, treatment with Triacsin C results in an accumulation of free fatty acids, which cannot be re-esterified into TAG, or used in any other metabolic pathway.

The relevance of lipid droplet biogenesis and catabolism for survival to starvation is evidenced by the toxic effect of drugs or siRNAs directed against the key enzymes that regulate this process. Inhibition of cPLA2α with py-2 abrogated lipid droplet formation, and dramatically accelerated cell death in all cell types tested, in a way that was mirrored by the effect of inhibiting β-oxidation with EX. Further, Triacsin C precluded the activation of fatty acids that initiates β-oxidation, and had a similar toxic effect on nutrient-deprived cells. Importantly, those treatments did not affect the survival of cells maintained in serum-free culture medium, which did not depend on fatty acid catabolism.

In agreement with previous observations from our group (Gubern et al., 2009b), inhibition of iPLA$_2$-VIA with BEL was very toxic for nutrient-deprived cells, and it also affected cells maintained in complete culture medium (not shown). Other than iPLA$_2$-VIA, BEL also inhibits phosphatidate phosphohydrolase (PAP) which mediates the dephosphorylation of phosphatidic acid, a major precursor of diacylglycerol (DAG)) (Balsinde and Dennis, 1996; Balboa et al., 1998). Therefore, targeting the formation of lipid droplets at the later step of cPLA$_2$α-mediated release from the ER membrane was a more specific approach.

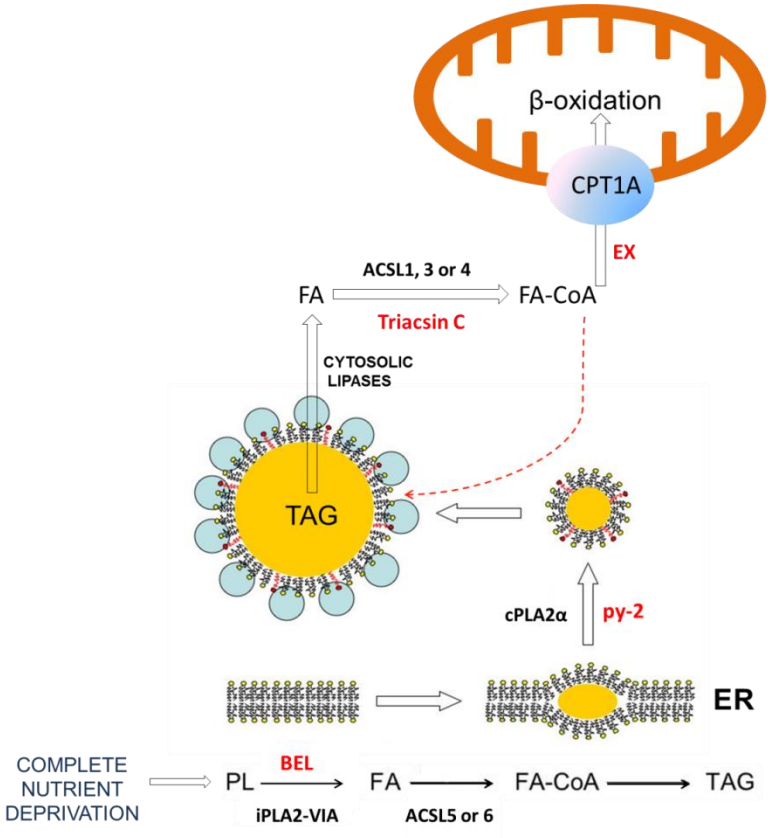

Figure 56. ***starvation-triggered lipid droplet formation and mobilization***

Taken together, our results evidence that lipid droplets induced by an external lipid source or stress due to complete nutrient deprivation have different functions, which are mirrored by differences in the processes mediating their formation and catabolism. This could reflect the existence of an orchestrated metabolic switch, aimed at sustaining cell survival to starvation.

Peroxisome-activated receptor α (PPARα) is a ligand-activated transcription factor whose expression is enriched in tissues with high fatty acid oxidation rates, although it is also expressed in many other tissues and cells (Pawlak et al., 2014). PPARα ligands are fatty acids or fatty acid derivatives formed during lipolysis, lipogenesis or fatty acid catabolism (Reid et al., 2008), and many of its target genes, such as CPT1 or ACSL, are involved in fatty acid metabolism (Reddy, 2001). Interestingly, perilipin 5 expression is also regulated by PPARα, and PPARα-induced expression of perilipin 5 in the fasted liver appears to be part of an expression program that shifts the metabolism from fatty acid storage to oxidation (Wolins et al., 2006; Dalen et al., 2007; Wang et al., 2011; Granneman et al., 2011). Interestingly, Laurenti and coworkers reported that hypoxia induces PPARα-mediated expression of lipid

metabolism enzymes in samples from human glioblastoma multiforme patients, in a way that highly correlated with lipid droplet content and the degree of malignancy (Laurenti et al., 2011).

Our results reflect that, under complete nutrient deprivation, cell survival becomes strictly dependent on lipid droplet-fueled β-oxidation of fatty acids. This process is preceded by the iPLA2-VIA-mediated release of fatty acids from phospholipids, and their activation by Triacsin C-insensitive ACSL isoforms for TAG synthesis, and accompanied by the overexpression of CPT1A. Preliminary findings using siRNA designed against perilipin 5 have shown that treatment with KH buffer without glucose, but not with FBS-containing medium, induces the appearance of cytosolic puncta which are detected by perilipin 5 antiserum, and sensitive to treatment with perilipin 5 siRNA.

In this context, it might be worth investigating a possible stress-induced activation of PPARα signaling, that could be involved in orchestrating a metabolic switch aimed at channeling phospholipid-linked fatty acids towards mitochondrial oxidation, to provide metabolic fuel and sustain cell survival.

CONCLUSIONS

The work presented in this Thesis has led to the following conclusions

- Lipid droplet biogenesis induced by complete nutrient deprivation is a cell survival strategy

- During complete nutrient deprivation, cell survival is sustained by a process of TAG synthesis from phospholipid-linked fatty acids, and their subsequent packaging into lipid droplets, which are later mobilized to fuel mitochondrial β-oxidation.

- Starvation-induced lipid droplet lipolysis is independent of autophagy, and is not regulated by perilipins 2 and 3.

- TAG synthesis and lipid droplet biogenesis induced by an external lipid source is sensitive to inhibition of ACSL1, 3 and 4 with Triacsin C. However, TAG synthesis and lipid droplet formation triggered by complete nutrient deprivation are initiated by Triacsin C-insensitive isoforms of ACSL.

BIBLIOGRAPHY

abcam. Flow cytometry guide.

Abounit, K., T.M. Scarabelli, and R.B. Mccauley. 2012. Autophagy in mammalian cells. *World J. Biol. Chem.* 3:1–6. doi:10.4331/wjbc.v3.i1.TOPIC.

Alonzi, T., C. Agrati, B. Costabile, C. Cicchini, L. Amicone, C. Cavallari, C. Della Rocca, A. Folgori, C. Fipaldini, F. Poccia, N. La Monica, and M. Tripodi. 2004. Steatosis and intrahepatic lymphocyte recruitment in hepatitis C virus transgenic mice. *J. Gen. Virol.* 85:1509–20.

Alvisi, G., V. Madan, and R. Bartenschlager. 2011. Hepatitis c virus and host cell lipids: An intimate connection. *RNA Biol.* 8:258–269. doi:10.4161/rna.8.2.15011.

Aon, M. a., N. Bhatt, and S.C. Cortassa. 2014. Mitochondrial and cellular mechanisms for managing lipid excess. *Front. Physiol.* 5:1–13. doi:10.3389/fphys.2014.00282.

Balboa, M., J. Balsinde, A. Dennis, and E.A. Dennis. 1998. Involvement of Phosphatidate Phosphohydrolase in Arachidonic Acid Mobilization in Human Amnionic WISH Cells Involvement of Phosphatidate Phosphohydrolase in Arachidonic Acid Mobilization in Human Amnionic WISH Cells *. *J. Biol. Chem.* 273:7684–7690. doi:10.1074/jbc.273.13.7684.

Balsinde, J., and E.A. Dennis. 1996. Bromoenol Lactone Inhibits Phosphohydrolase and Blocks Triacylglycerol Biosynthesis in Mouse Bromoenol Lactone Inhibits Magnesium-dependent Phosphatidate Phosphohydrolase and Blocks Triacylglycerol Biosynthesis in Mouse P388D. *J. Biol. Chem.* 271:3197–31941. doi:10.1074/jbc.271.50.31937.

Balsinde, J., R. Pérez, and M.A. Balboa. 2006. Calcium-independent phospholipase A2 and apoptosis. *Biochim. Biophys. Acta*. 1761:1344–50. doi:10.1016/j.bbalip.2006.07.013.

Barba, I., L. Chavarria, M. Ruiz-Meana, M. Mirabet, E. Agulló, and D. Garcia-Dorado. 2009. Effect of intracellular lipid droplets on cytosolic Ca2+ and cell death during ischaemia-reperfusion injury in cardiomyocytes. *J. Physiol.* 587:1331–41. doi:10.1113/jphysiol.2008.163311.

Barbero, P., E. Buell, S. Zulley, and S.R. Pfeffer. 2001. TIP47 is not a component of lipid droplets. *J. Biol. Chem.* 276:24348–51. doi:10.1074/jbc.M102468200.

Barth, S., D. Glick, and K.F. Macleod. 2010. Autophagy: assays and artifacts. *J. Pathol.* 221:117–24. doi:10.1002/path.2694.

BD Biosciences. 2000. Introduction to Flow Cytometry: A Learning Guide.

Belfrage, P., B. Jergil, P. Strålfors, and H. Tornqvist. 1977. Hormone-sensitive lipase of rat adipose tissue: identification and some properties of the enzyme protein. *FEBS Lett.* 75:259–64.

Bell, M., H. Wang, H. Chen, J.C. McLenithan, D.-W. Gong, R.-Z. Yang, D. Yu, S.K. Fried, M.J. Quon, C. Londos, and C. Sztalryd. 2008. Consequences of lipid droplet coat protein downregulation in liver cells: abnormal lipid droplet metabolism and induction of insulin resistance. *Diabetes*. 57:2037–45. doi:10.2337/db07-1383.

Beller, M., K. Thiel, P.J. Thul, and H. Jäckle. 2010. Lipid droplets: a dynamic organelle moves into focus. *FEBS Lett.* 584:2176–82. doi:10.1016/j.febslet.2010.03.022.

Bickel, P.E., J.T. Tansey, and M.A. Welte. 2009. PAT proteins, an ancient family of lipid droplet proteins that regulate cellular lipid stores. *Biochim. Biophys. Acta*. 1791:419–440. doi:10.1016/j.bbalip.2009.04.002.PAT.

Birnbaum, M.J. 2003. Lipolysis: more than just a lipase. *J. Cell Biol.* 161:1011–2. doi:10.1083/jcb.200306008.

Bligh, E.G., and W.J. Dyer. 1959. A rapid method of total lipid extraction and purification. *Can. J. Biochem. Physiol.* 37:911–7.

Boden, G., X. Chen, J. Ruiz, J. V White, and L. Rossetti. 1994. Mechanisms of fatty acid-induced inhibition of glucose uptake. *J. Clin. Invest.* 93:2438–46. doi:10.1172/JCI117252.

Boren, J., and K.M. Brindle. 2012. Apoptosis-induced mitochondrial dysfunction causes cytoplasmic lipid droplet formation. *Cell Death Differ.* 19:1561–70. doi:10.1038/cdd.2012.34.

Bortner, C.D., and J.A. Cidlowski. 2002. Apoptotic volume decrease and the incredible shrinking cell. *Cell Death Differ.* 9:1307–10. doi:10.1038/sj.cdd.4401126.

Bose, S.K., and R. Ray. 2014. Hepatitis C virus infection and insulin resistance. *World J. Diabetes*. 5:52–8. doi:10.4239/wjd.v5.i1.52.

Bosma, M., R. Minnaard, L.M. Sparks, G. Schaart, M. Losen, M.H. de Baets, H. Duimel, S. Kersten, P.E. Bickel, P. Schrauwen, and M.K.C. Hesselink. 2012. The lipid droplet coat protein perilipin 5 also localizes to muscle mitochondria. *Histochem. Cell Biol.* 137:205–16. doi:10.1007/s00418-011-0888-x.

Boström, P., L. Andersson, M. Rutberg, J. Perman, U. Lidberg, B.R. Johansson, J. Fernandez-Rodriguez, J. Ericson, T. Nilsson, J. Borén, and S.-O. Olofsson. 2007. SNARE proteins mediate fusion between cytosolic lipid droplets and are implicated in insulin sensitivity. *Nat. Cell Biol.* 9:1286–93. doi:10.1038/ncb1648.

Boulant, S., M.W. Douglas, L. Moody, A. Budkowska, P. Targett-Adams, and J. McLauchlan. 2008. Hepatitis C virus core protein induces lipid droplet redistribution in a microtubule- and dynein-dependent manner. *Traffic*. 9:1268–82. doi:10.1111/j.1600-0854.2008.00767.x.

Bozza, P.T., and J.P.B. Viola. 2010. Lipid droplets in inflammation and cancer. *Prostaglandins. Leukot. Essent. Fatty Acids*. 82:243–50. doi:10.1016/j.plefa.2010.02.005.

Brasaemle, D.L. 2007. Thematic review series: adipocyte biology. The perilipin family of structural lipid droplet proteins: stabilization of lipid droplets and control of lipolysis. *J. Lipid Res.* 48:2547–59. doi:10.1194/jlr.R700014-JLR200.

Brasaemle, D.L., T. Barber, N.E. Wolins, G. Serrero, E.J. Blanchette-Mackie, and C. Londos. 1997. Adipose differentiation-related protein is an ubiquitously expressed lipid storage droplet-associated protein. *J. Lipid Res.* 38:2249–63.

Brasaemle, D.L., and N.E. Wolins. 2012. Packaging of fat: An evolving model of lipid droplet assembly and expansion. *J. Biol. Chem.* 287:2273–2279. doi:10.1074/jbc.R111.309088.

Brown, W.J., K. Chambers, and A. Doody. 2003. Phospholipase A2 (PLA2) enzymes in membrane trafficking: mediators of membrane shape and function. *Traffic*. 4:214–21.

Buhman, K.K., H.C. Chen, and R. V Farese. 2001. The enzymes of neutral lipid synthesis. *J. Biol. Chem.* 276:40369–72. doi:10.1074/jbc.R100050200.

Cabodevilla, A.G., L. Sánchez-Caballero, E. Nintou, V.G. Boiadjieva, F. Picatoste, A. Gubern, and E. Claro. 2013. Cell survival during complete nutrient deprivation depends on lipid droplet-fueled β-oxidation of fatty acids. *J. Biol. Chem.* 288:27777–88. doi:10.1074/jbc.M113.466656.

Carracedo, A., L.C. Cantley, and P.P. Pandolfi. 2013. Cancer metabolism: fatty acid oxidation in the limelight Arkaitz. *Nat Rev Cancer*. 13:227–232. doi:10.1038/nrc3483.Cancer.

Carracedo, A., D. Weiss, A.K. Leliaert, M. Bhasin, V.C.J. De Boer, G. Laurent, A.C. Adams, M. Sundvall, S.J. Song, K. Ito, L.S. Finley, A. Egia, T. Libermann, Z. Gerhart-hines, P. Puigserver, M.C. Haigis, E. Maratos-flier, A.L. Richardson, Z.T. Schafer, and P.P. Pandolfi. 2012. A metabolic prosurvival role for PML in breast cancer. 122. doi:10.1172/JCI62129DS1.

Chang, B.H.-J., L. Li, A. Paul, S. Taniguchi, V. Nannegari, W.C. Heird, and L. Chan. 2006. Protection against fatty liver but normal adipogenesis in mice lacking adipose differentiation-related protein. *Mol. Cell. Biol.* 26:1063–76. doi:10.1128/MCB.26.3.1063-1076.2006.

Chaves, V.E., D. Frasson, and N.H. Kawashita. 2011. Several agents and pathways regulate lipolysis in adipocytes. *Biochimie*. 93:1631–40. doi:10.1016/j.biochi.2011.05.018.

Chen, B., X. Sun, Y. Zhang, X.-Q. Zhu, and H.-M. Shen. 2012. Use of inducible Atg5 deletion and expression cell lines in study of the pro-survival function of autophagy under starvation. *Biochem. Biophys. Res. Commun.* 427:11–7. doi:10.1016/j.bbrc.2012.08.117.

Christian, P., J. Sacco, and K. Adeli. 2013. Autophagy: Emerging roles in lipid homeostasis and metabolic control. *Biochim. Biophys. Acta*. 1831:819–24. doi:10.1016/j.bbalip.2012.12.009.

Cole, N.B., D.D. Murphy, T. Grider, S. Rueter, D. Brasaemle, and R.L. Nussbaum. 2002. Lipid droplet binding and oligomerization properties of the Parkinson's disease protein alpha-synuclein. *J. Biol. Chem.* 277:6344–52. doi:10.1074/jbc.M108414200.

Coleman, R.A., and R.M. Bell. 1978. Evidence that biosynthesis of phosphatidylethanolamine, phosphatidylcholine and triacylglycerol occurs on the cytoplasmic side of microsomal vesicles. *J. Cell Biol.* 76:245–253.

Czaja, M.J., W.-X. Ding, T.M. Donohue, S.L. Friedman, J.-S. Kim, M. Komatsu, J.J. Lemasters, A. Lemoine, J.D. Lin, J.J. Ou, D.H. Perlmutter, G. Randall, R.B. Ray, A. Tsung, and X.-M. Yin. 2013. Functions of autophagy in normal and diseased liver. *Autophagy*. 9:1131–58. doi:10.4161/auto.25063.

Dalen, K.T., T. Dahl, E. Holter, B. Arntsen, C. Londos, C. Sztalryd, and H.I. Nebb. 2007. LSDP5 is a PAT protein specifically expressed in fatty acid oxidizing tissues. *Biochim. Biophys. Acta*. 1771:210–27. doi:10.1016/j.bbalip.2006.11.011.

Debeer, L.J., J. Thomas, P.J. De Schepper, J. Thomas, and J. De Schepper. 1979. lipolysis in isolated rat hepatocytes . P Mannaerts Lysosomal Triacylglycerol Hepatocytes * Lipase and Lipolysis in Isolated Rat. *J. Biol. Chem.* 254:8841–8846.

Delikatny, E.J., S. Chawla, D.-J. Leung, and H. Poptani. 2011. MR-visible lipids and the tumor microenvironment. *NMR Biomed.* 24:592–611. doi:10.1002/nbm.1661.

Delikatny, E.J., C.M. Lander, T.M. Jeitner, R. Hancock, and C.E. Mountford. 1996. Modulation of MR-visible mobile lipid levels by cell culture conditions and correlations with chemotactic response. *Int. J. Cancer*. 65:238–45. doi:10.1002/(SICI)1097-0215(19960117)65:2<238::AID-IJC18>3.0.CO;2-9.

Diaz, G., M. Melis, B. Batetta, F. Angius, and A.M. Falchi. 2008. Hydrophobic characterization of intracellular lipids in situ by Nile Red red/yellow emission ratio. *Micron*. 39:819–24. doi:10.1016/j.micron.2008.01.001.

Diez, E., P. Louis-Flamberg, R.H. Hall, and R.J. Mayer. 1992. Substrate specificities and properties of human phospholipases A2 in a mixed vesicle model. *J. Biol. Chem.* 267:18342–8.

Djouadi, F., J.P. Bonnefont, A. Munnich, and J. Bastin. 2003. Characterization of fatty acid oxidation in human muscle mitochondria and myoblasts. *Mol. Genet. Metab.* 78:112–8.

Du, L., R.W. Hickey, H. Bayir, S.C. Watkins, V. a Tyurin, F. Guo, P.M. Kochanek, L.W. Jenkins, J. Ren, G. Gibson, C.T. Chu, V.E. Kagan, and R.S.B. Clark. 2009. Starving neurons show sex difference in autophagy. *J. Biol. Chem.* 284:2383–96. doi:10.1074/jbc.M804396200.

Ducharme, N. a, and P.E. Bickel. 2008. Lipid droplets in lipogenesis and lipolysis. *Endocrinology*. 149:942–9. doi:10.1210/en.2007-1713.

Dupont, N., S. Chauhan, J. Arko-Mensah, E.F. Castillo, A. Masedunskas, R. Weigert, H. Robenek, T. Proikas-Cezanne, and V. Deretic. 2014. Neutral lipid stores and lipase PNPLA5 contribute to autophagosome biogenesis. *Curr. Biol.* 24:609–20. doi:10.1016/j.cub.2014.02.008.

Edens, N.K., R.L. Leibel, and J. Hirsch. 1990. Mechanism of free fatty acid re-esterification in human adipocytes in vitro. *J. Lipid Res.* 31:1423–31.

Egan, J.J., a S. Greenberg, M.K. Chang, S. a Wek, M.C. Moos, and C. Londos. 1992. Mechanism of hormone-stimulated lipolysis in adipocytes: translocation of hormone-sensitive lipase to the lipid storage droplet. *Proc. Natl. Acad. Sci. U. S. A.* 89:8537–41.

Ellis, J.M., J.L. Frahm, L.O. Li, and R.A. Coleman. 2010. Acyl-coenzyme A synthetases in metabolic control. *Curr. Opin. Lipidol.* 21:212–7.

Farese, R. V, and T.C. Walther. 2009. Lipid droplets finally get a little R-E-S-P-E-C-T. *Cell*. 139:855–60. doi:10.1016/j.cell.2009.11.005.

Fredrikson, G., H. Tornqvist, and P. Belfrage. 1986. Hormone-sensitive lipase and monoacylglycerol lipase are both required for complete degradation of adipocyte triacylglycerol. *Biochim. Biophys. Acta*. 876:288–93.

Freitas, I., B. Bono, V. Bertone, P. Griffini, G.F. Baronzio, L. Bonandrini, and G. Gerzeli. 1996. Characterization of the metabolism of perinecrotic cells in solid tumors by enzyme histochemistry. *Anticancer Res.* 16:1491–502.

Freitas, I., P. Pontiggia, S. Barni, V. Bertone, M. Parente, A. Novarina, G. Roveta, G. Gerzeli, and P. Stoward. 1990. Histochemical probes for the detection of hypoxic tumour cells. *Anticancer Res.* 10:613–22.

Friis, M.B., C.R. Friborg, L. Schneider, M.-B. Nielsen, I.H. Lambert, S.T. Christensen, and E.K. Hoffmann. 2005. Cell shrinkage as a signal to apoptosis in NIH 3T3 fibroblasts. *J. Physiol.* 567:427–43. doi:10.1113/jphysiol.2005.087130.

Fujimoto, Y., H. Itabe, T. Kinoshita, K.J. Homma, J. Onoduka, M. Mori, S. Yamaguchi, M. Makita, Y. Higashi, A. Yamashita, and T. Takano. 2007. Involvement of ACSL in local synthesis of neutral lipids in cytoplasmic lipid droplets in human hepatocyte HuH7. *J. Lipid Res.* 48:1280–92. doi:10.1194/jlr.M700050-JLR200.

Granneman, J.G., H.-P.H. Moore, E.P. Mottillo, Z. Zhu, and L. Zhou. 2011. Interactions of perilipin-5 (Plin5) with adipose triglyceride lipase. *J. Biol. Chem.* 286:5126–35. doi:10.1074/jbc.M110.180711.

Greenberg, A.S., J.J. Egan, S.A. Wek, N.B. Garty, E.J. Blanchette-Mackie, and C. Londos. 1991. Perilipin, a major hormonally regulated adipocyte-specific phosphoprotein associated with the periphery of lipid storage droplets. *J. Biol. Chem.* 266:11341–11346.

Greenspan, P., E.P. Mayer, and S.D. Fowler. 1985. Nile red: a selective fluorescent stain for intracellular lipid droplets. *J. Cell Biol.* 100:965–73.

Gruber, A., I. Cornaciu, A. Lass, M. Schweiger, M. Poeschl, C. Eder, M. Kumari, G. Schoiswohl, H. Wolinski, S.D. Kohlwein, R. Zechner, R. Zimmermann, and M. Oberer. 2010. The N-terminal region of comparative gene identification-58 (CGI-58) is important for lipid droplet binding and activation of adipose triglyceride lipase. *J. Biol. Chem.* 285:12289–98. doi:10.1074/jbc.M109.064469.

Gubern, A., M. Barceló-Torns, D. Barneda, J.M. López, R. Masgrau, F. Picatoste, C.E. Chalfant, J. Balsinde, M. a Balboa, and E. Claro. 2009a. JNK and ceramide kinase

govern the biogenesis of lipid droplets through activation of group IVA phospholipase A2. *J. Biol. Chem.* 284:32359–69. doi:10.1074/jbc.M109.061515.

Gubern, A., M. Barceló-Torns, J. Casas, D. Barneda, R. Masgrau, F. Picatoste, J. Balsinde, M. a Balboa, and E. Claro. 2009b. Lipid droplet biogenesis induced by stress involves triacylglycerol synthesis that depends on group VIA phospholipase A2. *J. Biol. Chem.* 284:5697–708. doi:10.1074/jbc.M806173200.

Gubern, A., J. Casas, M. Barceló-Torns, D. Barneda, X. de la Rosa, R. Masgrau, F. Picatoste, J. Balsinde, M. a Balboa, and E. Claro. 2008. Group IVA phospholipase A2 is necessary for the biogenesis of lipid droplets. *J. Biol. Chem.* 283:27369–82. doi:10.1074/jbc.M800696200.

Gujar, S.K., S. Maheshwari, I. Björkman-Burtscher, and P.C. Sundgren. 2005. Magnetic resonance spectroscopy. *J. Neuroophthalmol.* 25:217–26.

Guo, F., Y. Ma, A.K.G. Kadegowda, J.L. Betters, P. Xie, G. Liu, X. Liu, H. Miao, J. Ou, X. Su, Z. Zheng, B. Xue, H. Shi, and L. Yu. 2013. Deficiency of liver Comparative Gene Identification-58 causes steatohepatitis and fibrosis in mice. *J. Lipid Res.* 54:2109–20. doi:10.1194/jlr.M035519.

Haemmerle, G., A. Lass, R. Zimmermann, G. Gorkiewicz, C. Meyer, J. Rozman, G. Heldmaier, R. Maier, C. Theussl, S. Eder, D. Kratky, E.F. Wagner, M. Klingenspor, G. Hoefler, and R. Zechner. 2006. Defective lipolysis and altered energy metabolism in mice lacking adipose triglyceride lipase. *Science*. 312:734–7. doi:10.1126/science.1123965.

Haemmerle, G., R. Zimmermann, M. Hayn, C. Theussl, G. Waeg, E. Wagner, W. Sattler, T.M. Magin, E.F. Wagner, and R. Zechner. 2002. Hormone-sensitive lipase deficiency in mice causes diglyceride accumulation in adipose tissue, muscle, and testis. *J. Biol. Chem.* 277:4806–15. doi:10.1074/jbc.M110355200.

Hakumäki, J.M., and R.A. Kauppinen. 2000. 1H NMR visible lipids in the life and death of cells. *Trends Biochem. Sci.* 25:357–62.

Harris, C., E. Herker, R. V Farese, and M. Ott. 2011. Hepatitis C virus core protein decreases lipid droplet turnover: a mechanism for core-induced steatosis. *J. Biol. Chem.* 286:42615–25. doi:10.1074/jbc.M111.285148.

Vander Heiden, M.G., L.C. Cantley, and C.B. Thompson. 2009. Understanding the Warburg Effect: The Metabolic Requirements of Cell Proliferation Matthew. *Science (80-.).* 324:1029–1033. doi:10.1126/science.1160809.Understanding.

Herker, E., and M. Ott. 2011. Unique ties between hepatitis C virus replication and intracellular lipids. *Trends Endocrinol. Metab.* 22:241–8. doi:10.1016/j.tem.2011.03.004.

Hernández-Gea, V., Z. Ghiassi-Nejad, R. Rozenfeld, R. Gordon, M.I. Fiel, Z. Yue, M.J. Czaja, and S.L. Friedman. 2012. Autophagy releases lipid that promotes fibrogenesis by activated hepatic stellate cells in mice and in human tissues. *Gastroenterology*. 142:938–46. doi:10.1053/j.gastro.2011.12.044.

Hirsch, a H., and O.M. Rosen. 1984. Lipolytic stimulation modulates the subcellular distribution of hormone-sensitive lipase in 3T3-L1 cells. *J. Lipid Res.* 25:665–77.

Huttunen, J.K., D. Steinberg, and S.E. Mayer. 1970. ATP-dependent and cyclic AMP-dependent activation of rat adipose tissue lipase by protein kinase from rabbit skeletal muscle. *Proc. Natl. Acad. Sci. U. S. A.* 67:290–5.

Igal, R. a, P. Wang, and R. a Coleman. 1997. Triacsin C blocks de novo synthesis of glycerolipids and cholesterol esters but not recycling of fatty acid into phospholipid: evidence for functionally separate pools of acyl-CoA. *Biochem. J.* 324 (Pt 2:529–534.

Imai, Y., G.M. Varela, M.B. Jackson, M.J. Graham, R.M. Crooke, and R.S. Ahima. 2007. Reduction of hepatosteatosis and lipid levels by an adipose differentiation-related protein antisense oligonucleotide. *Gastroenterology*. 132:1947–54. doi:10.1053/j.gastro.2007.02.046.

Imamura, M., T. Inoguchi, S. Ikuyama, S. Taniguchi, K. Kobayashi, N. Nakashima, and H. Nawata. 2002. ADRP stimulates lipid accumulation and lipid droplet formation in murine fibroblasts. *Am. J. Physiol. Endocrinol. Metab.* 283:E775–83. doi:10.1152/ajpendo.00040.2002.

Iorio, E. 2003. Triacsin C inhibits the formation of 1H NMR-visible mobile lipids and lipid bodies in HuT 78 apoptotic cells. *Biochim. Biophys. Acta - Mol. Cell Biol. Lipids*. 1634:1–14. doi:10.1016/j.bbalip.2003.07.001.

Jaber, N., Z. Dou, J.-S. Chen, J. Catanzaro, Y.-P. Jiang, L.M. Ballou, E. Selinger, X. Ouyang, R.Z. Lin, J. Zhang, and W.-X. Zong. 2012. Class III PI3K Vps34 plays an essential role in autophagy and in heart and liver function. *Proc. Natl. Acad. Sci. U. S. A.* 109:2003–8. doi:10.1073/pnas.1112848109.

Jacquier, N., S. Mishra, V. Choudhary, and R. Schneiter. 2013. Expression of oleosin and perilipins in yeast promotes formation of lipid droplets from the endoplasmic reticulum. *J. Cell Sci.* 126:5198–209. doi:10.1242/jcs.131896.

Jenkins, C.M., D.J. Mancuso, W. Yan, H.F. Sims, B. Gibson, and R.W. Gross. 2004. Identification, cloning, expression, and purification of three novel human calcium-independent phospholipase A2 family members possessing triacylglycerol lipase and acylglycerol transacylase activities. *J. Biol. Chem.* 279:48968–75. doi:10.1074/jbc.M407841200.

Jiang, H.P., and G. Serrero. 1992. Isolation and characterization of a full-length cDNA coding for an adipose differentiation-related protein. *Proc. Natl. Acad. Sci. U. S. A.* 89:7856–60.

Jiang, L., T.R. Greenwood, D. Artemov, V. Raman, P.T. Winnard, R.M. a Heeren, Z.M. Bhujwalla, and K. Glunde. 2012. Localized hypoxia results in spatially heterogeneous metabolic signatures in breast tumor models. *Neoplasia*. 14:732–41. doi:10.1593/neo.12858.

Jiang, P., M. Gan, W.-L. Lin, and S.-H.C. Yen. 2014. Nutrient deprivation induces α-synuclein aggregation through endoplasmic reticulum stress response and SREBP2 pathway. *Front. Aging Neurosci.* 6:268. doi:10.3389/fnagi.2014.00268.

Kassan, A., A. Herms, A. Fernández-Vidal, M. Bosch, N.L. Schieber, B.J.N. Reddy, A. Fajardo, M. Gelabert-Baldrich, F. Tebar, C. Enrich, S.P. Gross, R.G. Parton, and A. Pol. 2013. Acyl-CoA synthetase 3 promotes lipid droplet biogenesis in ER microdomains. *J. Cell Biol.* 203:985–1001. doi:10.1083/jcb.201305142.

Kaushik, S., J.A. Rodriguez-Navarro, E. Arias, R. Kiffin, S. Sahu, G.J. Schwartz, A.M. Cuervo, and R. Singh. 2011. Autophagy in hypothalamic AgRP neurons regulates food intake and energy balance. *Cell Metab.* 14:173–83. doi:10.1016/j.cmet.2011.06.008.

Khatchadourian, A., and D. Maysinger. Lipid droplets: their role in nanoparticle-induced oxidative stress. *Mol. Pharm.* 6:1125–37. doi:10.1021/mp900098p.

Khor, V.K., W.-J. Shen, and F.B. Kraemer. 2013. Lipid Droplet Metabolism. *Curr Opin Clin Nutr Metab Care*. 16:632–637. doi:10.1097/MCO.0b013e3283651106.Lipid.

Kim, J., and C. V Dang. 2006. Cancer's molecular sweet tooth and the Warburg effect. *Cancer Res.* 66:8927–30. doi:10.1158/0008-5472.CAN-06-1501.

Kim, M.H., and H. Kim. 2013. Oncogenes and Tumor Suppressors Regulate Glutamine Metabolism in Cancer Cells. *J. Cancer Prev.* 18:221–226. doi:10.15430/JCP.2013.18.3.221.

Kimmel, A.R., D.L. Brasaemle, M. McAndrews-Hill, C. Sztalryd, and C. Londos. 2010. Adoption of PERILIPIN as a unifying nomenclature for the mammalian PAT-family of intracellular lipid storage droplet proteins. *J. Lipid Res.* 51:468–71. doi:10.1194/jlr.R000034.

Kooijman, E.E., V. Chupin, B. de Kruijff, and K.N.J. Burger. 2003. Modulation of membrane curvature by phosphatidic acid and lysophosphatidic acid. *Traffic*. 4:162–74.

Kratky, D., S. Obrowsky, D. Kolb, and B. Radovic. 2014. Pleiotropic regulation of mitochondrial function by adipose triglyceride lipase-mediated lipolysis. *Biochimie*. 96:106–12. doi:10.1016/j.biochi.2013.06.023.

Kuramoto, K., T. Okamura, T. Yamaguchi, T.Y. Nakamura, S. Wakabayashi, H. Morinaga, M. Nomura, T. Yanase, K. Otsu, N. Usuda, S. Matsumura, K. Inoue, T. Fushiki, Y. Kojima, T. Hashimoto, F. Sakai, F. Hirose, and T. Osumi. 2012. Perilipin 5, a lipid droplet-binding protein, protects heart from oxidative burden by sequestering fatty acid from excessive oxidation. *J. Biol. Chem.* 287:23852–63. doi:10.1074/jbc.M111.328708.

Lafontan, M. 2008. Advances in adipose tissue metabolism. *Int. J. Obes. (Lond).* 32 Suppl 7:S39–51. doi:10.1038/ijo.2008.237.

Lake, A.C., Y. Sun, J.-L. Li, J.E. Kim, J.W. Johnson, D. Li, T. Revett, H.H. Shih, W. Liu, J.E. Paulsen, and R.E. Gimeno. 2005. Expression, regulation, and triglyceride hydrolase activity of Adiponutrin family members. *J. Lipid Res.* 46:2477–87. doi:10.1194/jlr.M500290-JLR200.

Lass, A., R. Zimmermann, G. Haemmerle, M. Riederer, G. Schoiswohl, M. Schweiger, P. Kienesberger, J.G. Strauss, G. Gorkiewicz, and R. Zechner. 2006. Adipose triglyceride

lipase-mediated lipolysis of cellular fat stores is activated by CGI-58 and defective in Chanarin-Dorfman Syndrome. *Cell Metab.* 3:309–19. doi:10.1016/j.cmet.2006.03.005.

Lass, A., R. Zimmermann, M. Oberer, and R. Zechner. 2011. Lipolysis - a highly regulated multi-enzyme complex mediates the catabolism of cellular fat stores. *Prog. Lipid Res.* 50:14–27. doi:10.1016/j.plipres.2010.10.004.

Laurenti, G., E. Benedetti, B. D'Angelo, L. Cristiano, B. Cinque, S. Raysi, M. Alecci, M.P. Cerù, M.G. Cifone, R. Galzio, A. Giordano, and A. Cimini. 2011. Hypoxia induces peroxisome proliferator-activated receptor α (PPARα) and lipid metabolism peroxisomal enzymes in human glioblastoma cells. *J. Cell. Biochem.* 112:3891–901. doi:10.1002/jcb.23323.

Lecoeur, H. 2002. Nuclear apoptosis detection by flow cytometry: influence of endogenous endonucleases. *Exp. Cell Res.* 277:1–14. doi:10.1006/excr.2002.5537.

Lee, J.M., M. Wagner, R. Xiao, K.H. Kim, D. Feng, M.A. Lazar, and D.D. Moore. 2014. Nutrient-sensing nuclear receptors coordinate autophagy. *Nature*. 516:112–5. doi:10.1038/nature13961.

Lee, S.-C., H. Poptani, S. Pickup, W.T. Jenkins, S. Kim, C.J. Koch, E.J. Delikatny, and J.D. Glickson. 2010. Early detection of radiation therapy response in non-Hodgkin's lymphoma xenografts by in vivo 1H magnetic resonance spectroscopy and imaging. *NMR Biomed.* 23:624–32. doi:10.1002/nbm.1505.

Lee, S.-J., J. Zhang, A.M.K. Choi, and H.P. Kim. 2013. Mitochondrial dysfunction induces formation of lipid droplets as a generalized response to stress. *Oxid. Med. Cell. Longev.* 2013:327167. doi:10.1155/2013/327167.

Lei, P., A. Baysa, H.I. Nebb, G. Valen, T. Skomedal, J.B. Osnes, Z. Yang, and F. Haugen. 2013. Activation of Liver X receptors in the heart leads to accumulation of intracellular lipids and attenuation of ischemia-reperfusion injury. *Basic Res. Cardiol.* 108:323. doi:10.1007/s00395-012-0323-z.

Lewis, G.F., A. Carpentier, K. Adeli, and A. Giacca. 2002. Disordered fat storage and mobilization in the pathogenesis of insulin resistance and type 2 diabetes. *Endocr. Rev.* 23:201–29. doi:10.1210/edrv.23.2.0461.

Li, L.O., J.M. Ellis, H. a Paich, S. Wang, N. Gong, G. Altshuller, R.J. Thresher, T.R. Koves, S.M. Watkins, D.M. Muoio, G.W. Cline, G.I. Shulman, and R. a Coleman. 2009. Liver-specific loss of long chain acyl-CoA synthetase-1 decreases triacylglycerol synthesis and beta-oxidation and alters phospholipid fatty acid composition. *J. Biol. Chem.* 284:27816–26. doi:10.1074/jbc.M109.022467.

Li, Z., M.R. Johnson, Z. Ke, L. Chen, and M.A. Welte. 2014. Drosophila Lipid Droplets Buffer the H2Av Supply to Protect Early Embryonic Development. *Curr. Biol.* 24:1485–1491. doi:10.1016/j.cub.2014.05.022.

Liefhebber, J.M.P., C. V Hague, Q. Zhang, M.J.O. Wakelam, and J. McLauchlan. 2014. Modulation of triglyceride and cholesterol ester synthesis impairs assembly of infectious hepatitis C virus. *J. Biol. Chem.* 289:21276–88. doi:10.1074/jbc.M114.582999.

Lin, H.H., S.-M. Lin, Y. Chung, S. Vonderfecht, J.M. Camden, P. Flodby, Z. Borok, K.H. Limesand, N. Mizushima, and D.K. Ann. 2014. Dynamic involvement of ATG5 in cellular stress responses. *Cell Death Dis.* 5:e1478. doi:10.1038/cddis.2014.428.

Listenberger, L.L., A.G. Ostermeyer-Fay, E.B. Goldberg, W.J. Brown, and D. a Brown. 2007. Adipocyte differentiation-related protein reduces the lipid droplet association of adipose triglyceride lipase and slows triacylglycerol turnover. *J. Lipid Res.* 48:2751–61. doi:10.1194/jlr.M700359-JLR200.

Liu, K., and M.J. Czaja. 2013. Regulation of lipid stores and metabolism by lipophagy. *Cell Death Differ.* 20:3–11. doi:10.1038/cdd.2012.63.

Liu, L., Q. Jiang, X. Wang, Y. Zhang, R.C.Y. Lin, S.M. Lam, G. Shui, L. Zhou, P. Li, Y. Wang, X. Cui, M. Gao, L. Zhang, Y. Lv, G. Xu, G. Liu, D. Zhao, and H. Yang. 2014. Adipose-specific knockout of SEIPIN/BSCL2 results in progressive lipodystrophy. *Diabetes*. 63:2320–31. doi:10.2337/db13-0729.

Lopes-Marques, M., I. Cunha, M.A. Reis-Henriques, M.M. Santos, and L.F.C. Castro. 2013. Diversity and history of the long-chain acyl-CoA synthetase (Acsl) gene family in vertebrates. *BMC Evol. Biol.* 13:271. doi:10.1186/1471-2148-13-271.

Marchesan, D., M. Rutberg, L. Andersson, L. Asp, T. Larsson, J. Borén, B.R. Johansson, and S.-O. Olofsson. 2003. A phospholipase D-dependent process forms lipid droplets containing caveolin, adipocyte differentiation-related protein, and vimentin in a cell-free system. *J. Biol. Chem.* 278:27293–300. doi:10.1074/jbc.M301430200.

Martin, S., and R.G. Parton. 2005. Caveolin, cholesterol, and lipid bodies. *Semin. Cell Dev. Biol.* 16:163–174. doi:10.1016/j.semcdb.2005.01.007.

Martin, S., and R.G. Parton. 2006. Lipid droplets: a unified view of a dynamic organelle. *Nat. Rev. Mol. Cell Biol.* 7:373–8. doi:10.1038/nrm1912.

Martinez-Vicente, M., Z. Talloczy, E. Wong, G. Tang, H. Koga, S. Kaushik, R. de Vries, E. Arias, S. Harris, D. Sulzer, and A.M. Cuervo. 2010. Cargo recognition failure is responsible for inefficient autophagy in Huntington's disease. *Nat. Neurosci.* 13:567–76. doi:10.1038/nn.2528.

Mashek, D.G., L.O. Li, and R.A. Coleman. 2010. Long-chain acyl-CoA synthetases and fatty acid channeling. 2:465–476.

Mashima, T., S. Sato, Y. Sugimoto, T. Tsuruo, and H. Seimiya. 2009. Promotion of glioma cell survival by acyl-CoA synthetase 5 under extracellular acidosis conditions. *Oncogene*. 28:9–19. doi:10.1038/onc.2008.355.

Milkevitch, M., H. Shim, U. Pilatus, S. Pickup, J.P. Wehrle, D. Samid, H. Poptani, J.D. Glickson, and E.J. Delikatny. 2005. Increases in NMR-visible lipid and glycerophosphocholine during phenylbutyrate-induced apoptosis in human prostate cancer cells. *Biochim. Biophys. Acta*. 1734:1–12. doi:10.1016/j.bbalip.2005.01.008.

Miura, S., J.-W. Gan, J. Brzostowski, M.J. Parisi, C.J. Schultz, C. Londos, B. Oliver, and A.R. Kimmel. 2002. Functional conservation for lipid storage droplet association among

Perilipin, ADRP, and TIP47 (PAT)-related proteins in mammals, Drosophila, and Dictyostelium. *J. Biol. Chem.* 277:32253–7. doi:10.1074/jbc.M204410200.

Miyoshi, H., J.W. Perfield, S.C. Souza, W.-J. Shen, H.-H. Zhang, Z.S. Stancheva, F.B. Kraemer, M.S. Obin, and A.S. Greenberg. 2007. Control of adipose triglyceride lipase action by serine 517 of perilipin A globally regulates protein kinase A-stimulated lipolysis in adipocytes. *J. Biol. Chem.* 282:996–1002. doi:10.1074/jbc.M605770200.

Miyoshi, H., S.C. Souza, H.-H. Zhang, K.J. Strissel, M. a Christoffolete, J. Kovsan, A. Rudich, F.B. Kraemer, A.C. Bianco, M.S. Obin, and A.S. Greenberg. 2006. Perilipin promotes hormone-sensitive lipase-mediated adipocyte lipolysis via phosphorylation-dependent and -independent mechanisms. *J. Biol. Chem.* 281:15837–44. doi:10.1074/jbc.M601097200.

Mizushima, N., B. Levine, A.M. Cuervo, and D.J. Klionsky. 2008. Autophagy fights disease through cellular self-digestion Noboru. *Nature*. 451:1069–1075. doi:10.1038/nature06639.Autophagy.

Mizushima, N., a. Yamamoto, M. Hatano, Y. Kobayashi, Y. Kabeya, K. Suzuki, T. Tokuhisa, Y. Ohsumi, and T. Yoshimori. 2001. Dissection of Autophagosome Formation Using Apg5-Deficient Mouse Embryonic Stem Cells. *J. Cell Biol.* 152:657–668. doi:10.1083/jcb.152.4.657.

Mizushima, N., T. Yoshimorim, and B. Levine. 2010. Methods in Mammalian Autophagy Research. *Cell*. 140:313–326. doi:10.1016/j.cell.2010.01.028.Methods.

Murphy, D.J. 2012. The dynamic roles of intracellular lipid droplets: from archaea to mammals. *Protoplasma*. 249:541–85. doi:10.1007/s00709-011-0329-7.

Namatame, I., H. Tomoda, H. Arai, K. Inoue, and S. Omura. 1999. Complete inhibition of mouse macrophage-derived foam cell formation by triacsin C. *J. Biochem.* 125:319–27.

Ohsaki, Y., J. Cheng, A. Fujita, T. Tokumoto, and T. Fujimoto. 2006. Cytoplasmic lipid droplets are sites of convergence of proteasomal and autophagic degradation of apolipoprotein B. *Mol. Biol. Cell*. 17:2674–83. doi:10.1091/mbc.E05-07-0659.

Osuga, J., S. Ishibashi, T. Oka, H. Yagyu, R. Tozawa, a Fujimoto, F. Shionoiri, N. Yahagi, F.B. Kraemer, O. Tsutsumi, and N. Yamada. 2000. Targeted disruption of hormone-sensitive lipase results in male sterility and adipocyte hypertrophy, but not in obesity. *Proc. Natl. Acad. Sci. U. S. A.* 97:787–92.

Patel, S., W. Yang, K. Kozusko, V. Saudek, and D.B. Savage. 2014. Perilipins 2 and 3 lack a carboxy-terminal domain present in perilipin 1 involved in sequestering ABHD5 and suppressing basal lipolysis. *Proc. Natl. Acad. Sci. U. S. A.* 111:9163–8. doi:10.1073/pnas.1318791111.

Paul, A., L. Chan, and P.E. Bickel. 2010. The PAT Family of Lipid Droplet Proteins in Heart and Vascular Cells. 10:461–466.

Pawlak, M., P. Lefebvre, and B. Staels. 2014. Molecular Mechanism of PPARα Action and its Impact on Lipid Metabolism, Inflammation and Fibrosis in Non-Alcoholic Fatty Liver Disease. *J. Hepatol.* doi:10.1016/j.jhep.2014.10.039.

Da Poian, A.T., T. El-Bacha, and M.R.M.. Luz. 2010. Nutrient Utilization in Humans: Metabolism Pathways. *Nat. Educ.* 3:11.

Pol, A., S.P. Gross, and R.G. Parton. 2014. Biogenesis of the multifunctional lipid droplet: Lipids, proteins, and sites. *J. Cell Biol.* 204:635–646. doi:10.1083/jcb.201311051.

Puri, V., S. Ranjit, S. Konda, S.M.C. Nicoloro, J. Straubhaar, A. Chawla, M. Chouinard, C. Lin, A. Burkart, S. Corvera, R. a Perugini, and M.P. Czech. 2008. Cidea is associated with lipid droplets and insulin sensitivity in humans. *Proc. Natl. Acad. Sci. U. S. A.* 105:7833–8. doi:10.1073/pnas.0802063105.

Reddy, J.K. 2001. Nonalcoholic Steatosis and Steatohepatitis III. Peroxisomal beta-oxidation, PPAR alpha, and steatohepatitis. *Am J Physiol Gastrointest Liver Physiol*. 281:1333–1339.

Reid, B.N., G.P. Ables, A. Oleg, G. Schoiswohl, W.S. Blaner, I.J. Goldberg, R.F. Schwabe, S.C. Chua, I.J. Goldberg, R.F. Schwabe, S.C. Chua, and L. Huang. 2008. Hepatic Overexpression of Hormone-sensitive Lipase and Adipose Triglyceride Lipase Promotes Fatty Acid Oxidation , Stimulates Direct Release of Free Fatty Acids , and. *J. Biol. Chem.* 283:13087–19099. doi:10.1074/jbc.M800533200.

Robenek, H., O. Hofnagel, I. Buers, M.J. Robenek, D. Troyer, and N.J. Severs. 2006. Adipophilin-enriched domains in the ER membrane are sites of lipid droplet biogenesis. *J. Cell Sci.* 119:4215–24. doi:10.1242/jcs.03191.

Ross, D.D., C.C. Joneckis, V. Ordonez, A.M. Sisk, R.K. Wu, A.W. Hamburger, and R.E. Nora. 1989. Estimation of Cell Survival by Flow Cytometric Quantification of Fluorescein Diacetate/Propidium Iodide Viable Cell Number1. 3776–3782.

Sandager, L., M.H. Gustavsson, U. Ståhl, A. Dahlqvist, E. Wiberg, A. Banas, M. Lenman, H. Ronne, and S. Stymne. 2002. Storage lipid synthesis is non-essential in yeast. *J. Biol. Chem.* 277:6478–82. doi:10.1074/jbc.M109109200.

Schafer, Z.T., A.R. Grassian, L. Song, Z. Jiang, H.Y. Irie, S. Gao, P. Puigserver, and J.S. Brugge. 2009. Antioxidant and Oncogene Rescue of Metabolic Defects Caused by Loss of Matrix Attachment. *Nature*. 461:109–113. doi:10.1038/nature08268.Antioxidant.

Scherer, P.E., P.E. Bickel, M. Kotler, and H.F. Lodish. 1998. Cloning of cell-specific secreted and surface proteins by subtractive antibody screening. *Nat. Biotechnol.* 16:581–6. doi:10.1038/nbt0698-581.

Schlaepfer, I.R., L. Rider, L.U. Rodrigues, M.A. Gijón, C.T. Pac, L. Romero, A. Cimic, S.J. Sirintrapun, L.M. Glodé, R.H. Eckel, and S.D. Cramer. 2014. Lipid Catabolism via CPT1 as a Therapeutic Target for Prostate Cancer. *Mol. Cancer Ther.* doi:10.1158/1535-7163.MCT-14-0183.

Schulze, R.J., S.G. Weller, B. Schroeder, E.W. Krueger, S. Chi, C. a Casey, and M. a McNiven. 2013. Lipid droplet breakdown requires dynamin 2 for vesiculation of autolysosomal tubules in hepatocytes. *J. Cell Biol.* 203:315–26. doi:10.1083/jcb.201306140.

Singh, R., and A.M. Cuervo. 2012. Lipophagy: connecting autophagy and lipid metabolism. *Int. J. Cell Biol.* 2012:282041. doi:10.1155/2012/282041.

Singh, R., S. Kaushik, Y. Wang, Y. Xiang, I. Novak, M. Komatsu, K. Tanaka, A.M. Cuervo, and M.J. Czaja. 2009. Autophagy regulates lipid metabolism. *Nature*. 458:1131–5. doi:10.1038/nature07976.

Sites, J.B.C.A. 1976. Purification hydrolyzing and Some Properties of a Monoacylglycerol-Enzyme of Rat Adipose Tissue *.

Skop, V., M. Cahová, Z. Papáčková, E. Páleníčková, H. Daňková, M. Baranowski, P. Zabielski, J. Zdychová, J. Zídková, and L. Kazdová. 2012. Autophagy-lysosomal pathway is involved in lipid degradation in rat liver. *Physiol. Res.* 61:287–97.

Söllner, T.H. 2007. Lipid droplets highjack SNAREs. *Nat. Cell Biol.* 9:1219–20. doi:10.1038/ncb1107-1219.

Soupene, E., and F.A. Kuypers. 2008. Mammalian Long-Chain Acyl-CoA Synthetases. *Exp Biol Med*. 233:507–521. doi:10.3181/0710-MR-287.Mammalian.

Straeter-Knowlen, I.M., W.T. Evanochko, J.A. den Hollander, P.E. Wolkowicz, J.A. Balschi, J.B. Caulfield, D.D. Ku, and G.M. Pohost. 1996. 1H NMR Spectroscopic Imaging of Myocardial Triglycerides in Excised Dog Hearts Subjected to 24 Hours of Coronary Occlusion. *Circulation*. 93:1464–1470. doi:10.1161/01.CIR.93.7.1464.

Stremmel, W., L. Pohl, A. Ring, and T. Herrmann. 2001. A new concept of cellular uptake and intracellular trafficking of long-chain fatty acids. *Lipids*. 36:981–9.

Subramanian, V., A. Rothenberg, C. Gomez, A.W. Cohen, A. Garcia, S. Bhattacharyya, L. Shapiro, G. Dolios, R. Wang, M.P. Lisanti, and D.L. Brasaemle. 2004. Perilipin A mediates the reversible binding of CGI-58 to lipid droplets in 3T3-L1 adipocytes. *J. Biol. Chem.* 279:42062–71. doi:10.1074/jbc.M407462200.

Sztalryd, C., M. Bell, X. Lu, P. Mertz, S. Hickenbottom, B.H.-J. Chang, L. Chan, A.R. Kimmel, and C. Londos. 2006. Functional compensation for adipose differentiation-related protein (ADFP) by Tip47 in an ADFP null embryonic cell line. *J. Biol. Chem.* 281:34341–8. doi:10.1074/jbc.M602497200.

Sztalryd, C., G. Xu, H. Dorward, J.T. Tansey, J. a Contreras, A.R. Kimmel, and C. Londos. 2003. Perilipin A is essential for the translocation of hormone-sensitive lipase during lipolytic activation. *J. Cell Biol.* 161:1093–103. doi:10.1083/jcb.200210169.

Tanida, I., T. Ueno, and E. Kominami. 2008. LC3 and Autophagy. *Methods Mol. Biol.* 445:77–88. doi:10.1007/978-1-59745-157-4_4.

Tansey, J.T., C. Sztalryd, J. Gruia-Gray, D.L. Roush, J. V Zee, O. Gavrilova, M.L. Reitman, C.X. Deng, C. Li, a R. Kimmel, and C. Londos. 2001. Perilipin ablation results in a lean mouse with aberrant adipocyte lipolysis, enhanced leptin production, and resistance to diet-induced obesity. *Proc. Natl. Acad. Sci. U. S. A.* 98:6494–9. doi:10.1073/pnas.101042998.

Taschler, U., F.P.W. Radner, C. Heier, R. Schreiber, M. Schweiger, G. Schoiswohl, K. Preiss-Landl, D. Jaeger, B. Reiter, H.C. Koefeler, J. Wojciechowski, C. Theussl, J.M. Penninger, A. Lass, G. Haemmerle, R. Zechner, and R. Zimmermann. 2011. Monoglyceride lipase deficiency in mice impairs lipolysis and attenuates diet-induced insulin resistance. *J. Biol. Chem.* 286:17467–77. doi:10.1074/jbc.M110.215434.

Than, N.G., B. Sumegi, S. Bellyei, T. Berki, G. Szekeres, T. Janaky, A. Szigeti, H. Bohn, and G.N. Than. 2003. Lipid droplet and milk lipid globule membrane associated placental protein 17b (PP17b) is involved in apoptotic and differentiation processes of human epithelial cervical carcinoma cells. *Eur. J. Biochem.* 270:1176–88.

Tirinato, L., C. Liberale, S. Di Franco, P. Candeloro, A. Benfante, R. La Rocca, L. Potze, R. Marotta, R. Ruffilli, V.P. Rajamanickam, M. Malerba, F. De Angelis, A. Falqui, E. Carbone, M. Todaro, J.P. Medema, G. Stassi, and E. Di Fabrizio. 2014. Lipid droplets: A New Player in Colorectal Cancer Stem Cells Unveiled by Spectroscopic Imaging. *Stem Cells*. doi:10.1002/stem.1837.

Trump, B.E., I.K. Berezesky, S.H. Chang, and P.C. Phelps. 1997. The Pathways of Cell Death: Oncosis, Apoptosis, and Necrosis. *Toxicol. Pathol.* 25:82–88. doi:10.1177/019262339702500116.

Ujimoto, Y.F., J.O. Noduka, K.J.H. Omma, S.Y. Amaguchi, M.M. Ori, Y.H. Igashi, M.M. Akita, T.K. Inoshita, J.N. Oda, and H.I. Tabe. 2006. Long-Chain Fatty Acids Induce Lipid Droplet Formation in a Cultured Human Hepatocyte in a Manner Dependent of Acyl-CoA Synthetase. 29:2174–2180.

Villena, J. a, S. Roy, E. Sarkadi-Nagy, K.-H. Kim, and H.S. Sul. 2004. Desnutrin, an adipocyte gene encoding a novel patatin domain-containing protein, is induced by fasting and glucocorticoids: ectopic expression of desnutrin increases triglyceride hydrolysis. *J. Biol. Chem.* 279:47066–75. doi:10.1074/jbc.M403855200.

Viscarra, J.A., and R.M. Ortiz. 2013. Cellular mechanisms regulating fuel metabolism in mammals: role of adipose tissue and lipids during prolongued food deprivation. *Metabolism*. 62:889–897. doi:10.1016/j.metabol.2012.12.014.Cellular.

Walther, T.C., and R. V Farese. 2009. The life of lipid droplets. *Biochim. Biophys. Acta*. 1791:459–466. doi:10.1016/j.bbalip.2008.10.009.The.

Wang, H., M. Bell, U. Sreenivasan, U. Sreenevasan, H. Hu, J. Liu, K. Dalen, C. Londos, T. Yamaguchi, M. a Rizzo, R. Coleman, D. Gong, D. Brasaemle, and C. Sztalryd. 2011. Unique regulation of adipose triglyceride lipase (ATGL) by perilipin 5, a lipid droplet-associated protein. *J. Biol. Chem.* 286:15707–15. doi:10.1074/jbc.M110.207779.

Wang, H., L. Hu, K. Dalen, H. Dorward, A. Marcinkiewicz, D. Russell, D. Gong, C. Londos, T. Yamaguchi, C. Holm, M. a Rizzo, D. Brasaemle, and C. Sztalryd. 2009. Activation of hormone-sensitive lipase requires two steps, protein phosphorylation and binding to the

PAT-1 domain of lipid droplet coat proteins. *J. Biol. Chem.* 284:32116–25. doi:10.1074/jbc.M109.006726.

Watkins, P. a, D. Maiguel, Z. Jia, and J. Pevsner. 2007. Evidence for 26 distinct acyl-coenzyme A synthetase genes in the human genome. *J. Lipid Res.* 48:2736–50. doi:10.1194/jlr.M700378-JLR200.

Wee, K., W. Yang, S. Sugii, and W. Han. 2014. Towards a mechanistic understanding of lipodystrophy and seipin functions. *Biosci. Rep.* doi:10.1042/BSR20140114.

Weidberg, H., E. Shvets, and Z. Elazar. 2009. Lipophagy: selective catabolism designed for lipids. *Dev. Cell*. 16:628–30. doi:10.1016/j.devcel.2009.05.001.

Weng, L.-C., B. Pasaribu, I.-P. Lin, C.-H. Tsai, C.-S. Chen, and P.-L. Jiang. 2014. Nitrogen deprivation induces lipid droplet accumulation and alters fatty acid metabolism in symbiotic dinoflagellates isolated from Aiptasia pulchella. *Sci. Rep.* 4:5777. doi:10.1038/srep05777.

Wilfling, F., J.T. Haas, T.C. Walther, and R.V.F. Jr. 2014. Lipid droplet biogenesis. *Curr. Opin. Cell Biol.* 29:39–45. doi:10.1016/j.ceb.2014.03.008.

Wilfling, F., H. Wang, J.T. Haas, N. Krahmer, T.J. Gould, J. Cheng, M. Graham, R. Christiano, F. Fröhlich, K.K. Buhman, R.A. Coleman, J. Bewersdorf, R. V Farese, and T.C. Walther. 2013. Growth by Relocalizing from the ER to Lipid Droplets. 24:384–399. doi:10.1016/j.devcel.2013.01.013.Triacylglycerol.

Winstead, M. V, J. Balsinde, and E.A. Dennis. 2000. Calcium-independent phospholipase A(2): structure and function. *Biochim. Biophys. Acta*. 1488:28–39.

Wolins, N.E., B.K. Quaynor, J.R. Skinner, M.J. Schoenfish, A. Tzekov, and P.E. Bickel. 2005. S3-12, Adipophilin, and TIP47 package lipid in adipocytes. *J. Biol. Chem.* 280:19146–55. doi:10.1074/jbc.M500978200.

Wolins, N.E., B.K. Quaynor, J.R. Skinner, A. Tzekov, M. a Croce, M.C. Gropler, V. Varma, A. Yao-Borengasser, N. Rasouli, P. a Kern, B.N. Finck, and P.E. Bickel. 2006. OXPAT/PAT-1 is a PPAR-induced lipid droplet protein that promotes fatty acid utilization. *Diabetes*. 55:3418–28. doi:10.2337/db06-0399.

Wolins, N.E., B. Rubin, and D.L. Brasaemle. 2001. TIP47 associates with lipid droplets. *J. Biol. Chem.* 276:5101–8. doi:10.1074/jbc.M006775200.

Wolins, N.E., J.R. Skinner, M.J. Schoenfish, A. Tzekov, K.G. Bensch, and P.E. Bickel. 2003. Adipocyte protein S3-12 coats nascent lipid droplets. *J. Biol. Chem.* 278:37713–21. doi:10.1074/jbc.M304025200.

Xiong, X., R. Tao, R.A. DePinho, and X.C. Dong. 2012. The autophagy-related gene 14 (Atg14) is regulated by forkhead box O transcription factors and circadian rhythms and plays a critical role in hepatic autophagy and lipid metabolism. *J. Biol. Chem.* 287:39107–14. doi:10.1074/jbc.M112.412569.

Xu, G., C. Sztalryd, X. Lu, J.T. Tansey, J. Gan, H. Dorward, A.R. Kimmel, and C. Londos. 2005. Post-translational regulation of adipose differentiation-related protein by the ubiquitin/proteasome pathway. *J. Biol. Chem.* 280:42841–7. doi:10.1074/jbc.M506569200.

Yamaguchi, T. 2010. Crucial role of CGI-58/alpha/beta hydrolase domain-containing protein 5 in lipid metabolism. *Biol. Pharm. Bull.* 33:342–5.

Yamaguchi, T., S. Matsushita, K. Motojima, F. Hirose, and T. Osumi. 2006. MLDP, a novel PAT family protein localized to lipid droplets and enriched in the heart, is regulated by peroxisome proliferator-activated receptor alpha. *J. Biol. Chem.* 281:14232–40. doi:10.1074/jbc.M601682200.

Yamaguchi, T., and T. Osumi. 2009. Chanarin-Dorfman syndrome: deficiency in CGI-58, a lipid droplet-bound coactivator of lipase. *Biochim. Biophys. Acta*. 1791:519–23. doi:10.1016/j.bbalip.2008.10.012.

Yamashita, Y., T. Kumabe, Y.Y. Cho, M. Watanabe, J. Kawagishi, T. Yoshimoto, T. Fujino, M.J. Kang, and T.T. Yamamoto. 2000. Fatty acid induced glioma cell growth is mediated by the acyl-CoA synthetase 5 gene located on chromosome 10q25.1-q25.2, a region frequently deleted in malignant gliomas. *Oncogene*. 19:5919–25.

Yang, L., P. Li, S. Fu, E.S. Calay, and G.S. Hotamisligil. 2010. Defective hepatic autophagy in obesity promotes ER stress and causes insulin resistance. *Cell Metab.* 11:467–78. doi:10.1016/j.cmet.2010.04.005.

Yu, W., P.T. Bozza, D.M. Tzizik, J.P. Gray, J. Cassara, a M. Dvorak, and P.F. Weller. 1998. Co-compartmentalization of MAP kinases and cytosolic phospholipase A2 at cytoplasmic arachidonate-rich lipid bodies. *Am. J. Pathol.* 152:759–69.

Zaugg, K., Y. Yao, P.T. Reilly, K. Kannan, R. Kiarash, J. Mason, P. Huang, S.K. Sawyer, B. Fuerth, B. Faubert, A. Elia, X. Luo, V. Nadeem, D. Bungard, S. Yalavarthi, J.D. Growney, A. Wakeham, Y. Moolani, J. Silvester, A.Y. Ten, W. Bakker, K. Tsuchihara, S.L. Berger, R.P. Hill, R.G. Jones, M. Tsao, and M.O. Robinson. 2011. Carnitine palmitoyltransferase 1C promotes cell survival and tumor growth under conditions of metabolic stress. 1041–1051. doi:10.1101/gad.1987211.Freely.

Zechner, R., P.C. Kienesberger, G. Haemmerle, R. Zimmermann, and A. Lass. 2009. Adipose triglyceride lipase and the lipolytic catabolism of cellular fat stores. *J. Lipid Res.* 50:3–21. doi:10.1194/jlr.R800031-JLR200.

Zhang, H.H., S.C. Souza, K. V Muliro, F.B. Kraemer, M.S. Obin, and A.S. Greenberg. 2003. Lipase-selective functional domains of perilipin A differentially regulate constitutive and protein kinase A-stimulated lipolysis. *J. Biol. Chem.* 278:51535–42. doi:10.1074/jbc.M309591200.

Zietkowski, D., G.S. Payne, E. Nagy, M.A. Mobberley, T.A. Ryder, and N.M. deSouza. 2012. Comparison of NMR lipid profiles in mitotic arrest and apoptosis as indicators of paclitaxel resistance in cervical cell lines. *Magn. Reson. Med.* 68:369–77. doi:10.1002/mrm.23265.

Zimmermann, R., J.G. Strauss, G. Haemmerle, G. Schoiswohl, R. Birner-Gruenberger, M. Riederer, A. Lass, G. Neuberger, F. Eisenhaber, A. Hermetter, and R. Zechner. 2004. Fat mobilization in adipose tissue is promoted by adipose triglyceride lipase. *Science*. 306:1383–6. doi:10.1126/science.1100747.

Zou, J., S. Ganji, I. Pass, R. Ardecky, M. Peddibhotla, M. Loribelle, S. Heynen-Genel, M. Sauer, S. Vasile, S. E, M. S, V.M. Mangravita-Novo A, M. D, C. A, D. S, S. S, S. Y, Z. FY, P. AB, S. LH, K. S, N. H, D. J, H. AJ, C. R, M. PM, and C. TDY. 2014. Potent inhibitors of lipid droplet formation. *Probe Reports from NIH Mol. Libr. Progr. [Internet]. Bethesda Natl. Cent. Biotechnol. Inf.* 23762932 [PubMed].

Zoula, S., P.F.J.W. Rijken, J.P.W. Peters, R. Farion, B.P.J. Van der Sanden, a J. Van der Kogel, M. Décorps, and C. Rémy. 2003. Pimonidazole binding in C6 rat brain glioma: relation with lipid droplet detection. *Br. J. Cancer*. 88:1439–44. doi:10.1038/sj.bjc.6600837.